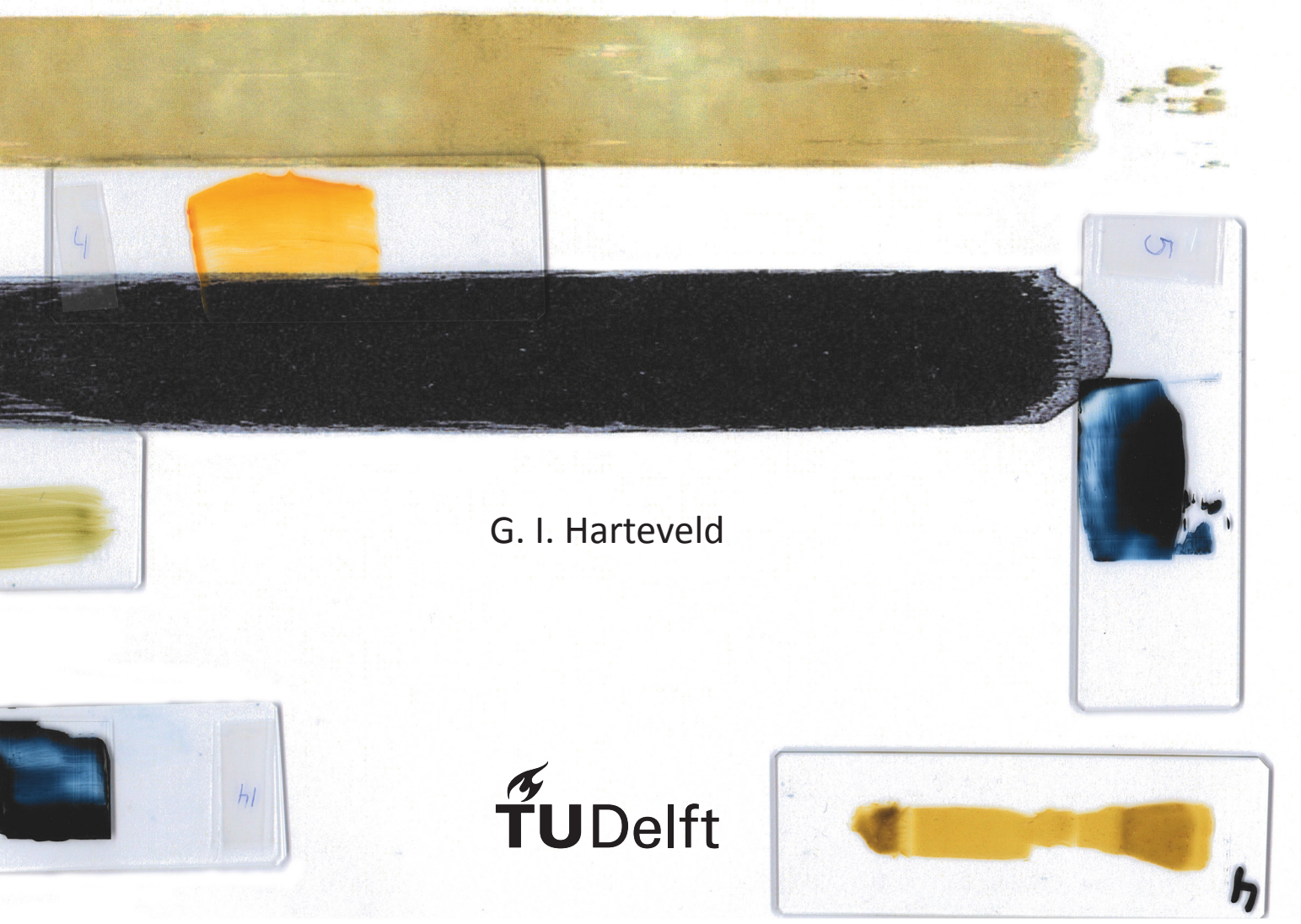


An Approach using Optical Properties of Paints and Rendering Techniques



# Investigation of the Effect of the Green Glaze Layer in the Background of Girl with a Pearl Earring by Johannes Vermeer

An Approach using Optical Properties of Paints and Rendering Techniques

Ву

G. I. Harteveld

in partial fulfilment of the requirements for the degree of

#### **Master of Science**

in Materials Science and Engineering

at the Delft University of Technology, to be defended publicly on Thursday May 23, 2019 at 14:00.

Student number: 4007522

Supervisors: Prof. dr. J. Dik

Prof. dr. ir. J. M. P. Geraedts

Thesis committee: Prof. dr. J. Dik (Chair), TU Delft

Prof. dr. ir. J. M. P. Geraedts, TU Delft dr. M. W. E. M. Alfeld, TU Delft dr. A. L. S. Vandivere, Mauritshuis

This thesis is confidential and cannot be made public until December 31, 2019.

An electronic version of this thesis is available at http://repository.tudelft.nl/.

#### Abstract

A novel combination of analytical techniques for measuring optical properties of glaze and paint as input for computer modelling is used to investigate the influence of the green glaze layer present on top of the black underpainting in the background of Girl with a Pearl Earring. The absorption spectra of paint layers from paint reconstructions and samples of the original painting were determined using micro spectrophotometry. Additionally, Bidirectional Reflectance Distribution Function (BRDF) measurements were done on paint reconstructions to determine the reflection distribution from multiple illumination and observation angles. Already existing height and layer thickness information was compiled in a digital 3D model of the painting which, in combination with the optical properties, was used as a base for rendering using the Mitsuba render engine. The experimental results clearly show that the green glaze layer under specific angles darkens the appearance of the black paint onto which it is applied. The computer simulation shows promising results for digitally recreating the painting.

#### Preface

After I finished my bachelor degree in Architecture I started my journey to the master Materials Science and Engineering. The direction of materials in art caught my interest as a way to combine my interest for art and science. My parents taught me that it is more important to do something that makes you happy, rather than earning a lot of money. Keeping this in mind, the switch from Architecture to Materials Science turned out to be a good one since I have come home bouncing off the walls from excitement many times since the beginning of my master's (ask my boyfriend, he can confirm).

A thank you is in order for prof. dr. Joris Dik who has given me the opportunity to do my graduation project in the field I find so interesting. Together with prof. dr. ir. Jo Geraedts he made a good supervising team giving me the opportunity to do research at many different departments and organisations. After a roller coaster graduation project filled with a lot of exciting moments, it is time to finish after (almost) a decade of studying.

Guusje Harteveld Delft, May 12th 2019

## Table of Contents

1- Introduction	1
1.1- Girl with a Pearl Earring	1
1.2- Reproductions of Paintings	1
1.3- Research Aim	2
1.4- Build-up Thesis	3
2- Theoretical Background- Optical Properties of Paint	4
2.1- Paint and Paintings	
2.1.1 - What is Paint?	4
2.1.2 - Glaze	4
2.1.3 - Interaction of Light with a Painting	5
2.2- Previous Research on Girl with a Pearl Earring	6
2.3 - Acquisition of Experimental Data	8
2.3.1 - Acquisition of Optical Data from Paint	8
2.3.2 - Acquisition of Data from Paintings	11
2.4- Theoretical Description of Paint and Paint Layers	13
2.4.1 - Description of Theoretical Models	13
2.4.2 - Comparing Theoretical Models and their Application	16
2.4.3 - Conclusion	17
3- Experiment- Characterisation of Optical Properties	19
3.1- Assumptions made within Experiment	19
3.2- Paint Samples	
3.2.1 - Samples from the Original Painting	20
3.2.2 - Reconstructions with Pigments Similar to Pigments in Original Painting	
3.2.3 - Reconstructions with Modern Paint	
3.3 - Measurement of Optical Properties	
3.3.1 - Ellipsometry	23
3.3.2 - Micro Spectrophotometry	24
3.3.3 - BRDF Measurements	
3.4- Results	
3.4.1 - Ellipsometry Measurements	25
3.4.2 - Absorption Measurements	
3.4.3 - BRDF Measurements	28
4- Theoretical Background- Rendering and 3D Modeling	33
4.1- Rendering of Layered Structures	
4.2- Ray Tracing	36
5- Experiment- 3D Model and Simulation	
5.1- Assumptions made within Experiment	37
5.2- Creation of 3D Model	
5.3- Rendering using Mitsuba	38
5.4- Results	
5.4.1 - Absorption Spectra as Input	38

6- Discussion and Conclusion	40
6.1- Discussion	40
6.2- Conclusions	42
6.3- Limitations	43
6.4- Recommendations	43
Acknowledgements	44
Bibliography	45
Appendix A- Sample Preparation	49
Appendix B- Literature Study	55

#### 1 - Introduction

#### 1.1- Girl with a Pearl Earring

The Girl with a Pearl Earring (c. 1665-1666) (Figure 1.1) by Johannes Vermeer is one of the most iconic and well-known paintings in the world. Next to Rembrandt van Rijn and Jan Steen, Vermeer is one of the famous painters from the Dutch Golden Age. Girl with a Pearl Earring shows the portrait of a girl with a blue headdress and an earring in front of a dark background. The portrait appeals to many viewers because of its appearance and mystery. There is a soft-focus effect in the painting that, up until this date, raises questions amongst art historians.[53] Some suggest that Vermeer might have used a camera obscura to create the almost photograph-like effect of the portrait.[34]. In the television programme Het Geheim van de Meester a test is done with a camera obscura to study the effect and compare it to the painting. The soft-focus effect in the painting was visible using the camera obscura, which could be a suggestion that Vermeer might have looked through a lens and used the effect as inspiration for the Girl with a Pearl Earring. [66] When comparing looking at an object through a lens and with the naked eye, the dynamic range can be significantly reduced when looking Figure 1.1. Girl with a Pearl Earring (c.1665-1666). through the lens. This could result in the dark areas appearing more [44] dark and the light areas appearing more light.



At first sight the background of the painting appears black but there is a green translucent glaze layer present as seen in the cross section. The glaze is applied on top of a black layer of paint.[25] The question rises why the glaze layer is applied on top of the black layer and whether the presence of the glaze layer influences the visual appearance of the background compared to only a black layer of paint. It could be suggested that the combination of the glaze layer and the textured black paint beneath it cause the soft-focus or the optical effect experienced when looking through a lens. To test this, research should be done on the role of the glaze layer and whether the effect can be simulated to relate it to the characteristic appearance of the portrait painted by Vermeer.

#### 1.2- Reproductions of Paintings

Reproductions of fine art can be made for multiple purposes. For example, 3D printed versions of paintins are made for research as well as merchandise purposes. Researchers in the field of conservation and restoration can use reproductions to study the painting, its ageing process and possible approaches for restoration and conservation. Next to physically reproducing fine art, it can be of interest to virtually reproduce a painting. Museums are more often digitising their collections to make the fine arts more accessible to a wide public. The digital versions are, however, still only a 2D image of the art work, therefore the topography information of the painting is lost in the images. A digital 3D model combined with the optical properties of the paint layers will result in a completely new experience of the paintings.

Creating digital 3D versions of paintings will provide new insights in paintings, their interaction with light and the influence of their physical properties on the appearance of the paintings. In advanced modelling software it can be possible to examine a painting under different lighting situations. Knowing about the layered structure of the painting and being able to digitally model it, makes it possible to examine a painting layer by layer and perhaps peal away overpaintings without having to physically touch the painting.

Over the past decades, more techniques have become available to non-destructively -without damaging the painting- analyse a painting. Advancements in this field have lead to more knowledge than ever about paintings and their history. By digitally simulating the optical properties of the paint used in the painting, a

prediction can be made of the visual appearance of the painting with and without the glaze layer. By using the optical properties of freshly made paint, an indication can be made of the appearance when the painting was only just painted. These optical properties of the paints could also contribute to the knowledge of the optical properties which must be recreated by means of 3D printing to create an even more convincing 3D printed reproduction. The combination of these novel techniques and the acquired measurement data makes it possible to come closer to the secrets of paintings and how these were made by the great masters in the past.

#### 1.3 - Research Aim

As mentioned above, researching the optical properties of paint and glaze can provide insight in the effects which influence the appearance of a painting. The influence of the glaze layer present in the background of *Girl with a Pearl Earring* can be studied using data of the layered structure of the painting, the optical parameters of the paint and glaze layers and model these using rendering software. This is a novel approach in the field of fine art due to the combination of the used techniques and could lead to new insights in the reasons behind the use of i.e. glaze layers in paintings and digitally recreating painted structures. The aim is to gain more information about the effect of the glaze layer in the background of the painting on the visual appearances of the painting. By determining whether the needed parameters of paint and glaze layers provide the information needed to create a digital 3D simulation of the painting, it is studied if this approach can lead to a realistic simulation of the glaze layer in the background of *Girl with a Pearl Earring*.

Determining the optical effect of the glaze layer in the background of *Girl with a Pearl Earring* on the visual appearance of the painting will be done by means of a computer simulation. To create a computer simulation of the original painting, optical properties of the paint (layers) and a 3D model of the painting are required as input (see Figure 1.2). The acquisition of data can be divided into two streams, measurements of the optical properties of paint and measurements on the layered structure and topography of the painting. The painting cannot be recreated without any one of these elements. Measurements on the layered structure of the painting have been done by Callewaert [9] and will provide the base for a 3D model of the painting. The optical properties of the paint and glaze in the painting have not been determined up until now. The focus of this research will be on that stream in Figure 1.2.

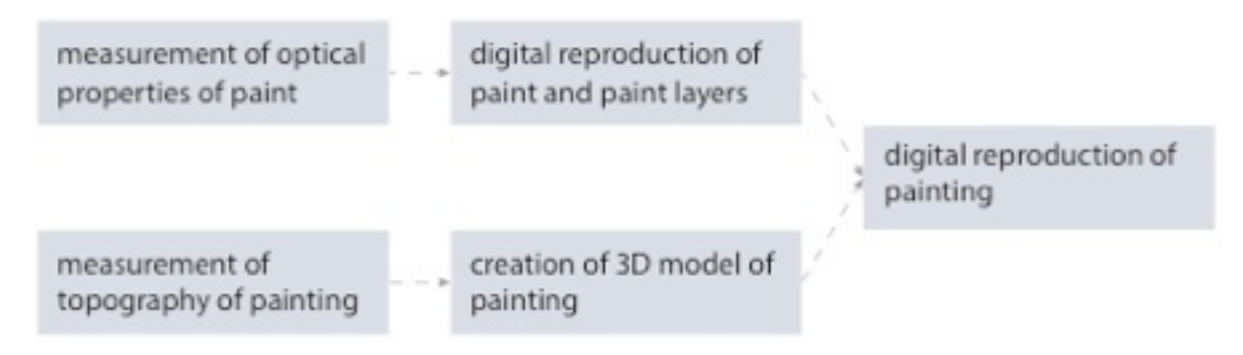


Figure 1.2. Overview of research build-up.

During this research, absorption of the original paint, paint reconstructions and modern oil paint is measured using micro spectrophotometry. Tests are done to determine the refractive index of paint using ellipsometry. The reflectance of the paints is determined by BRDF (Bidirectional Reflection Distribution Function) measurements. A 3D model of the painting is created by using OCT scan data as input for the height and layer thicknesses of the painting. [9] These parameters should create enough input for the Mitsuba render software to simulate the visual appearance of the painting. Eventually, this model might be suitable to use as a base for (further improving the quality) of 3D printed reproductions of paintings.

The fact that this is a novel approach could lead to some difficulties or uncertainties during the research. The use of ellipsometry to determine the refractive index of paint has not been previously done. Using the Mitsuba render engine to simulate paint layers is also unprecedented and therefore an uncertain factor within the research.

#### 1.4- Build-up Thesis

The research can be divided into two sections with firstly the determination of the optical properties of paint and the theoretical models to calculate the optical behaviour of the paint layers and secondly the building of a 3D model to represent the painting and the models used to create a computer simulation of the paint layers. The structure of the paint, the painting and previous research on *Girl with a Pearl Earring* are discussed in Chapter 2. Also, methods of analysing several properties of paintings and theoretical models representing the optical properties of paint layers are discussed. The following Chapter 3, describes the experimental determination of optical properties of the paint present in the original painting and of the paint reconstructions created for this research. The results of the experiment are also discussed in Chapter 3. Advancements in rendering of layered structures can be found in Chapter 4, followed by the experimental section about testing the implementation of the measured data in the 3D model and render software as a means to digitally simulate the original painting in Chapter 5. The discussion, conclusion and recommendations can be found in Chapter 6.

## 2 - Theoretical Background - Optical Properties of Paint

#### 2.1- Paint and Paintings

The paint forms the basis of a painting. This section describes what paint is, what the differences are between paint and glaze and how a painting is built up.

#### 2.1.1 - What is Paint?

The most basic version of paint is a mixture of pigment and a binder. The pigment provides the colour and the binder, for example linseed oil, binds the pigment particles to each other and to the support on which the paint is applied. A vehicle can be added to the paint to dilute the mixture of pigment and binding medium to decrease its viscosity. Other additions could be materials to alter the optical or textural characteristics of the paint or to accelerate or slow down the drying of the paint. The production of paint in the seventeenth century was done in painter's studios by grinding the pigment and binder together with a muller, a flat-bottomed glass or stone instrument, on a flat surface to create a paste which could be applied onto the support. (Figure 2.1)

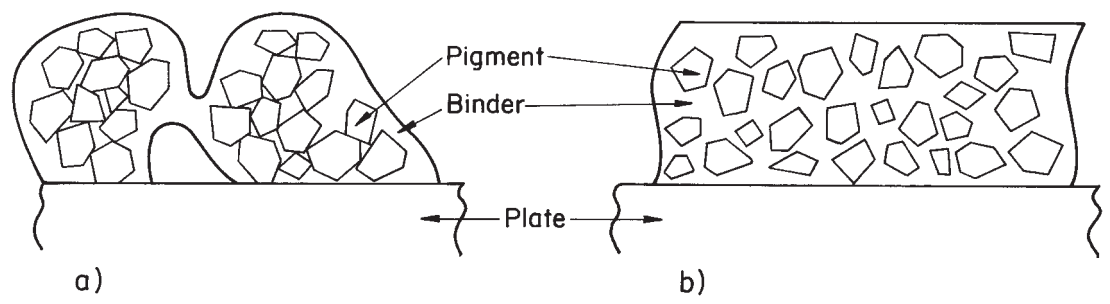


Figure 2.1. Production of paint. Pigment particles are combined with a binding medium into a paste (a) which is ground on a flat plate in order to distribute the pigment particles uniformly within the binding medium (b).[55]

#### 2.1.2 - Glaze

As mentioned above, the binding medium is the vehicle to bind pigment together and to the substrate on which the paint is applied. Usually, pigment particles are not soluble in the binding medium. Depending on the composition of the paint, it can be translucent or opaque. The optical properties of the pigment and oil in combination with the ratio of binding medium to pigment determine the translucency of the paint. A translucent or transparent paint layer is usually referred to as a glaze. The translucency of the glaze makes it possible for light rays to partially move through the glaze and interact with the, often opaque, paint layer underneath the glaze. (Figure 2.2) The main difference between an opaque paint layer and a glaze is the ratio of pigment to binding medium which results in a more or less translucent layer.[55] Glazes were often applied on top of dry opaque underpaintings to create more intense colours and a luminosity which could not be achieved by using opaque paints. Because the glaze was applied on a dry paint layer, the two layers do not mix physically. However, due to the translucency of the glaze, the layers do mix optically. The pigments used for glazes were, other than the pigments in opaque paints, inherently transparent and organic.[31]

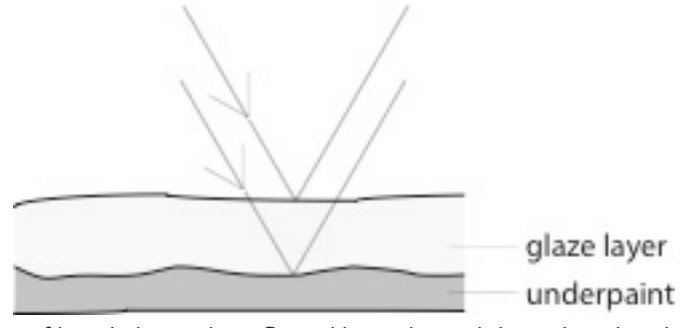


Figure 2.2. Schematic representation of how light can be reflected by and travel through a glaze layer.

The influence of a glaze on the visual appearance of a paint layer has been of interest to multiple artists in history. Glazes could be used to create richer and more intense colours and to create soft, dark areas without using opaque paints. Glaze layers have been applied by for example Leonardo da Vinci to create the darker areas in faces as can be seen in Figure 2.3. Using X-ray fluorescence, Viguerie analysed the layered structure in several faces in paintings from Leonardo da Vinci. The virtual cross sections of two faces are shown in Figure 2.3 where the thickness of the glaze layer becomes larger towards the shadow area of the face. Da Vinci used multiple glaze layers to create darker areas in his paintings instead of using dark opaque paint. The use of a glaze in combination with how it was applied by Da Vinci resulted in a softer appearance at the edge of the faces compared to dark paint.[58]

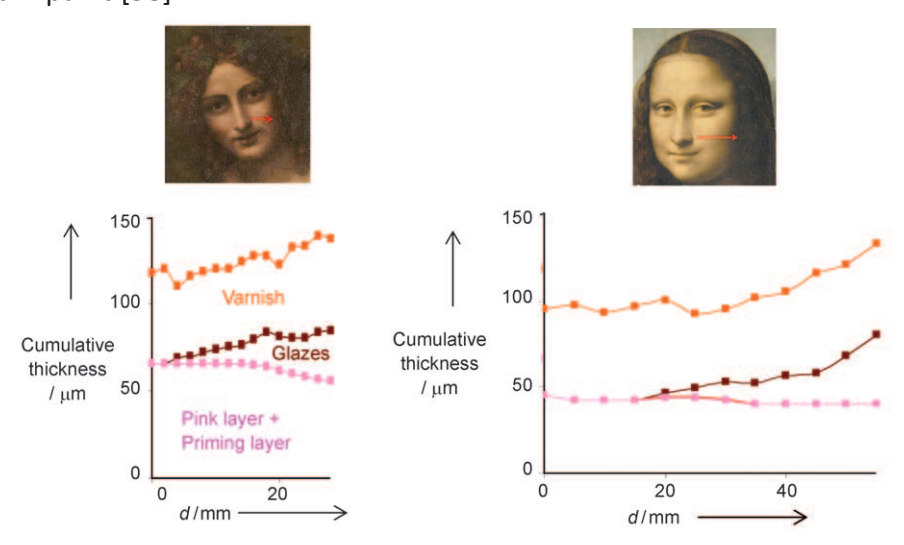


Figure 2.3. Virtual cross sections of faces in Leonardo da Vinci paintings. Left: Bacchus, right: Mona Lisa. The pink line indicates the thickness of the priming layer combined with the pink flesh tones. The dark red line indicates the thickness of the glaze and the orange layer indicates the thickness of the varnish layer.[58]

Not only Da Vinci used glaze layers in his painting, also in paintings by Rembrandt glazes have been applied. The painting of Isaac and Rebecca, known as 'the Jewish Bride', contains a cochineal red glaze layer which has been applied on top of a vermilion red underpainting resulting a rich red skirt. (Figure 2.4) [61]



Figure 2.4. Details of Isaac and Rebecca, known as 'the Jewish Bride' by Rembrandt van Rijn. The red skirt of Rebecca contains a red cochineal glaze on top of a vermilion underpainting resulting in a deep red skirt.[29]

#### 2.1.3 - Interaction of Light with a Painting

A painting is a layered structure as schematically shown in Figure 2.5. The canvas is the base of the painting on top of which a layer of ground paint is applied. On top of the ground, one or more layers of paint are applied which form the image of the painting. Often a varnish layer is applied on top of the paint to preserve the paint and bring out the colours and depth of the painting. The optical properties of the varnish and paint influence how a painting is seen by the viewer.

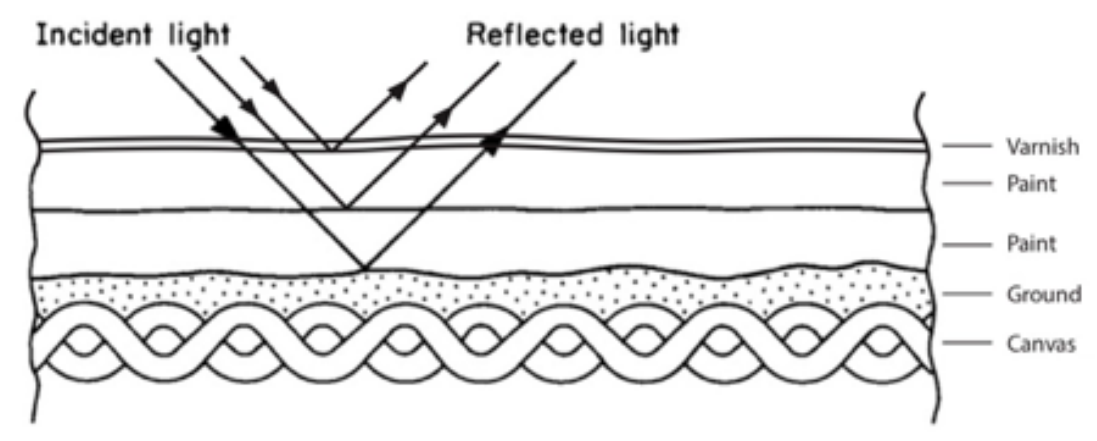


Figure 2.5. Schematic cross section of a painting, after Taft.[55]

When a light ray emitted by a certain light source interacts with a paint layer several effects occur simultaneously. Depending on the properties of the light and the paint, the light can be reflected from the surface, absorbed by the paint or transmitted through the paint or a combination occurs where light is partially reflected, partially absorbed and/or partially transmitted. If, in the case of reflection the angle of reflection of the ray is equal to the incident angle, there is specular or mirror reflection. When the light is reflected in every direction, also known as scattering, diffuse reflection takes place. When the paint or glaze layer is translucent, light can be transmitted through it. This transmitted light can be specular or diffuse, like reflected light, depending on whether or not the light is scattered when passing through the paint.[27] The spectral distribution of the light source combined with the wavelengths absorbed by a material determine the colour the material appears to be to the observer. For example, a red object appears red because the material absorbs all wavelengths of the visible spectrum except for the red. Some paint can exhibit different colours under different light sources, this is also known as metamerism.[55] The type of reflection of light from a surface determines partially how light or dark a surface appears. A surface with diffuse reflection appears similarly light or dark from each viewing angle. (Figure 2.6a) In the case of reflection with a specular component, Figure 2.6b, the surface will appear lighter when looking from the angle where the specular reflection is directed to and darker when the surface is observed from another angle. This is similar for the reflection shown in Figure 2.6c where the largest amount of light is reflected in the direction of the incident light. This makes it possible for a surface to appear darker or lighter depending on the observation angle.[3]

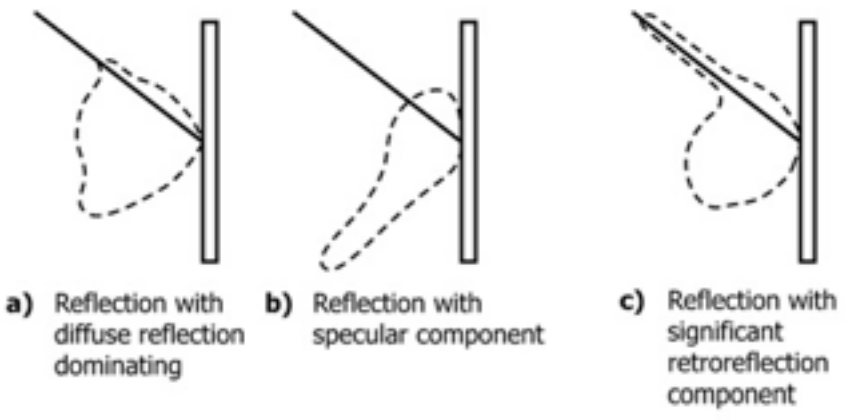


Figure 2.6. Different types of reflection that can occur. The black solid lines indicate the incident light, the dashed lines indicate the reflection.[3]

#### 2.2- Previous Research on Girl with a Pearl Earring

The Girl with a Pearl Earring was examined and restored extensively at the Mauritshuis museum in 1994-1995. During the examination it was confirmed that earlier restorations had been severe. Several pieces of paint had become dislodged and some were stuck upside down on top of the paint surface. These pieces of paint provided samples from the painting without having to cut into the painting (Figure 2.8). The background of the painting turned out to be more green than black. The old retouches appeared to have shielded the original paint from moisture and light. That is probably the reason why areas underneath the retouches were darker compared to the other areas. Figure 2.7 shows a cross section of the background background and the green

colour of the paint is visible in the left image. The cross section originates from the background between the left side of the painting and the forehead of the girl (Figure 2.8, sample 26). Sample 26 was one of the samples that became dislodged in a previous restoration and was found at the location indicated in Figure 2.8. It is unclear from which exact spot the sample originates, but it there is no doubt this is a sample from the background of the painting.[25] In the cross section in Figure 2.7 three distinct layers are visible. The bottom layer (1) is the ground, consisting of chalk, lead white, a little fine ochre and black. The 12  $\mu$ m middle layer (2) is a black underpainting, according to the latest research consisting of a combination of mainly charcoal black and bone black, pigments created by burning wood and bones.

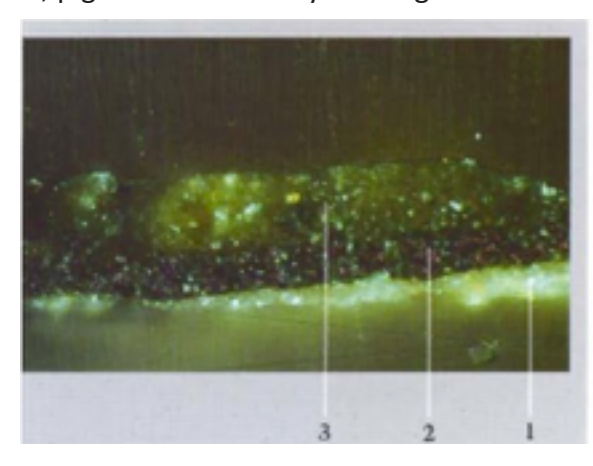




Figure 2.7. Cross section of a background sample (sample 26) left of the forehead of Girl with a Pearl Earring. The left image was taken under regular light, the right image under fluorescent light both with 305x magnification. 1 Indicates the ground, 2 the black underpaint of 12  $\mu$ m thickness and 3 is the translucent green glaze layer of 28  $\mu$ m containing weld, chalk, indigo and a little red ochre.[25]

The top layer visible in the cross section (3) is a 28 µm thick translucent green layer consisting of weld, indigo, chalk and a little red ochre. Weld is a natural yellow dye obtained from the Reseda luteola and was used for dying woollen and silk materials. It is very transparent and therefore an ideal pigment for glazes.[32] The primary colouring substance of weld is luteolin which is extracted by boiling the Reseda luteola in an alkaline solution with water and potash (potassium containing salts). Different mordants, i.e. chalk or aluminium, can



Figure 2.8. Overview of samples available of the painting.[57]

be used to bind the luteolin. Depending on the used mordant, the colour can range from bright yellow to green. [60] High-Performance Liquid Chromatography (HPLC) results show the presence of the proteinaceous material which might originate from the woollen textiles dyed with weld used as a pigment in the paint. [57] The indigo pigment is, like weld, extracted from a plant. The leaves of a plant of the indigofera species, often indigofera tinctoria, are steeped in alkaline water in order to start the fermentation of the leaves. The soaked leaves are stirred or beaten to a pulp to oxidise the mass until the indigo forms as a precipitate which is then dried. The pigment was ground for use in a paint. [15]

#### 2.3- Acquisition of Experimental Data

Optical properties of the paint and the structure of the painting determine the visual appearance of the painting. The absorption and reflection of light by the paint influences the colour of the paint and next to the topography, the reflection can also be an indication of the glossiness of the paint.

The refractive index of the materials is a measure for the relation between the transmitted and reflected light at an interface between two materials. These factors all influence the appearance of the paint and therefore need to be taken into account when simulating the visual appearance of the paint. The different properties of paint and paintings are discussed here as well as available techniques to determine these properties.

#### 2.3.1 - Acquisition of Optical Data from Paint

#### Refractive index

The refractive properties of a material are expressed as a complex refractive index ( $\tilde{n}$ ), consisting of the refractive index (n) and the extinction coefficient (k) (eq. 2.1).

$$\tilde{n} = n + ik$$
 eq. 2.1

The refractive index (n) is the ratio of the velocities of light in vacuum and the respective medium. It influences the appearance of objects, especially at the interface of different media, e.g. the distortion visible when looking through water in a glass. Differences in the real part of the RI also influence how transparent objects appear when placed against each other. The extinction coefficient (k) is a measure how much light energy is absorbed in a material.[41]

Figure 2.9 demonstrates the impact of these material properties on the wavelength and intensity of the light passing through the materials. As light waves move from air to the absorbing film 1 with a RI of 4, the wavelength becomes shorter with the change in the velocity of light at constant frequency, while the intensity decays proportionally to e<sup>(-kl)</sup>, with I being the penetration depth of the light. When the waves move into Film 2 with a RI of 2, the wavelengths become larger again compared to these in Film 1.[41]

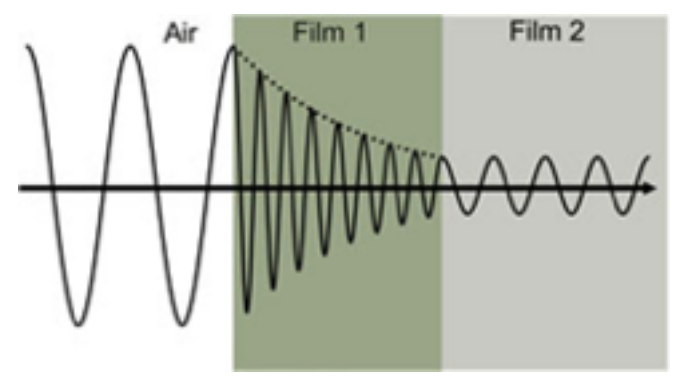


Figure 2.9. Movement of waves through different mediums.[41]

The refractive index of paint and varnish is an important factor for the appearance of a painting as it is an indicator to how transparent the varnish layer appears compared to the underlying paint layer and can drastically alter the appearance of the painting. Factors determining this impact are the refractive indices of the paint and varnish, the optical contact between the layers, the method in which both layers are applied, as well as other optical properties of both paint and varnish, respectively. To visualise the effect of different varnish refractive indices on the appearance of a painting, Berns created a computer simulation modelling varnish layers with different RI on paintings. [6] Applying a varnish layer usually reduces the surface roughness of the painting which increases contrast, spatial image quality and colour gamut.

Within the field of restoration and conservation of paintings the RI is mainly used to determine how a new varnish layer will appear and/or if a pigment used for restoration will appear similar to the original. Additionally, the ratio of refractive indices of a pigment compared to the binding medium of a paint is an indicator for the transparency of the paint. The closer the RI of the pigment to the RI of the binding medium, the more transparent the paint will appear.

Until now, the RI of paint is only determined in limited cases in the field of conservation and restoration of paintings. The method of choice in this field is the immersion method, in which a pigment is immersed in a binding medium with known RI to estimate the RI of the pigment. Typically a set of oils used as binding medium in artists paints with known RI is used to get a close approximation.[4] For conservation and restoration purposes, the exact refractive index is often not required, so the pigment is usually only compared to commonly used binding media. However, this method only approximates the real part of the complex refractive index.

#### Ellipsometry

An alternative to the immersion method is ellipsometry, a technique that can be used to determine the film thickness and optical constants, under which both the real and complex part of the refractive index. A schematic representation of the principles of an ellipsometer is shown in Figure 2.10. Light from a light source is linearly polarised and incident on the sample. Due to the optical properties and thickness of the sample, a change in amplitude ( $\Psi$ ) and phase ( $\Delta$ ) of the polarised light occurs resulting in elliptically polarised light.[19] From the change in polarization the thickness and refractive index of the investigated film can be determined. [45]

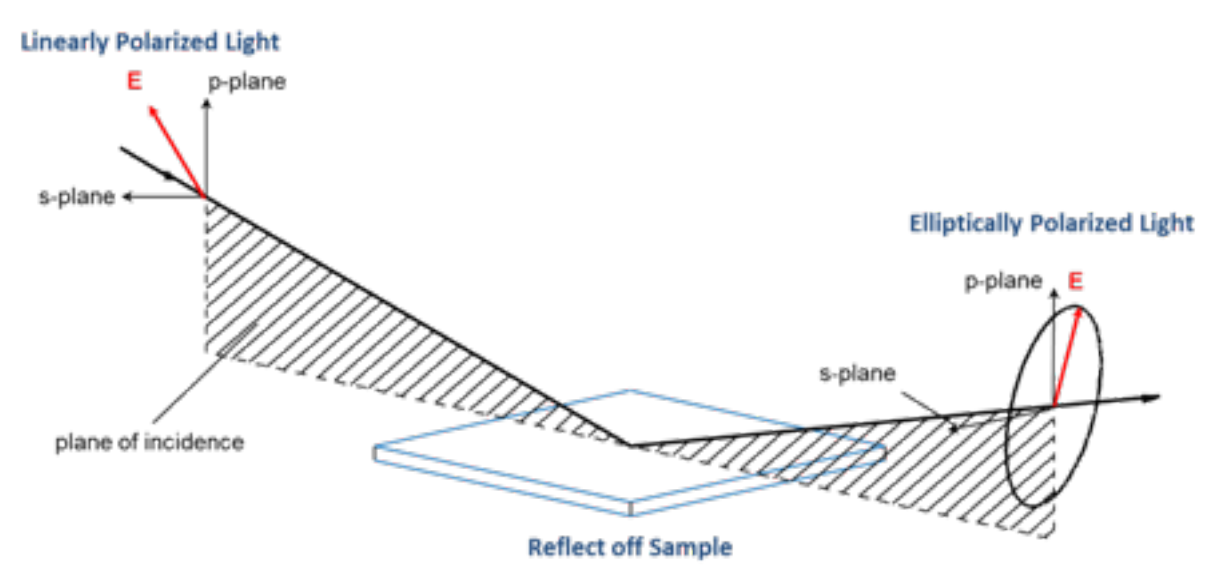


Figure 2.10. Schematic representation of ellipsometry where linearly polarised light is reflected off the sample and shifts to elliptically polarised light.[19]

The method was used by Polikreti who examined two different fresh varnishes using spectroscopic ellipsometry in order to determine whether they could determine their optical properties, their thicknesses and whether a distinction could be made between two different varnishes.[50] This technique shows promising results as it might be a non-destructive method to determine the varnish present on a painting which is useful for conservation and restoration purposes. The absence of pigment particles in the varnish, compared to paint, probably contributed to the promising results of this research. However, up until now the RI and thickness of actual paint layers have not been examined using ellipsometry.

#### Micro Spectrophotometer

As mentioned in section 2.1.3, absorption and reflection of an object influence the colour under which it appears to the observer, as the reflected wavelengths are registered by our eyes and brain. This wavelength dependent reflection and absorption can be measured using a spectrophotometer. For extremely small samples, for example paint samples, a micro spectrophotometer can be used to measure areas as small as 1 by 1  $\mu$ m.

A possible setup for a micro spectrophotometer is shown in Figure 2.11 where a spectroscopic segment is added to a regular microscope. The microscope with transmission illumination contains a condenser which focusses the light onto the sample from below. The microscopes objective is used to collect the light transmitted through the sample and focusses it on the spectrophotometer detector, which measures the absorption spectrum of the sample, i.e. the intensity of light transmitted through the sample per wavelength.[12]

Next to absorption measurements, reflection measurements can be done using a spectrophotometer as is done by Geldof to determine input parameters for the Kubelka-Munk theory discussed in section 2.4.1 to simulate the original appearance of the Field with irises near Arles painting by Van Gogh. The painting has degraded significantly over the past ninety years and the aim of the research was to digitally reconstruct the original appearance of the painting. Geldof calculated the absorption and reflection parameters of different mixtures of paint in order to extrapolate these and to determine what would have been the ratio of the original paint and what would therefore have been the appearance of the painting when it was just painted. [24]

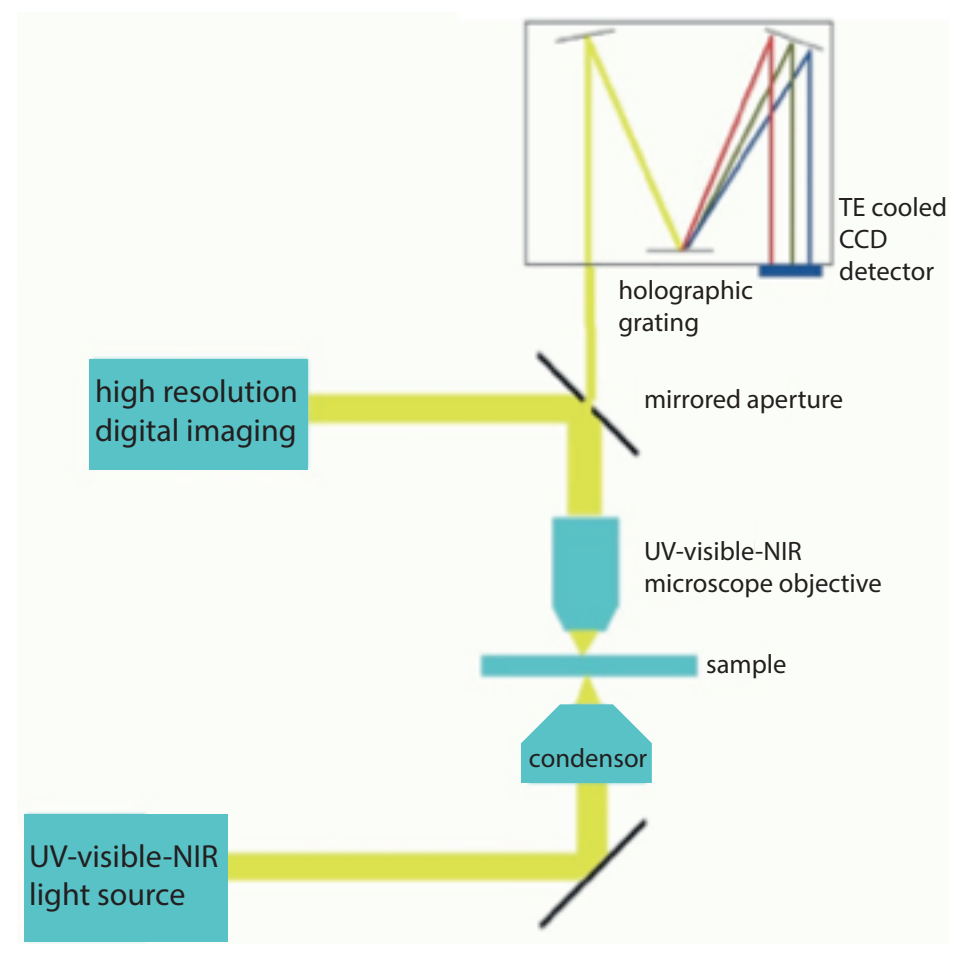


Figure 2.11. Schematic representation of a micro spectrophotometer.[12]

#### **BRDF** and Colour Measurements

The Bidirectional Reflection Distribution Function (BRDF) is a mathematical model to characterise the relation between the incident and reflected energy when light is incident on a surface. This technique is often applied for reflectance measurements on car paints to provide input for the animation of cars in for example car commercials.

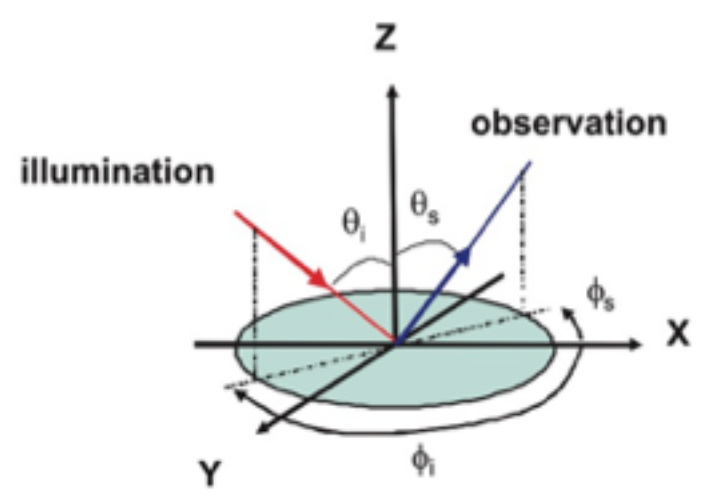


Figure 2.12. Schematic representation of the coordinate system showing the spherical coordinates for illumination and observation angles during BRDF measurements.[22]

The sample is illuminated with different wavelengths under illumination angles  $\theta_i$  and  $\phi_i$  and the reflected light is measured under the observation angles  $\theta_s$  and  $\phi_s$ . (Figure 2.12) to determine the spectral and angular intensity distribution of light reflected from the surface.

The angular distribution is an indication of the reflectivity at specific angles. Measurements of the spectral reflection and angular distribution of paint samples provide the parameters for calculating the BRDFs of the samples. [22][23][51]

The system described by Ferrero includes a spectrophotometer which can be used to determine the colour of a painted surface in the CIELab colour space as well as the BRDF.[23] Using this spectrophotometer, the a\* and b\* values can be determined and depending on these values the colour can be indicated on a diagram like the diagram in Figure 2.13.

The CIELab colour space is a way of representing colour on a 3-axis system. (Figure 2.13) The horizontal (a\*) axis displays a value of green and red and the vertical (b\*) axis displays the value of blue and yellow. The radius of the circle is an indication of the chroma of the colour, i.e. the level of colour in the sample. The smaller the radius, the paler the colour. The larger the radius, the brighter the colour. The L\* axis is the z-axis and is a measure of the lightness of the colour. A L\* value of 0 means black, the more this value increases, the lighter it is.[46]

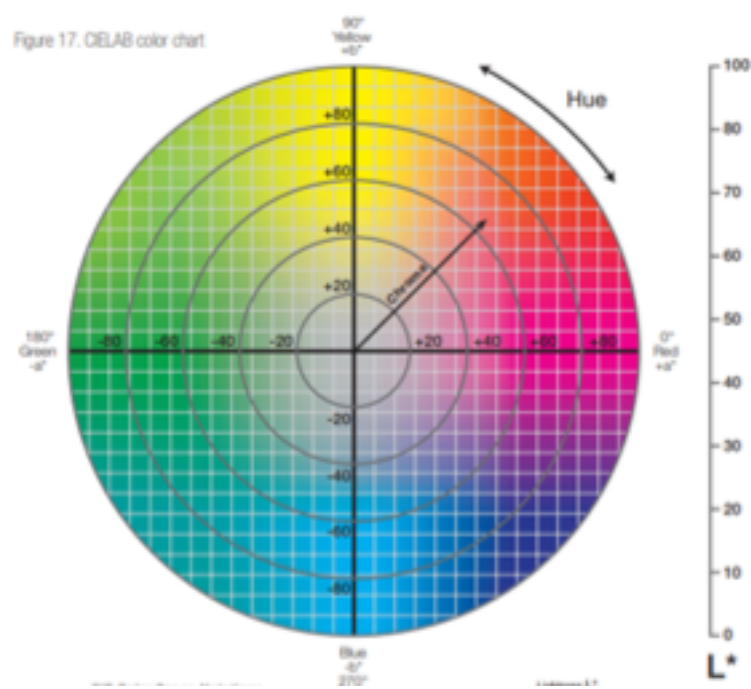


Figure 2.13. CIELab Colour chart a method to represent colour, towards +a\* is more red, towards -a\* is more green. The vertical axis, b\* indicates the level of yellow and blue. The radius of the circle determines chroma, level of colour, and the angle indicates the hue. L\* is an indication of the lightness where 0 means black and 100 means white.[46]

#### 2.3.2 - Acquisition of Data from Paintings

In recent years museums have increased their efforts to digitize their collections to make cultural heritage more accessible to the general public, e.g. for education, art historical research and conservation and restoration purposes. Currently paintings are mostly reproduced in 2D. A painting, however, does have a certain topography and is not completely flat. Next to the well-known 2D techniques as photographs and micrographic examinations, more advanced techniques are developed to include additional physical parameters to improve the accuracy of the reproduction. This data represents the 3D character of the paintings in a more precise manner and is at the moment mainly used as input for 3D printed reproductions. The data could also be used as input for a digital model of the painting. The measurement techniques discussed in this section focus on parameters such as colour, gloss, texture and translucency, which influence each other and the visual appearance of a painting (Figure 2.14).

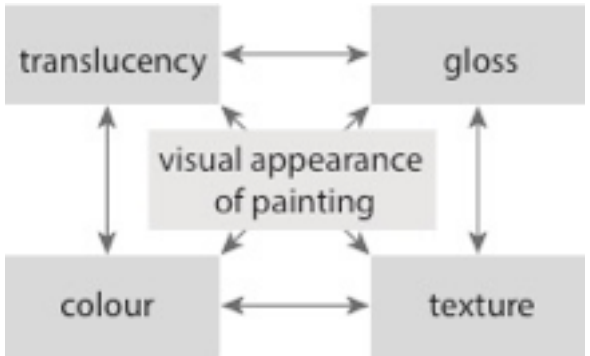


Figure 2.14. Relation of physical properties of a painting to each other and the visual appearance of a painting.

#### Texture

A hybrid system of a stereo vision camera rig with a projected fringe pattern was developed by Zaman to collect high resolution topography and colour data of a painting. The scanner provided the researchers with enough data to recreate paintings of Van Gogh and Rembrandt using a 3D printer of Océ.[64][65]

The reconstructions are created by a 3D printed relief print with the addition of one or several full colour ink layers on top of the relief. This leads to a print with minimal translucency and gloss variations, improvements in these areas will increase the quality of a reproduction of the original painting.

#### Gloss

Variations in gloss give a 3D print a more life-like appearance compared to a 2D poster. As gloss is mainly determined by specular reflection, Elkhuizen used a method in which an area of a surface is illuminated, and the reflected light is measured under the Brewster angle. At this specific angle, the specular reflected light is polarised which makes it possible to distinguish it from the unpolarised diffusely scattered light (Figure 2.15). Illuminating only a small patch of the surface and scanning the incident light beam makes the creation of a gloss map possible.[16][17] The data acquired by this scanning method may be used as input for a digital 3D model and - if combined with the optical properties of the paint - an indication can be made of how a 3D printed reproduction will appear before physically printing it.

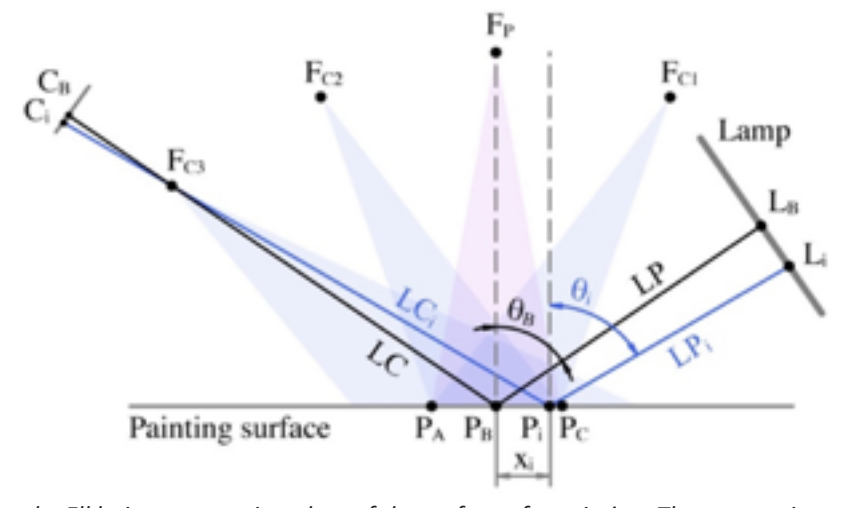


Figure 2.15. Setup of scanner by Elkhuizen measuring gloss of the surface of a painting. The camera is positioned at C on the left and a lamp positioned on the right. The Brewster angle is based on the averaged refractive index of oil paint and is used as the angle between line FpPB and LBPB.[16]

#### Internal Structures of Paint Layers

Optical Coherence Tomography (OCT) is a non-destructive analysis technique to analyse layered structures based on differences in light penetration. It has recently been applied in the field of fine arts by Cheung as well as Callewaert.[11][8]

In his method, a beam of light is split with one half being directed to a reference mirror and the other half to the sample. The scattering between the two beams is compared, which allows to determine the penetration depth of the light into the sample. Scanning the beam over the area of the sample results in a cross-sectional map representing the 3D build-up of the sample layers.[48]

OCT is usually applied in medical applications where it is for example used for the examination of eyes. The depth resolution of commercially available systems does not meet the accuracy required for the examination of the thin layers present in a painting. To accommodate for this, Cheung used ultra-high resolution Fourier domain OCT to examine the stratigraphy of the paint and varnish layers.

Because of its high dynamic range and depth selection capabilities it is a very sensitive technique for revealing preparatory drawings and the topography of the paint layers. The technique can be applied to investigate changes that occur in the ageing of a painting or the cleaning process in a case of restoration. Next to that, using OCT can help determining the layer thicknesses and topography of paintings.

Measurements were done by Callewaert on a volume of varnish to a depth of 19 millimeters.[7] During recent research on the Girl with a Pearl Earring, OCT scans were made of the painting by Callewaert. The scans provide information of the thicknesses of the paint and glaze layers present in the painting as well as the topography of the layers. These layers can be virtually separated when interpreting the OCT data. Due to the absorbance of the black layer in the background of the Girl with a Pearl Earring, no data can be retrieved from underneath that layer. A dark layer of paint is therefore a limiting factor in the use of OCT scans in the examination of paintings.

#### 2.4- Theoretical Description of Paint and Paint Layers

Theoretical descriptions of paint are for example used in the paint industry to describe and predict the optical behaviour of paint layers. The interaction between light and matter forms an important base for the theoretical models described in this section. These theoretical models should make it possible to predict the appearance of a 3D printed reproduction based on measured optical properties of paint in paintings and inks used for 3D printing.

#### 2.4.1 - Description of Theoretical Models

For this research, three leading models which describe the interaction between light and materials are considered;

- The Kubelka-Munk model, which is specifically designed to describe paint layers, including reflection, absorption and scattering,
- the Fresnel model describing the relation between transmitted and reflected light related by the refractive index and
- the Mie scattering model, which is a solution of Maxwells equations on particles with a size in the order of the wavelength.

In this section these three models are further described.

#### Kubelka-Munk

The Kubelka-Munk (K-M) theory is used to model the behaviour of light in multi-layer structures. The most simplified version of the K-M theory is based on the optical behaviour of a single layer on top of a substrate.

The incoming and outgoing flux of light on a surface is related by the albedo, i.e. the intensity of the incident light (i) multiplied with the albedo (H) of the surface equals reflected light (j). The reflectance of the substrate on which the paint is applied is given by  $R_{\rm g}$ . (Figure 2.16)

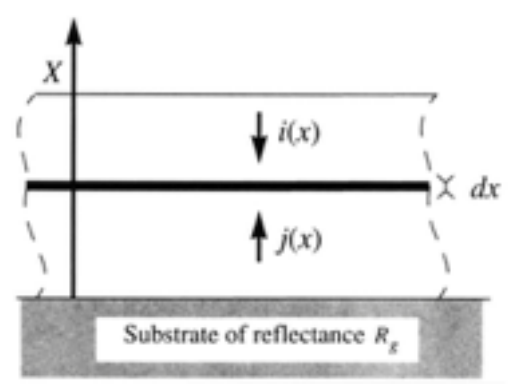


Figure 2.16. Schematic overview of light flux through material with i(x) the downward moving light at distance x from the surface, j(x) the light moving up at distance x from the surface. [20]

In a paint layer, at a point at distance x from the surface, the light fluxes going in (i) and out of the paint layer (j) are given by equation 2.2.

$$-di = -(r+s)i dx + r j dx$$

$$dj = -(r+s)j dx + r i dx$$
eq. 2.2

The absorption constant (s) and scattering constant (r) influence the portion of light being reflected and absorbed, respectively. The scattering constant is determined by the scattering properties of the pigment particles and the absorption constant is determined by the absorption of the bulk material which is mainly the binding medium of the paint.[37] For a thin enough layer, some of the light is passing through the investigated layer into the next. This flux of light through several layers is used for the prediction of the behaviour of a stack of materials.[37]

The classical version of the theory is applicable in the case of strongly scattering layers which are in optical contact with each other. The Kubelka-Munk model has been used by Geldof in the investigation of the original colour used by Van Gogh when painting his Field of irises in Arles.

To predict the measured reflection of the paint, an adapted version of the K-M theory (eq. 2.3), the Saunderson correction (eq. 2.4) was used.

$$R_{t} = \frac{(a+b)(a-b-R_{g})exp(-2bSD) - (a+b-R_{g})(a-b)}{(a-b-R_{g})exp(-2bSD) - (a+b-R_{g})}$$
eq. 2.3

$$a = 1 + \frac{K}{S}$$

$$b = \sqrt{a^2 - 1}$$

$$eq. 2.3a$$

 $R_t$  is the theoretical reflectance of the paint including the influence from the substrate. The thickness of the paint layer is given by D, S is the scattering parameter and K the absorption parameter.

$$R_m = \alpha k_1 + \frac{(1 - k_1)(1 - k_2)R_t}{1 - k_2R_t}$$
 eq. 2.4

$$\left(\frac{K}{S}\right)_{mixture} = \frac{c_1 K_1 + c_2 K_2 + \dots + c_N K_N}{c_1 S_1 + c_2 S_2 + \dots + c_N S_N}$$
 eq. 2.5

The measured reflection data was used as input for the relationship proposed by Duncan (eq. 2.5) to determine the reflectance factors of a mixture of N pigments with weight concentration c. This was used as a basis to determine the appearance of the original paint and create a digital reproduction of the original painting.[24]

Based on the Kubelka-Munk theory two-flux and four-flux models are designed to simulate the spectral behaviour of layered materials. A discrete version can be used in the case of a stack of non-scattering materials. This poses a limitation of the K-M theory, the layers within the stack need to be in optical contact in order for the model to work.

The classical and discrete versions are the most general of the theory. Four other versions meant for different stacks are discussed by Hébert.

- -The continuous-symmetrical version for cases of uniform scattering use the classical K-M formulas.
- -The discrete-symmetrical version created for stacks of identical layers which have the same reflectance on either face.
- -A discrete non-symmetrical version for stacks of identical layers with different reflectance on either face.
- -A continuous non-symmetrical version

for stacks of layers that have different absorption and scattering coefficients according to the forward and backward flux directions.

The accuracy of these generalised models still need to be tested with stacks of halftone ink layers.[28]

#### Fresnel

When a light wave travels from one medium to another, part of it is transmitted and another part is reflected. The Fresnel equations (eq. 2.6) relate the refractive indices and incident angle with the reflection and transmission of the light into a medium.

$$R_{s}(\theta) = \left(\frac{n_{1}\cos\theta_{i} - n_{2}\cos\theta_{t}}{n_{1}\cos\theta_{i} + n_{2}\cos\theta_{t}}\right)^{2}$$

$$eq. 2.6$$

$$R_{p}(\theta) = \left(\frac{n_{1}\cos\theta_{t} - n_{2}\cos\theta_{i}}{n_{1}\cos\theta_{t} + n_{2}\cos\theta_{i}}\right)^{2}$$

Rs and Rp are the reflection coefficients that correspond to the perpendicular and parallel directions to the surface.[16]

While the reflected light is always reflected at an angle equal to the incident angle (law of reflection), the transmitted light is bent, depending on the ratio of the refractive indices (Snells law, eq. 2.7).

$$\frac{n_2}{n_1} = \frac{\sin(\theta_i)}{\sin(\theta_t)} \quad \Rightarrow \quad \cos(\theta_t) = \sqrt{1 - \left(\frac{n_1}{n_2}\sin(\theta_i)\right)^2}$$
 eq. 2.7

When the refractive index of medium 1 (fast medium) is smaller than of medium 2 (slow medium) the angle of the transmitted light to the normal plane is decreased compared to the angle of incidence (Figure 2.17).

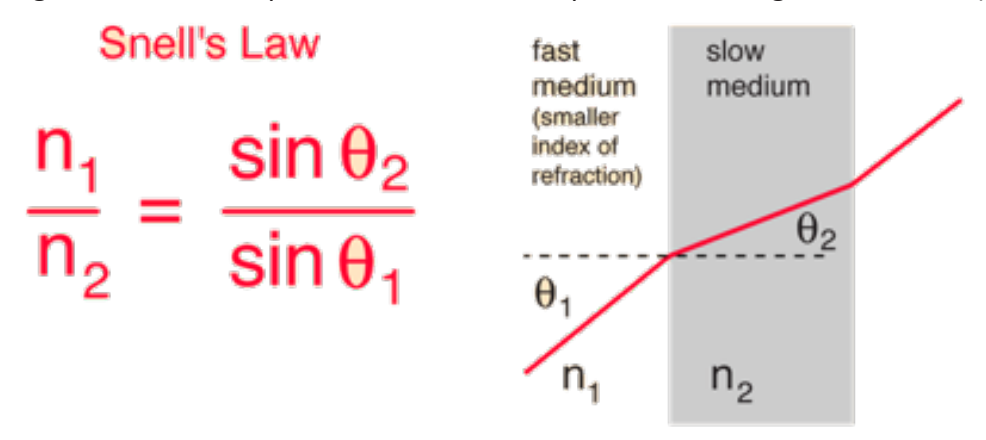


Figure 2.17. Snell's Law relating the refractive indices to the angles to the normal of the refracted beam. The fast medium 1 has a smaller refractive index compared to medium 2, resulting in a smaller  $\theta$ , compared to  $\theta$ , [47]

Snell's Law is derived from the Fresnel equations and can be seen as a simplified version of these equations, suitable for dielectric materials.[33][47] Elkhuizen used the Fresnel equations and the simplified Snell's law (eq. 2.7) to determine the Brewster angle during the gloss measurements of painting surfaces.

#### Mie Scattering

Light can be considered as an electromagnetic wave. When an object is illuminated by an electromagnetic wave, the wave excites electric charges in the object which causes an oscillation due to the interaction with the electric field of the incident wave. The oscillating charge scatters electromagnetic energy in every direction. Therefore, scattering can be seen as an interaction with particles causing a redirection of radiation from the original trajectory. Amongst others, reflection and refraction are forms of scattering. Next to scattering, absorption also attenuates a light beam.[63]

A model to describe the scattering of an electromagnetic wave is the Mie scattering model which is one of the solutions to Maxwell's equations. This theory specifically describes the scattering by a homogeneous spherical medium in which the wave travels at a different speed compared to the speed of the wave in the original material, i.e. materials with different refractive indices.[1]

Using the scattering of electromagnetic radiation, the Mie scattering model provides a basis for measuring the size of particles.[63] A particle much smaller than the wavelength of a light ray causes spherical scattering as is shown in Figure 2.18. Mie scattering occurs when the diameter of the particles is in the order of magnitude of the wavelength of light.[33]

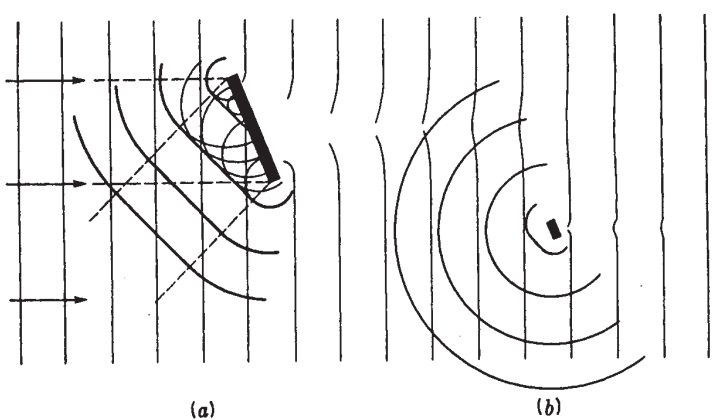


Figure 2.18. Reflection and diffraction of light by objects which are small compared to the wavelength of light.[33]

Joshi applied a multi-flux model based on Mie scattering to model optical properties of coloured pigmented paint films. The relation between the pigment particle size, the pigment particle distribution and reflection spectra is studied. A complex relation exists between the morphological characteristics of pigments and the colour the system exhibits.[35] Pigment particles are in the order of micrometers in size. This means that pigment particles are roughly around one order of magnitude larger than the wavelength of light and therefore spherical scattering might not occur.

#### 2.4.2 - Differences Between Theoretical Models and their Application

The theoretical models provide an indication of the appearance of the paint layers based on the measured optical parameters. This research focusses on the determination of the optical properties of paints as a base for the simulation of the paint and paint layers using render software. The theoretical calculation is useful to get an understanding of the significant parameters in the interaction of light with paint.

#### General Characteristics and Application to Paint

The Kubelka-Munk model is designed for the theoretical simulation of paint layers. Since the model is purpose built, it should be suitable for most paint layers and should also yield proper results in this case. It can be seen as a simplified version of Mie scattering and uses the absorption and scattering coefficients as input parameters. The Fresnel and Mie scattering models are a generic physical approach, based on fundamental optical

properties of the materials as input parameters.

For the Fresnel model the refractive index is used to calculate the reflected and transmitted light in a layered system. Scattering is not considered which means that scattering effects due to the presence of e.g. pigment particles in a paint layer are not considered. For a heterogeneous medium like a paint layer, this might pose a problem prohibiting the use of the Fresnel model. In the case of a homogeneous layer, as might be assumed for a glaze or varnish, the Fresnel model may be suitable to predict the properties of the layer.

While the Mie scattering model specifically does include particle scattering, as would be expected to be relevant in paint layers, the aforementioned work of Joshi has shown, that the relationship between the morphological characteristics of the pigment and the perceived colour are complex and go beyond the scope of this work.[35]

#### Application to Glaze Layers

A glaze is a special case of paint where pigment particles have dissolved into the binding medium. In this case the assumption can be made that there is no scattering taking place due to pigment particles in the glaze layer. The discussed theoretical models could be simplified for that reason. The equations discussed in the Kubel-ka-Munk section 2.4.1 apply to paint layers in which pigment particles cause scattering of the light. When considering the special case of a glaze where no scattering takes place, the scattering coefficient r in equation 2.2, can be considered zero. This leads to the set of equations in eq. 2.8 with i, j, s and x as in eq. 2.2. Integrating these equations leads to equation 2.9 for the albedo of a glaze layer.

$$-di = -sidx,$$

$$di = -sidx$$
eq. 2.8

$$H = H'e^{-2sX}$$
 eq. 2.9

H' in eq. 2.9 is the albedo of the substrate on which the glaze is applied and X is the thickness of the glaze layer. When considering the layered structure present in the background of Girl with a Pearl Earring the glaze layer is applied on top of a black underpainting. Due to the negative exponential in eq. 2.9, the albedo of the glaze layer applied on top of a substrate will be lower compared to the albedo of the substrate and therefore the glaze layer will appear darker compared to the black paint.[37]

#### Application to Rendering

Both the K-M and the Fresnel model have been used as a base for digital rendering of paints.[5][59] Most render engines are based on ray tracing where the light rays are traced back via a scene to the light source which often uses the Fresnel parameters as input.[52]

The K-M model yields in most paint simulations a reliable result, however, it is not always accurate enough. [59] The physical model used by the software for this work - path tracing - is a variation on ray tracing and provides the basis for the rendering of the layers in the background of *Girl with a Pearl Earring* in combination with the measured optical parameters, this will be discussed further in section 4.3.

As a means to check the performance of the render software, the resulting image could be compared to the original painting by eye or by using the measured parameters as input for the theoretical models to calculate the predicted appearance and compare this to the rendered result.

#### 2.4.3 - Conclusion

The Kubelka-Munk has proven to be a suitable model to describe paints and paint layers. It is, however, an approximation and therefore not accurate enough for simulation in render software. Considering the glaze layer, the Mie scattering model is complicated and not applicable in this situation because the assumption is made that in a glaze layer no scattering takes place. The Fresnel model is a suitable and accurate model for a homogeneous layer e.g. a glaze or a varnish layer. For heterogeneous paint layers the Fresnel model is less accurate since scattering caused by the pigment particles is not taken into account.

For heterogeneous paint layers, the K-M model should yield a reliable result when using it as a base for rendering. Rendering using the Fresnel model should give a good approximation of a homogeneous glaze or varnish layer. In the case of translucent materials, refraction could take place when light is incident on the material. When using ray tracing (discussed in section 4.2) for rendering, next to absorption and reflection the refraction taking place in translucent materials is taken into account. In that case Fresnel would lead to a more accurate approximation of the glaze layer compared to the K-M model.

### 3 - Experiment - Characterisation of Optical Properties

To determine the role of the glaze layer in the appearance of the painting, the optical properties of the paint are determined to serve as input for the computer model used in the second part of this research. Paint samples of the original painting *Girl with a Pearl Earring*, reconstructions with pigments similar to the pigments in the painting and reconstructions using modern store-bought oil paint (see Table 3.1) were analysed to retrieve optical properties of the paints.

Table 3.1. Overview of paint present in researched samples.

	Yellow	Blue	Black	Green
Original paint (OP)	Weld (substrate containing Ca and little AI) probably in linseed oil binding medium	Indigo probably in lin- seed oil binding medium	Mainly charcoal black, very little bone black probably in linseed oil binding medium	Glaze layer consists of mixture of weld, indigo and little red ochre
Reconstruction with pigment similar to pigments in painting (RU)	Weld with CaCO3 -potash substrate mixed with hot bodied linseed oil	Indigo tinctoria in heat bodied linseed oil	Charcoal black of beech with heat bodied lin- seed oil	Approximately 30:1 and 20:1 mixed weld and indigo
Reconstruction with sto- re-bought paint (RM)	Stil de grain from Rem- brandt series (Talens)	Indigo from Rembrandt series (Talens)	Ivory black from Rem- brandt series (Talens)	About 3:1 mixed stil de grain and indigo

The input parameters for the Mitsuba render engine are the absorption and refractive indices of the different layers in the 3D model and the Bidirectional Reflectance Distribution Function (BRDF) of the painted surfaces. The first renders could be made with assumed values, but to test the physical model of the render software, measured values of original paint samples are needed to compare the visual appearance of the render with that of the original painting. The creation of the 3D model and render model is discussed in Chapter 5 in the second part of the experiment.

#### 3.1- Assumptions made within Experiment

The research done by Groen was mainly qualitative to determine the different components that make up the paints and glaze in the *Girl with a Pearl Earring*. This research however, was not a quantitative analysis which means that the exact compositions of the paint and glaze in the original painting were not determined.[25] Because the quantitative compositions of the original paint and glaze are not known, several assumptions needed to be made when creating the reconstructions.

The black underpainting in the background of Girl with a Pearl Earring consists of charcoal black and a very limited amount of bone black. The assumption is made that the underpainting only consists of charcoal black, therefore, the reconstructions of the black underpainting are made with charcoal black. The main components of the glaze are weld and indigo, the exact amount of red ochre and drying agent (copper) present in the glaze is unknown. The reconstructions are therefore made with only weld and indigo in different ratios to approach the colour of the glaze. The small amount of aluminium present in the glaze indicates a mordant made with a mixture of chalk and aluminium, probably 5% aluminium potash and 95% chalk. [42] Because the main ingredient is chalk, the weld reconstruction is created with a chalk mordant with a small addition of potash. The ratio of yellow to blue paint in the reconstructions is done by eye because the pigment ratio of the original glaze is unknown.

#### 3.2- Paint Samples

Two available samples of the background of the original painting Girl with a Pearl Earring are a thin section stuck to a microscope slide with tape and a dispersion of the paint between a microscope slide and cover slide. Measurements of optical properties are also done on the two types of reconstructions. The preparation of the reconstructions is discussed in Appendix A.

#### 3.2.1 Samples from the Original Painting

During the previous and current research on Girl with a Pearl Earring [25][57] samples have been taken from



Figure 3.1. Overview of samples available of the painting.[57]

the painting (Figure 3.1). Sample 19 (OP 19) in the bottom right corner is taken from the background in '94-'95 to answer specific research questions. The sample is preserved in the form of a dispersion between a microscope slide and cover slide. A microscope image can be seen in Figure 3.2. Sample 26 (OP 26), left of the forehead, was taken from the varnish on the painting during the research in '94-'95 and is from an unknown location in the background of the painting. This sample is a thin section of a cross section and adhered to a piece of white tape. (Figure 3.3) Both samples show the charcoal black underpainting with on top of that the glaze layer. Sample OP\_19 contains another layer on top of the glaze layer, this could be varnish or dirt. The separation of top layer and the paint layer underneath is often due to the ageing of the varnish layer. The glaze layer in sample OP 19 is mainly yellow in appearance, there are some darker areas visible in the middle of the glaze layer. These might have a higher indigo content; however no clear pigment particles are visible in the sample.

The glaze in sample OP\_26 appears even more homogeneous compared to that in sample OP\_19. The thickness of the glaze layer in sample OP\_19 is between 21 and 26  $\mu$ m and the glaze layer in OP\_26 has a thickness of around 25  $\mu$ m. This is similar to the thickness in sample 26 discussed in section 2.2.

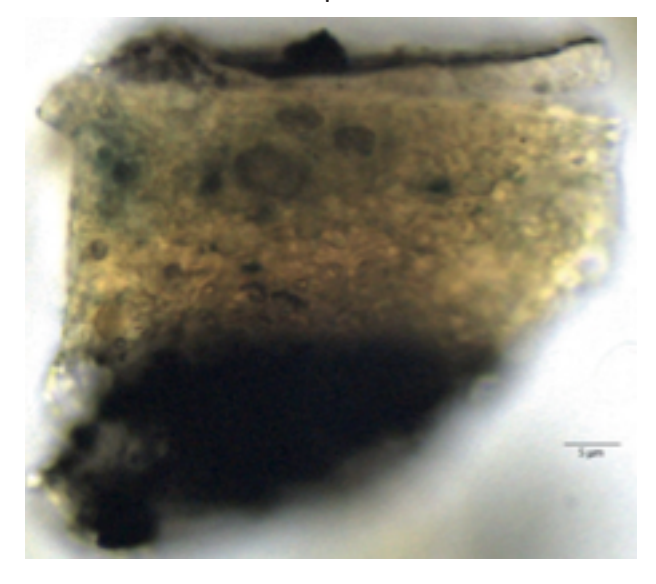


Figure 3.2.Dispersion of background sample 19 (OP\_19) from Girl with a Pearl Earring. On the bottom of the image the black underpainting can be seen, on top of that the glaze layer and on top of that the varnish layer, 40x magnification.

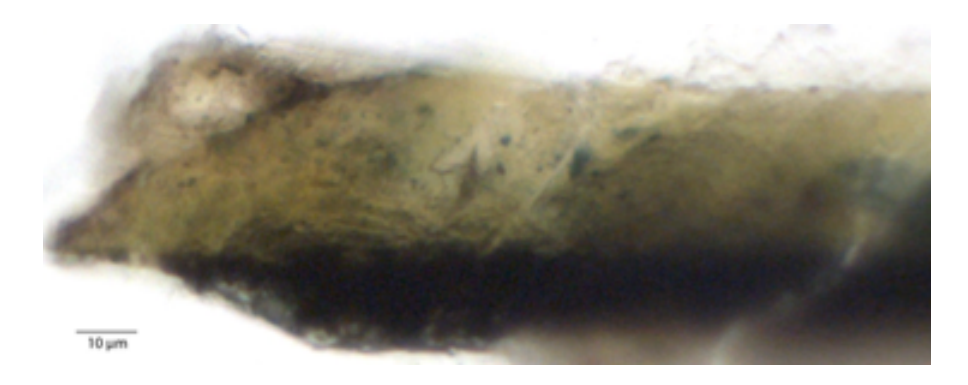


Figure 3.3. Thin section of background paint sample 26 from Girl with a Pearl Earring attached to a piece of tape. On the bottom the black underpainting and on top of that the glaze layer, 40x magnification.

#### 3.2.2 - Reconstructions with Pigments Similar to Pigments in Original Painting

The first set of reconstructions was made with pigments which are similar to the pigments that were found during examination of Girl with a Pearl Earring.[25] The reconstructions were made in corporation with Fahed Ibrahim, a Technical Art History student at the University of Amsterdam. The pigments were ground with linseed oil to form the paint. The ingredients used are listed in Table 3.1, the recipes and further description of the making of the reconstructions can be found in Table A1.1 of Appendix A. The paint was applied on microscope slides (Figure 3.4), microscope cover slides, opacity charts and a single crystal silicon wafer. The set of paints was used to recreate the layers present in the background of the painting.

The charcoal black layer represents the underpainting layer in the original painting. The glaze layer is reconstructed by a mixture of weld and indigo. The mixture of weld and indigo is a simplified version of the glaze in the original painting. Groen states that the glaze of sample 26 contains not only weld and indigo but also small amounts of chalk and red ochre.[25] The chalk most likely originates from the weld as it is probably used as the mordant for the yellow pigment. The red ochre is left out in the reconstruction since it is only present in a very small amount. The weld and indigo are mixed in approximately 30:1 and 20:1 ratios to create the layer that represents the translucent green glaze layer in the original painting. (Figure 3.4) Since the exact ratio of the weld and indigo in the original samples is unknown, these ratios are an estimation done by eye.

Application of the paint is done using a drawdown bar, a brush and with a spatula. (Figure 3.4) The paint applied with the drawdown bar is  $50~\mu m$  thick, twice the tickness of the glaze layer in the original sample. Indigo tinctoria is used as pigment for the indigo, it is a little more opaque compared to genuine indigo. Indigo tinctoria is the most historically correct indigo and the available raw pigment was easier to work. However, the transparency was an important factor of the glaze layer, the workability of the raw pigment was leading in this case. Mixing the indigo with weld resulted in a translucent green glaze (Figure 3.4).

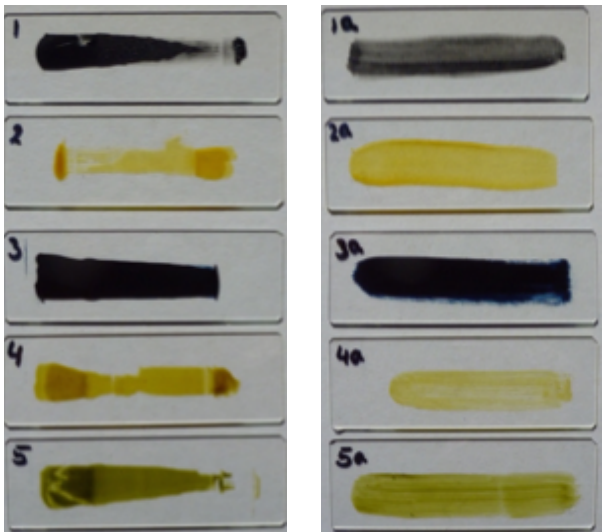


Figure 3.4. Reconstruction paint outs created with pigments present in the original painting. Left column applied using a drawdown bar ( $50\mu m$ ) and right column applied with a brush. 1 and 1a are charcoal black, 2 and 2a are weld, 3 and 3a are indigo, 4 and 4a are a roughly 30:1 mixture of weld and indigo, 5 and 5a are a roughly 20:1 mixture of weld and indigo.

#### 3.2.3 - Reconstructions with Modern Paint

The second set of reconstructions is made with store-bought modern oil paint from the Rembrandt series of Talens (see Table A1.2). Paint outs are made with yellow, blue and black on microscope slides (Figure 3.5), cover slides, single crystal silicon wafer, a canvas board and on a transparent plastic film. As the reconstructions with the original pigments, this set of paints is also used to recreate the different layers in the background of the original painting. The ivory black represents the underpainting layer, the stil de grain and indigo are mixed in a 3:1 ratio to create the translucent green glaze layer. The ratio is based on the colouring strength of indigo compared to stil de grain. To influence the transparency of the glaze, extra linseed oil is added to several of the reconstructions. The application of the paint is done using a spatula and a thin as possible layer is applied.



Figure 3.5. Reconstruction paint outs created with modern paints from the Rembrandt series created by Talens. 18) Ivory black, 4) Stil de grain, 5) Indigo, 7) 3:1 mixture of Stil de grain and Indigo. The samples are applied using a spatula.

#### 3.3- Measurement of Optical Properties

The three sets of samples discussed above have been analysed to determine optical properties needed as input for rendering. An overview of which analysis is done on which sample can be found in Table 3.2. Absorption measurements using a micro spectrophotometer is done on reconstructions on microscope slides. The BRDF measurements are done on a set of reconstructions applied on Leneta opacity charts of type 2A2 and 5C (Figure 3.8), microscope slides and canvas board which is a piece of canvas applied on wood.

Table 3.2. Overview of optical analysis of samples. In the case of BRDF measurements, it is also indicated on which substrate the paint was applied. Opacity Chart (OC) (black (b), white (w) or both), Microscope Slide (MS) or Canvas Board (CB).

Sample name	Sample description	Optical microscopy	Absorption (micro spectrophotome-ter)	Ellipsometry	BRDF
OP_19	Original Painting (OP) dispersion, bottom right corner, property of Mau- ritshuis (sample 1687-19, 4048 A)		Dispersion		
OP_26	Original Painting thin section, left from forehead, property of Mau- ritshuis (sample 1687-26, 4054 B)		Thin section		
RU_1	Reconstruction UvA (RU) Charcoal black				OC2w
RU_2	Weld		MS		OC2w, OC5b
RU_3	Indigo		MS		OC2
RU_4	Weld and Indigo mixed (ratio 30:1)		MS		OC2, MS
RU_5	Weld and Indigo mixed (ratio 20:1)		MS		OC5, MS
RM_1	Reconstruction Modern paint (RM) Ivory black				СВ
RM_4	Stil de grain with added linseed oil		MS		
RM_5	Indigo with added linseed oil		MS		
RM_6	Stil de grain and Indigo mixed (ratio 3:1)		MS		CB, MS
RM_7	Stil de grain with added linseed oil and Indigo with added linseed oil mixed (ratio 3:1)		MS		

#### 3.3.1 - Ellipsometry

Ellipsometry measurements can provide the complex refractive index and thickness of a material. Both types of reconstructions were applied on top of the single crystal silicon wafer which is polished on one side with an oxide layer applied on top of the wafer. The characteristics of the wafers are well known within ellipsometry measurements; therefore, the measured paint characteristics can be well distinguished from the properties of the wafer. Application was done using a spatula to create an as thin as possible paint layer. A layer thicker than 5 µm is considered bulk in ellipsometry measurements.

Several test measurements are done to test the possibility of determining the refractive index of paint using this technique. Measurements are done on sample RM\_2 using a J. A. Woollam RC2 ellipsometer with a wavelength range of 210 nm to 1690 nm. In steps of 5° measurements are done from 50° to 70°. The measured spectrum is analysed using the process steps shown in Figure 3.6 where a standardised model is fitted to the experimental data in order to determine both the regular and complex part of the refractive index.[18]

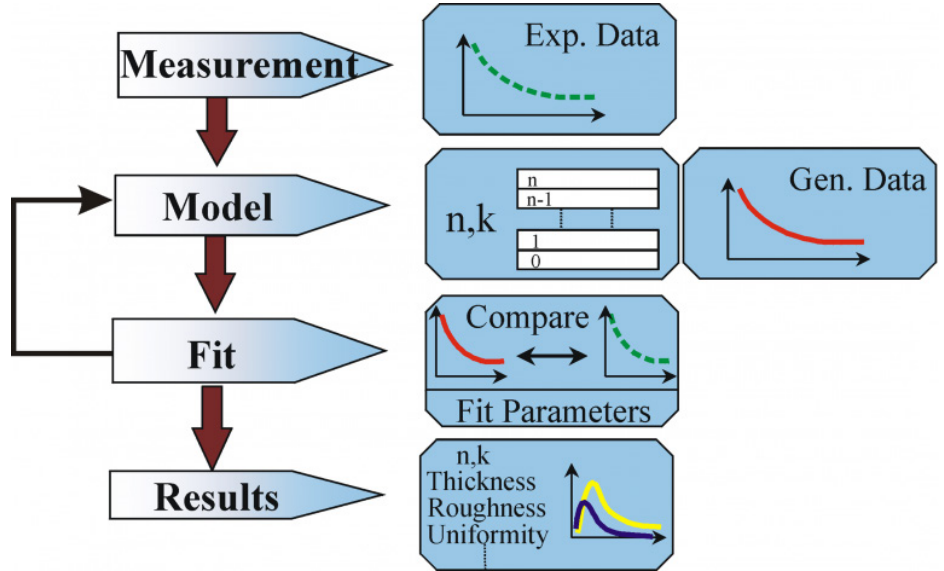


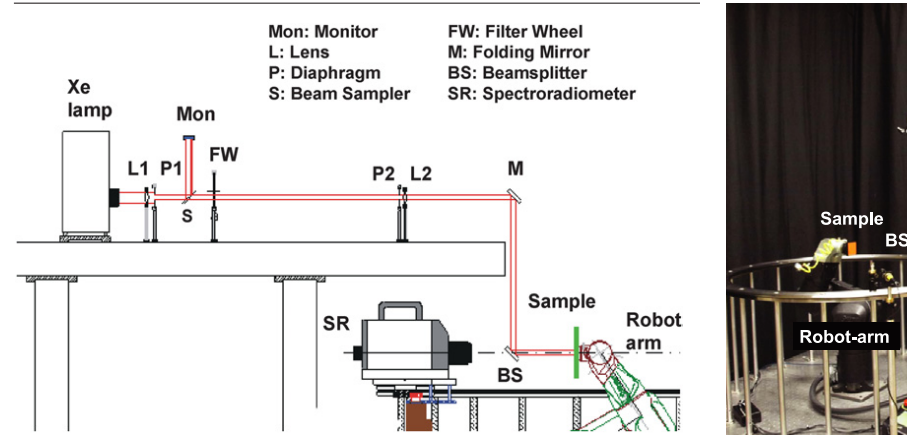
Figure 3.6. Schematic representation of the process of ellipsometry measurements from measurement through fitting of a model to the results.[18]

#### 3.3.2 - Micro Spectrophotometry

The samples from the original painting are too small to get absorption spectra of the individual paint layers when using regular spectroscopy devices since the resolution of these devices are around 1 mm by 1 mm. Therefore, micro spectrophotometry is done to determine the absorption of micrometer scale samples. A micro spectrophotometer can measure up to a resolution of 1  $\mu$ m by 1  $\mu$ m. Due to its high resolution, micro spectrophotometry is a suitable technique for measuring the absorption of the individual paint layers. The measurements are performed using a Craic QDI 302 micro spectrophotometer. Two different diaphragms are used resulting in measured areas of 2.5  $\mu$ m by 2.5  $\mu$ m and 5  $\mu$ m by 5  $\mu$ m. The measurements were done in transmission with the sample located between the light source and the detector. The light source is a Carl Zeiss VIS-LED emitting light with wavelengths between 400 and 700 nm with a peak at 460 nm. The absorption spectra are measured in the visible spectrum from 380 nm to 800 nm and at room temperature. The analysed samples are listed in Table 3.2. Before each measurement a reference spectrum is measured next to the sample for example on the microscope slide. This reference spectrum is subtracted from the measured paint spectrum by the software, with the result that the exported spectra are the absorption spectra of the paint samples.

#### 3.3.3 - BRDF Measurements

BRDF measurements are been done on a selection of paint reconstructions, indicated in the right column of Table 3.2. The measurements are done at the Spanish Council for Scientific Research's Optics Institute (IO-CSIC) in Madrid using the setup shown in Figure 3.7. The left image of Figure 3.7 shows a schematic representation of the setup with the xenon light source on the left. The light beam is directed through a set of lenses, diaphragms and a filter wheel towards mirrors in a periscope setup and the sample on the right side of the figure. The sample is attached to a robot arm by a vacuum suction mechanism which makes it possible to move the sample in every direction.



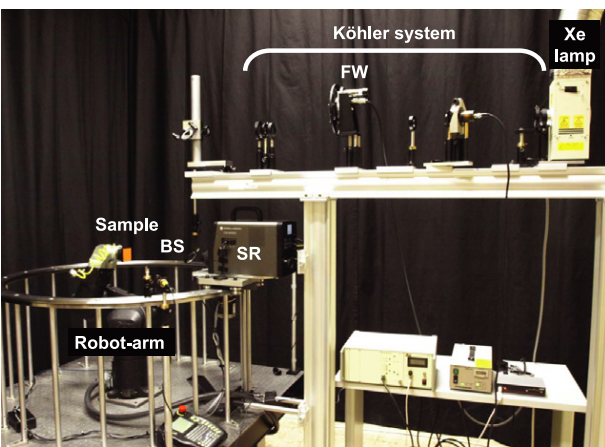


Figure 3.7. Left: Schematic representation of the setup for BRDF and spectral reflection measurements. [51] Right: Setup of system for BRDF and spectral reflection measurements. The light source is located at the top right corner, the sample is attached to the robot arm on the left of the image. [21]

-24-

The ring construction around the robot arm (see Figure 3.7 right) is a cogwheel on which the Konica-Minolta CS-2000 spectroradiometer is moved around to measure the spectral radiance in the visible range (380 nm to 780 nm) with a bandwidth of 5 nm.

The measurements are mainly done on the reconstructions applied onto the opacity charts (Figure 3.8). The BRDF is measured as a function of wavelength and angular distribution. Next to that the radio spectrophotometer measures the CIELab colour distribution of the sample. The angles under which the data is measured are listed in Table 3.3. The illumination angle is varied between 15°, 45° and 75° and for each illumination angle the observation angle is varied from 0° to 75° at 5° intervals. The 0° observation angle is perpendicular to the surface of the painted surface. The used angles result in 96 geometries or variables.

Table 3.3. Overview of used geometries in BRDF measurements. For each illumination angle, the observation angles are varied from  $0^{\circ}$  to  $75^{\circ}$  in steps of  $5^{\circ}$  with  $0^{\circ}$  perpendicular to the surface of the measured object.

			'													
Illumination angle $(\theta_i)$	15°	45°	75°													
Observation angle $(\theta_r)$	0°	5°	10°	15°	20°	25°	30°	35°	40°	45°	50°	55°	60°	65°	70°	75°
Illumination angle $(\phi_i)$	0°															
Observation angle $(\phi_r)$	0°	180°														



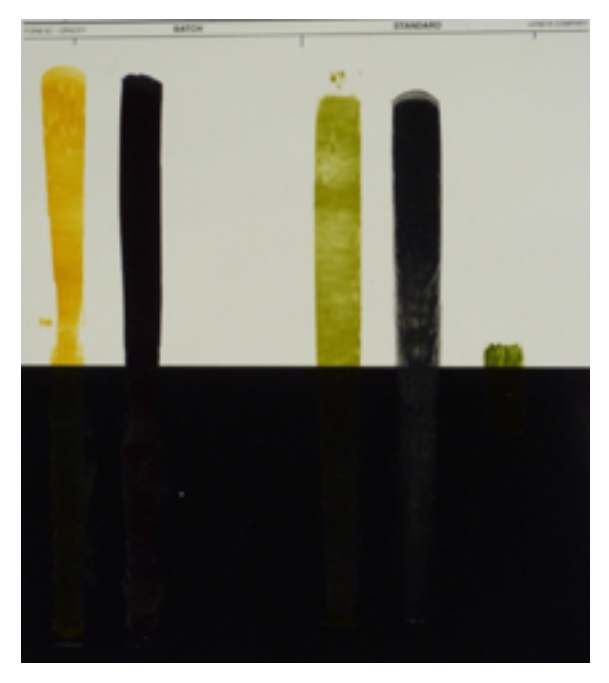


Figure 3.8. Reconstructions created using pigments found in the original painting. Left image Leneta Opacity Chart N2A-2 unsealed. Paint is applied with a drawdown bar ( $50\mu m$ ). From left to right: Weld ( $RU_2$ ), Indigo ( $RU_3$ ), Weld and Indigo mixed (30:1 ratio) ( $RU_4$ ), Charcoal black ( $RU_1$ ).

Right image Leneta Opacity Chart 5C, first 4 paints are applied with a drawdown bar (50μm), right paint applied with a brush. From left to right: Weld (RU\_2), Indigo (RU\_3), Weld and Indigo mixed (20:1 ratio) (RU\_5), Charcoal black (RU\_1), Weld and Indigo mixed (20:1 ratio) (RU\_5).

#### 3.4- Results

The results of the ellipsometer, absorption and BRDF measurements done on the paint samples are described in this section.

#### 3.4.1 - Ellipsometry Measurements

The ellipsometry measurements are done on sample RM\_2 applied onto a single crystal silicon wafer using a spatula. For ellipsometry measurements a layer thicker than a few microns is considered bulk, therefore the paint sample is very thick compared to the layers usually analysed using ellipsometry. Unfortunately, the intensity of the light on the detector is too low for the ellipsometer to measure the refractive index of the paint

sample. More tests need to be done on even thinner paint samples in order to get reliable results.

#### 3.4.2 - Absorption Measurements

Absorption spectra of a selection of samples are measured. The samples of the original painting and the yellow, blue and green reconstructions are studied using the Craic micro spectrophotometer. The measurements are done from 380 nm to 800 nm, due to the noise on the lower side of the spectrum, the spectra shown here run from 400 nm to 800 nm. The absorption spectrum of the stil de grain modern yellow paint is shown in Figure 3.9. A clear and broad peak is visible around 425 nm, the remaining spectrum is relatively flat with some noise at the edges of the measured spectrum.

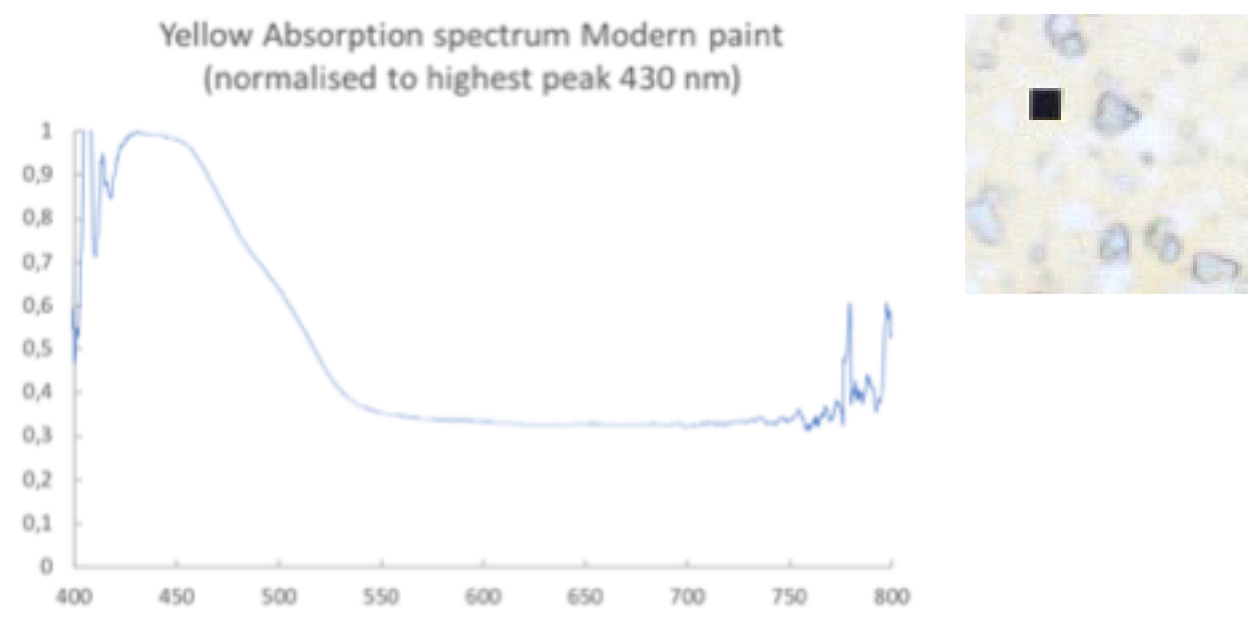


Figure 3.9. Absorption spectrum of the Stil de grain modern paint reconstruction, clear peak around 425 nm. Right a microscope image, the spectrum is measured in a yellow area. The size of the black square is 5  $\mu$ m by 5  $\mu$ m. The spectrum is normalised to the highest measured value.

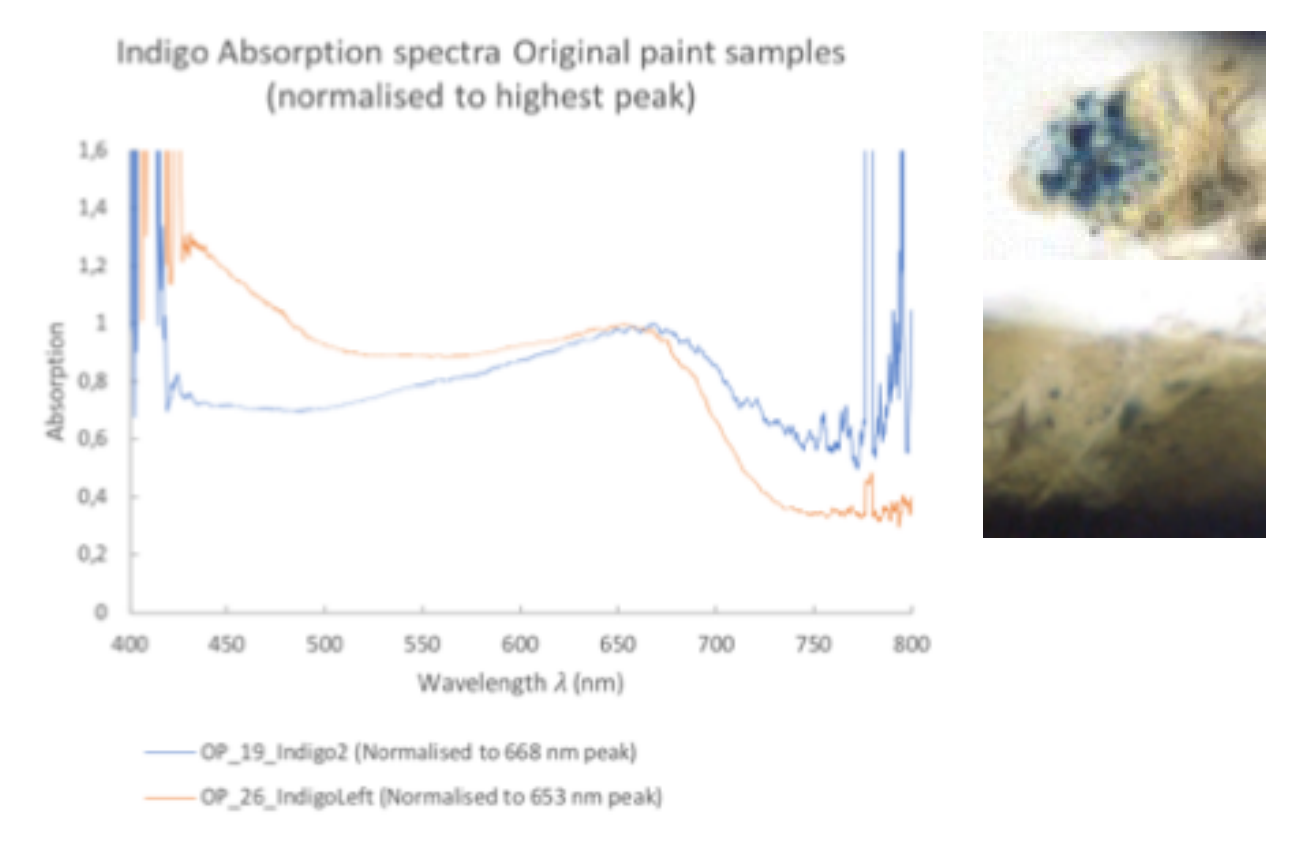


Figure 3.10. Absorption spectra of the indigo pigment in samples of the original painting. A bump around 660 nm indicating the indigo pigment. Right microscope images of the measurement locations, top image is the indigo cluster in OP\_19, bottom image OP\_26 where the measurement is done in the darker spots. The spectra are normalised to the indigo peak at 660 nm.

The absorption spectra of indigo pigments in the samples of the original painting are shown in Figure 3.10. The measurements are done on an indigo pigment cluster, sample OP\_19, below the cross section in Figure 3.2 and on the darker areas in sample OP\_26. A clear broad peak is visible around 660 nm indicating the indigo pigment. A peak is also visible at 430 nm in the spectrum of sample OP\_26, this is an indication of the yellow (weld) pigment which means the dark areas in OP\_26 are a mixture of weld and indigo.

Absorption measurements on the different indigo pigments result in the spectra in Figure 3.11. Both spectra of the reconstructions show a lot of noise especially towards the larger wavelengths. The indigo peaks of the reconstructions are shifted compared to the original samples and show a lot of noise within the spectrum. The peak of the MP\_5 reconstruction is around 620 nm and the peak of the RU\_3 reconstruction is around 600 nm. As with the other spectra, a lot of noise is also visible at the edges of the measured spectra. The differences in relative absorption around 430 nm indicate the changing amount of yellow pigment present in the paint samples. Since the measurements of the original samples are done on mixed paint, more yellow pigment is present in these areas compared to the reconstructions created from only indigo pigment.

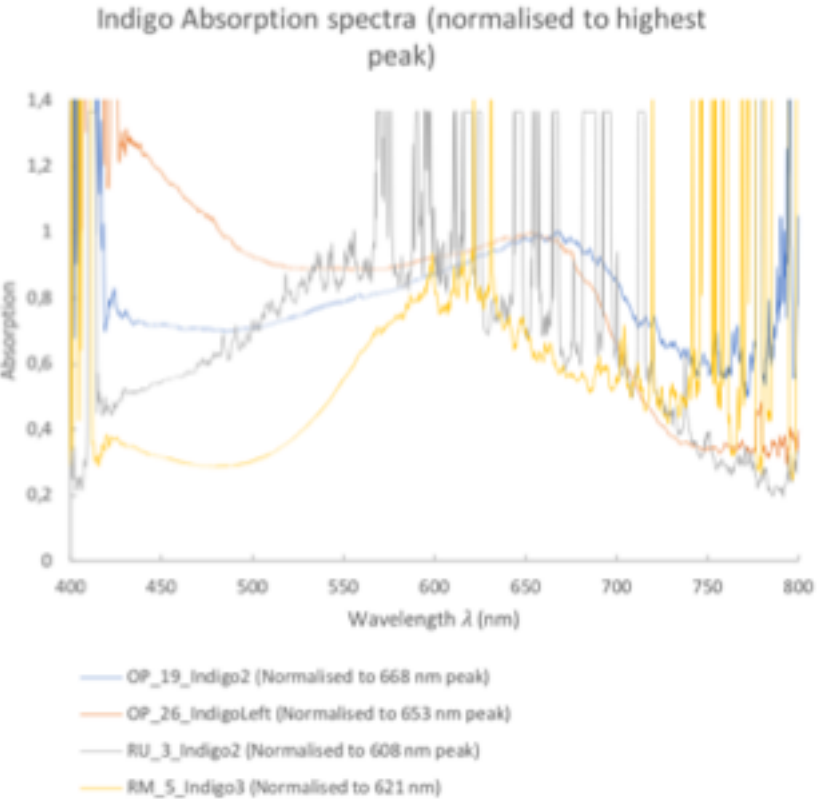


Figure 3.11. Absorption spectra of the indigo pigments in OP\_19, OP\_26, RU\_3 and RM\_5. The spectra are normalised to the blue pigment peak. A lot of noise is visible in the spectra of the reconstructions.

The individual yellow and blue spectra can be added to form the spectra of the green glaze. Absorption spectra of the green glazes in samples OP\_19, OP\_26, RU\_5 and RM\_7 are measured to compare the absorption peaks for the green glazes. (Figure 3.12) It can be seen that all four samples show a significant peak for the yellow pigment around 430 nm. The width of the peaks differs per sample with the RU\_5 spectrum narrow and the RM\_7 spectrum broad compared to the OP spectra. The blue and yellow lines in Figure 3.12 indicate the absorption spectra of the glaze layers in OP\_19 and OP\_26. When normalised, the lines follow the same trend and show peaks at the same wavelengths. As in Figure 3.11, the peaks of the indigo in RM\_7 and RU\_4 are clearly shifted compared to the peaks of the samples of the original painting. The paint created together with Fahed Ibrahim are shifted around 25-30 nm to the higher part of the spectrum. The Indigo in the modern paint is shifted relatively far to the left, around 40-45 nm compared to the indigo in the original painting. The shift of the indigo peak of the RU\_4 reconstruction is towards the larger wavelength, this is different from the shift visible in Figure 3.11.

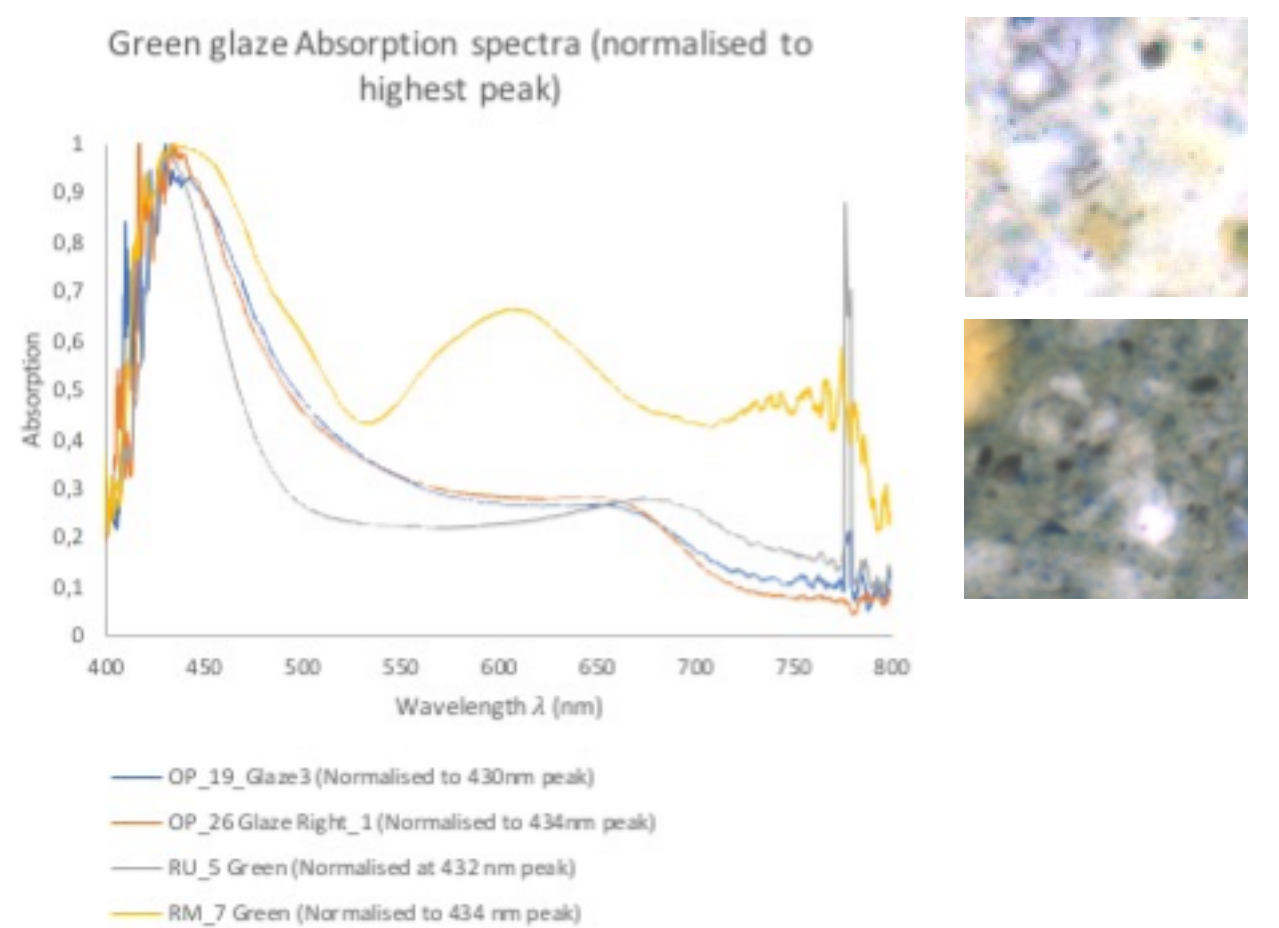


Figure 3.12. Absorption spectra of the green glazes in OP\_19, OP\_26, RU\_5 and RM\_7. The spectra are normalised to the yellow pigment peak. Much noise is visible at the edges of the spectra of the reconstructions. Top right RU\_5 an bottom right RM\_6.

#### 3.4.3 - BRDF Measurements

BRDF measurements are done on the two sets of reconstructions to determine the spectral reflectance distribution, the angular reflectance distribution and CIELab colour distribution. The analysed samples are indicated in Table 3.2. The measurements have been done on the paints on different substrates, the white and black areas of opacity charts, on microscope slides and on canvas board. Figure 3.13 shows the spectral distributions of the green glazes RU\_4 and RU\_5 on both the black and white part of two opacity charts. It can be observed that the reflectance of the paints on the white substrate is roughly 1.5 order of magnitude higher compared to the reflectance of the paints on the black substrate. Dips are present in the spectra around 420 nm and around 670 nm, this matches the observations of the absorption spectra in section 3.4.2. The spectrum of the darker green RU\_5 on the white substrate shows a larger dip in around 670 nm compared to the lighter green RU\_4 spectrum.

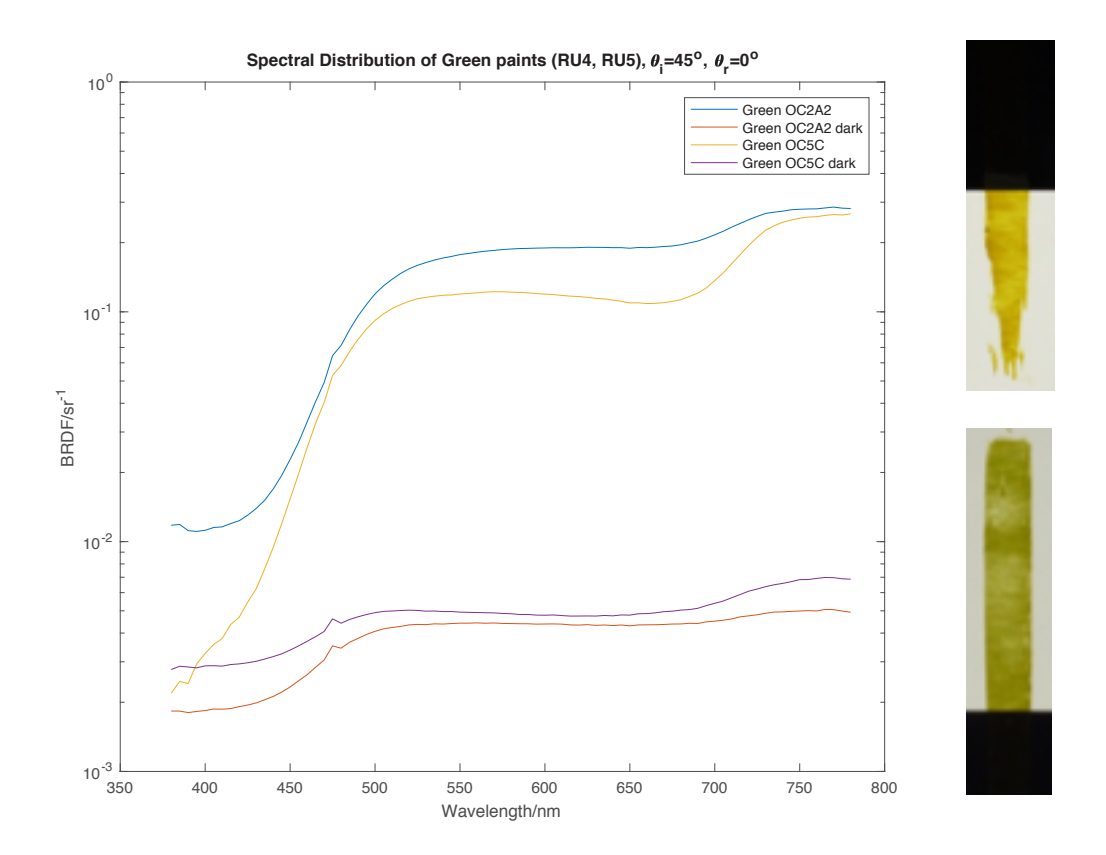
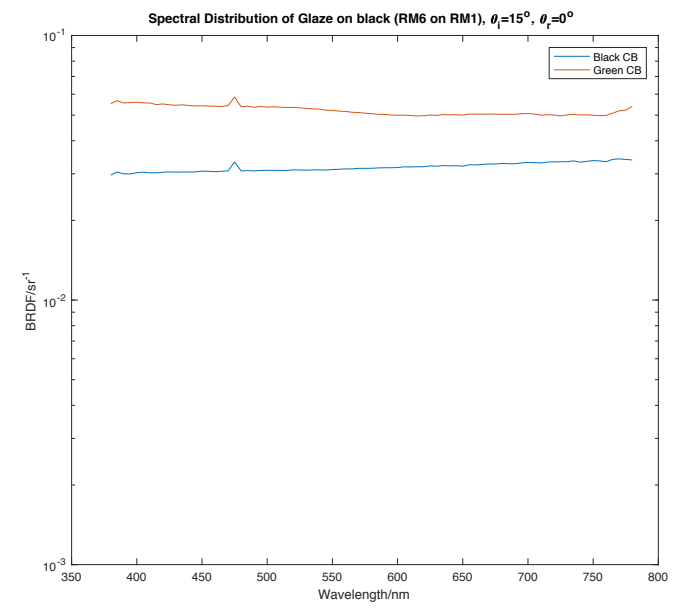


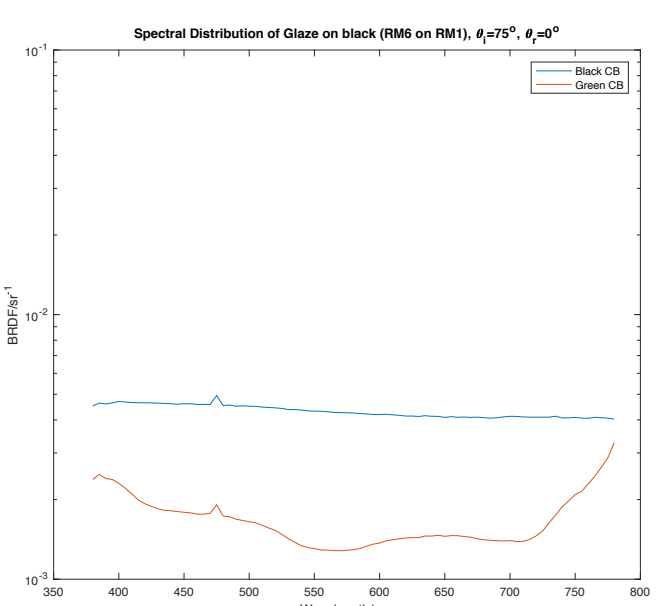
Figure 3.13. Spectral distribution of the reconstructions RU\_4 and RU\_5 applied using a drawdown bar on opacity charts 2A2 (RU\_4) and 5C (RU\_5). The graphs indicated with 'dark' in the legend are of the paints applied on the black areas of the opacity charts. Top right: sample RU\_4 on opacity chart 2A2, bottom right: sample RU\_5 on opacity chart 5C. The incident angle ( $\theta_i$ ) is 45° and the observation angle ( $\theta_i$ ) is 0°.



Figure 3.14. Left: Canvas board with on the left ivory black (RM\_1) applied with a spatula and in the middle green glaze (RM\_7) applied on top of the ivory black paint, again with a spatula. Incident diffuse light at approximately  $45^{\circ}$  and the observation angle is  $0^{\circ}$  (normal to the plane). Right: The observation angle in each image is  $45^{\circ}$ , the angle of the directional incident light with theviewing angle is  $a_0^{\circ}$ ,  $a_$ 

The spectral distribution of the green glaze (RM\_7) on top of a black layer of paint (RM\_1) applied on a canvas board (Figure 3.14) is compared to the spectral distribution of the black layer without the green glaze for  $\theta_i$  = 45° and  $\theta_r$  = 0°. (Figure 3.15, top right) The intensity of the reflection (BRDF) measured is an indication of how dark the painted surface is perceived. In Figure 3.15 it is visible that the reflected intensity of the black paint is about half an order of magnitude higher than the reflected intensity of the green glaze applied on top of the black paint. This suggests that the black paint appears darker when a green glaze is applied on top of it. When considering the glaze layer on the black paint in Figure 3.14, looking at the painted surface at an observation angle of 0° (along the surface normal) with light incident at an approximate angle of 45°, the glazed area appears darker compared to the black paint without glaze. The lighter areas on the glaze layer is caused by specular reflection from the surface.





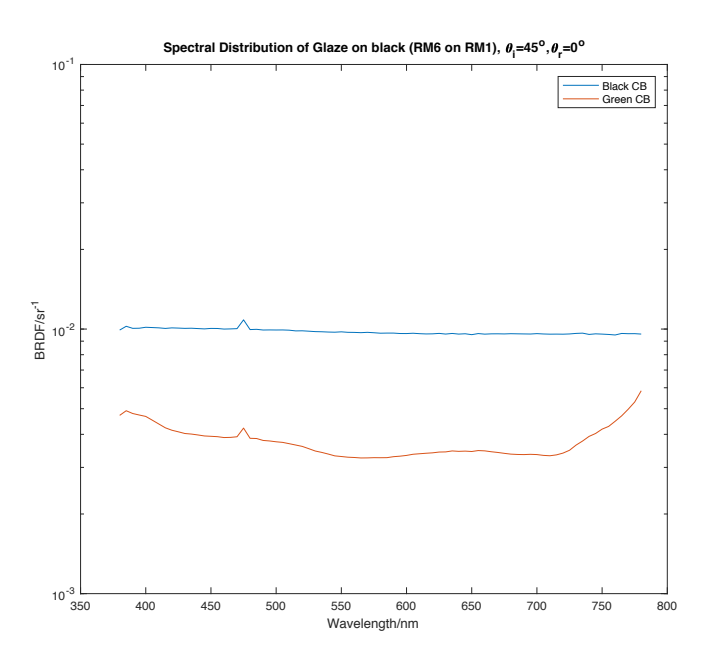


Figure 3.15. Spectral distribution of the BRDF of black paint on canvas board (blue line, sample RM\_1) compared to the spectral distribution of the BRDF of the green glaze applied on top of the black paint (RM\_7). Top left: the incident angle ( $\theta_{i}$ ) is 15° and the observation angle ( $\theta_{r}$ ) is 0° or perpendicular to the surface. Top right: the incident angle ( $\theta_{i}$ ) is 45° and the observation angle ( $\theta_{r}$ ) is 0°. Bottom left: the incident angle ( $\theta_{i}$ ) is 75° and the observation angle ( $\theta_{r}$ ) is 0° or perpendicular to the surface.

Comparing the three spectra in Figure 3.15, it becomes clear that for  $\theta_i$  = 15° and  $\theta_r$  = 0° the green glaze layer shows a higher BRDF value compared to the black paint while for the other two spectra the opposite is the case. Changing the illumination angle clearly influences how dark the glaze appears compared to the black paint.

The angular distribution of the BRDF indicates the type of reflection at specified angles. A flat graph is an indication of very diffuse reflection whereas sharp peaks indicate a specular reflection. Figure 3.16 shows a comparison of the angular distribution of the same four green paint samples as in Figure 3.13. Sample RU\_4 at opacity chart 2A2 appears diffuse on the white surface but shows some specular reflection on the black substrate. The sample RU\_5 on opacity chart 5C shows specular reflection on both substrates, however the reflectivity on the black substrate is about three orders of magnitude larger compared to RU\_5 on the white substrate. In the case of specular reflection, the incident angle is equal to the reflected angle. In Figure 3.16, the observation angles at which specular reflections occur coincide with the illumination angles indicating that these are indeed specular reflections.

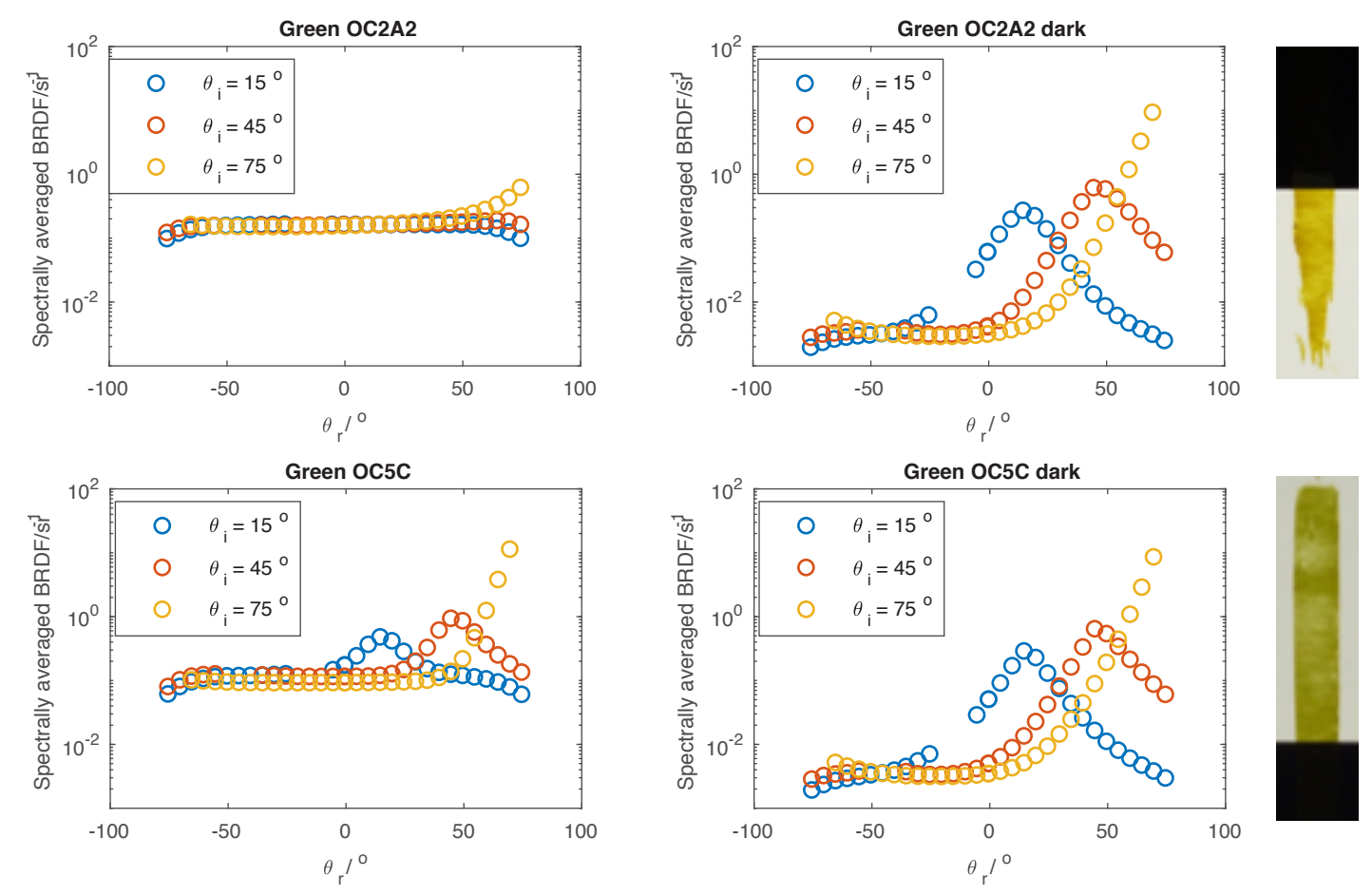


Figure 3.16. Angular distribution of the spectrally averaged BRDF. The blue circles indicate the illumination angle of 15°, the red circles are  $\theta_i = 45^\circ$  and the yellow circles  $\theta_i = 75^\circ$ . The observation angle ( $\theta_i$ ) is varied from -90° to 90°. The peaks clearly visible in the two graphs on the right indicate specular reflection from the surface. Top right: sample RU\_4 on opacity chart 2A2, bottom right: sample RU\_5 on opacity chart 5C.

The CIELab colour chart (Figure 3.17) displays the distribution of the analysed samples based on the level of red, green, yellow and blue present in the samples. RU\_2 on the white area of the opacity chart 2A2 (top right of Figure 3.16) is in the yellow-green quadrant, close to the yellow axis. Samples RU\_4 and RU\_5 on the opacity charts end up more towards to the positive b\* axis compared to the RU\_4 and RU\_5 samples applied on the microscope slides. Sample RM\_6 on the microscope slide is in the yellow-green quadrant close to the x-axis. When this is compared to the RM\_6 on the ivory black layer on top of the canvas board, it becomes clear that RM\_6CB is located on the other side of the origin, in the red-blue spectrum. The differences between the measured colours on different substrates indicates that the surface on which the paint is applied influences the measured colour of the paint.

The level of chroma related to the lightness of the paint samples is shown in Figure 3.18. The samples RU\_2, RU\_4 and RU\_5 applied on the white areas of the opacity charts are light and with high chroma compared to the other paint samples. In the intermediate area are the green samples (RU\_4 and RU\_5) applied on microscope slides. The remaining samples are located in the bottom left corner of the graph, meaning low chroma and lightness values.

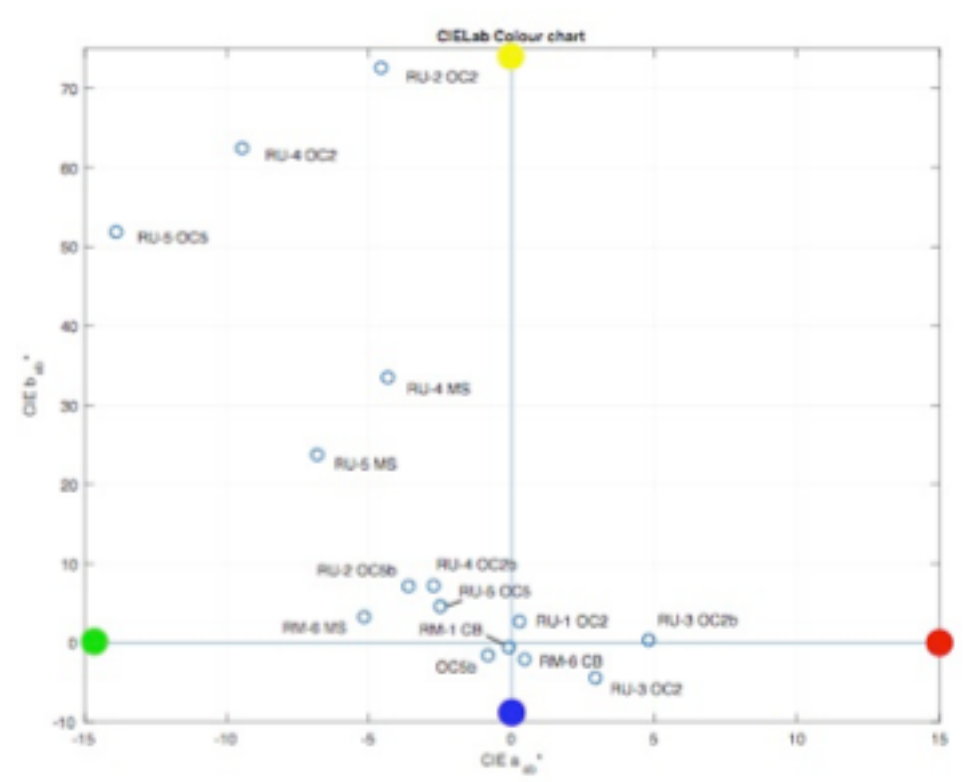


Figure 3.17. CIELab Colour distribution chart with the analysed samples displayed in a grid with the x-axis from  $-a^*$  (green) to  $+a^*$  (red) and the y-axis from  $-b^*$  (blue) to  $+b^*$  (yellow). OC2 is opacity chart 2A2, OC5 is opacity chart 5C, the addition of b indicates the black area of the opacity chart. MS is microscope slide and CB is the canvas board.

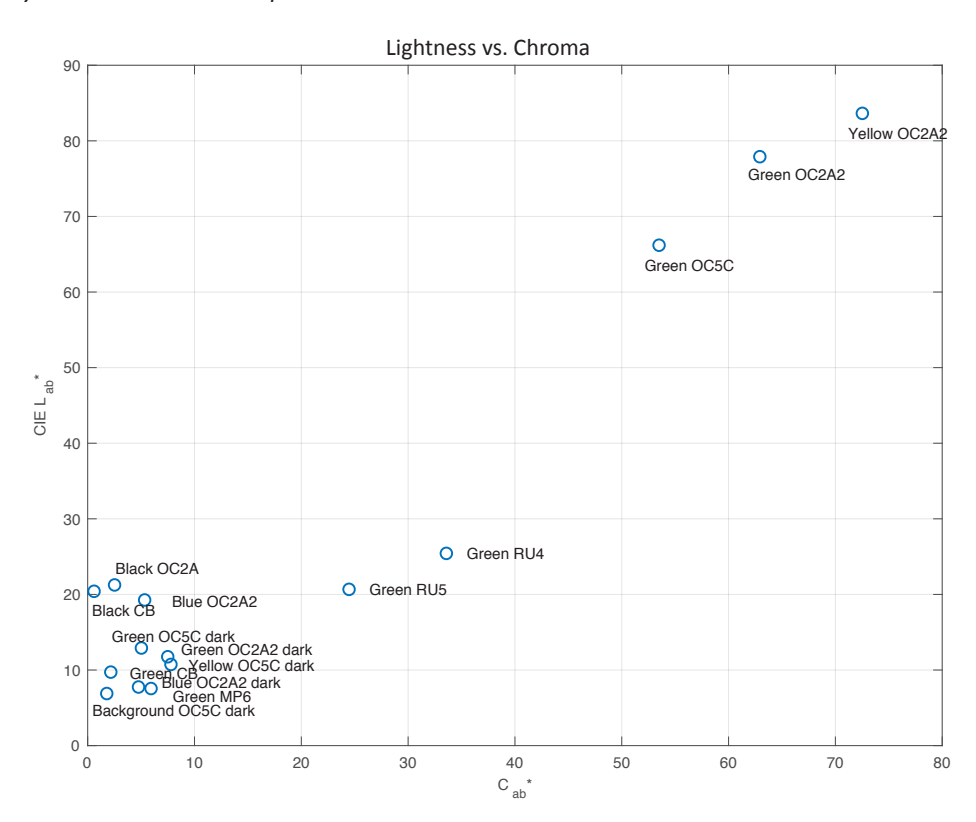


Figure 3.18. Chroma vs. Lightness of the analysed samples. Large cluster of the samples in the bottom left corner, RU\_2, RU\_4 and RU\_5 on the white area of the opacity charts are lighter and contain more chroma compared to the other analysed samples.

# 4 - Theoretical Background - Rendering and 3D Modeling

Theoretical calculations and calculations made using the theoretical models like described in Chapter 2 can be used to simulate the behaviour of a layered paint structure. Rendering software could visualise the paint layers digitally and thus provide more insight in the influence of the optical properties of paint on the visual appearance of paintings. Several analytical reflectance models have been developed for the field of computer graphics which can be divided into empirical and physically based models. The physically based computations focus on the interaction of light with matter to create realistic depictions of surfaces whereas the empirical models are formed experimentally. With increasing computing power, ray tracing has become a more important factor in rendering.[54]

#### 4.1- Rendering of Layered Structures

The behaviour of light in layered structures can be described theoretically as is discussed in Chapter 2. By using render software, these theoretical models can be visualised. Rendering virtual representations of paint can be used to create more realistic digital paintings. Several systems created for this purpose are described in this section.

BRDF is used by Yan as a base to create four different analytical models. Two empirical models (Blinn-Phong model and Ward model) and two microfacet-based models (Cook-Torrance model and Ashikhim-Shirley model) are tested on their performance. The Ward model showed the best results in terms of accuracy and speed. This is used as a starting point for further research to develop the BRDF model.[62] A BRDF model for subsurface scattering is set up by Dong. The Bidirectional subsurface scattering reflection distribution function (BSSRDF) is a general model to describe the surface appearance of translucent materials. The description is in terms of the light transport between every pair of surface points. This is used to compute the optimal layer layout of the output volume, thickness of the layers and the distribution of basis materials.[13]

Jakob developed a method for rendering and in that way simulating layered materials. By using transport-the-oretical models of isotropic or anisotropic scattering layers and smooth or rough boundaries of dielectrics and conductors as input, Bidirectional Scattering Distribution Function (BSDFs) of layered materials can be computed. Therefore, more realistic rendering results can be achieved because the multiple scattering within and between layers can be simulated using their systems reflectance models. The system can be considered a computational language for describing surface structure which can be combined to describe a layered structure. This forms the basis for the Mitsuba render engine. To solve the scattering matrices of medium layers, this system uses the adding-doubling technique which assumes that multiple scattering is a higher-order effect that can be neglected for sufficiently thin layers. These very thin layers are used to find the scattering matrices of a layer double the thickness by joining two identical layers. This process of joining two identical layers is repeated until the desired thickness is achieved.[30]

Weidlich proposed a physically plausible Bidirectional Reflectance Distribution Function (BRDF) model capable of simulating smooth and rough multi-layered surfaces. The model includes absorption within the layers and the total internal reflection. They have tested several layered structures with different material properties in order to replicate the visual appearances of multiple types of paint. (see Figure 4.1) The glossy paint (Figure 4.1a) consists of a clear varnish on top of a coloured solid. This is the application of a Lambertian surface, with diffuse reflection, covered with a smooth layer. It can be a simulation of a paint layer covered with a varnish. The tinted glazing (Figure 6b) is a Lambertian colourless surface covered with a tinted varnish or glaze layer. [59] A combination of these two models could be an approximation of the paint layers present in the background of the Girl with a Pearl Earring. The model proposed by Weidlich does however still fail to reproduce wave effects like iridescence.

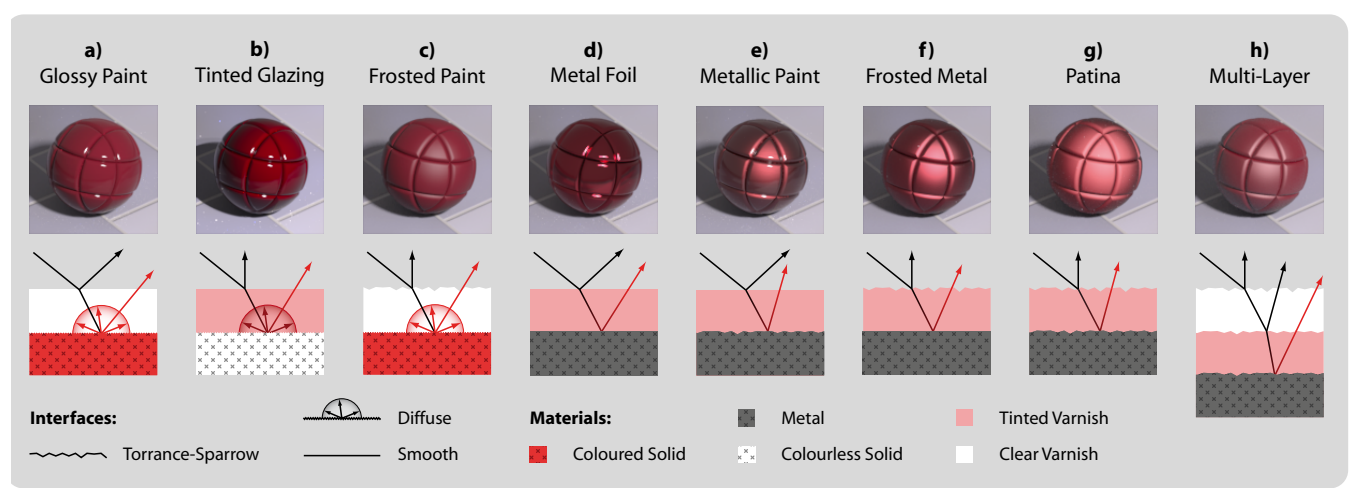


Figure 4.1. Examples of various surface types generated using the layered model created by Weidlich, Spheres are rendered under same illumination conditions. To distinguish the various cases, the micro-facets of the surface are much smaller than the layer thickness in the drawings.[59]

A method was set up by Levin to construct the spatially varying reflectance at resolutions up to 220 dpi. A consequence of the higher resolution is a lower angular resolution. Levin presents an analysis of incoherent reflectance based on wave optics which provides guidelines for the relation between the shape and size of particles and their reflectance functions. Wave optics are taken into account when, beyond a certain scale, geometric optics models do not apply. Other than the model from Weidlich, this model does take into account wave interference in order to fabricate a range of reflection effects.[40]

Moving more towards the realistic depiction of real objects in the digital environment, there are several researches done on digitally imaging paint and other objects. In several cases of the paint simulation, Kubel-ka-Munk is used as a basis to calculate the absorption and reflection parameters in order to digitally replicate the paint.

An example of digitally recreating a painting is Pigmento. It consists of an algorithm created by Tan to model a per-pixel mixture of a limited number of pigments with an RGB image as input. The multispectral scattering and absorption coefficients of the pigments are determined by using the K-M model. The system makes is possible to build up an original RGB image of pigments in order to make tonal adjustments by editing the properties of the pigments. Several applications are possible, for example recolouring, selection masking, edge enhancement and more. In the future it might be possible to use this technique for the identification of pigments in paintings from RGB images. There are at the moment still some limitations regarding the pigment database and the number of primary pigments used in the reconstruction of the image. Next to that, the approach does only provide plausible results enabling paint-like editing.[56]

Chen simulated the appearance of paint applied on a BTF (Bidirectional Texture Function) material. The BTF is a function representing the appearance of the surface of a material as a function of location, viewing direction and lighting direction. It is captured from a real material and can therefore produce a realistic digital representation of that material. This BTF data is used to set up the physical information of the surface including the geometry and reflectance. The properties of the paint are added to this model. The reflectance of the paint is computed using the K-M model. The use of the K-M model has its limitations and causes this system to not yet support complex lighting effects due to the directions of the fluxes in the K-M model. A more physically accurate model could lead to a more realistic result.[10]

To create a realistic depiction of a painting while it is being made, Baxter created a model which can be used in interactive painting systems. This model simulates both the numerical aspect as the physical flow of paint during the application on a surface. It can be used on paint styles similar to oil and acrylic paint and several different painting styles are possible, for example thick impasto and semi-transparent glazes.

The user of the model can draw on a tablet the brush strokes of the painting and the system will calculate the behaviour of the applied paint and its interaction with the surface and the brush. One active wet layer is taken into account together with an unlimited number of dry paint layers and each layer is represented by a height field. A set of pigments was selected by the developers in advance to build up the images. The spectral properties of the pigments were included in the set. By representing the colours in terms of pigments rather than RGB allows the system to show the painting under different lighting conditions because the appearance of the pigments can be adjusted with the emitted spectrum of the light source. (Figure 4.2) The physical flow of paint is used to simulate the application of paint live, however, the simulation is based on approximations with added heuristics which model the behaviours not covered by the physical terms. The full-spectrum reflectance of several oil paints commonly used were measured and imported into the system for users to work with. To model as accurate as possible the chromatic behaviour of paint blending, a colour blending and compositing engine based on the K-M model is added to the system as well. Limitations of the model are the limited resolution due to computational costs and the fact that K-M is an idealisation of the situation which does not exactly simulate the light transport through the paint layer. [5] Creating the appearance of a painted surface from a 2D image is done by Lee. An algorithm was generated to introduce 3D brush strokes to a 2D photograph to create the suggestion of an oil painting. Using a photometric stereo technique, brush strokes have been converted into 3D models. These could be integrated into the image by decreasing brush stroke radius to approach the effect of the painted image.[39]



Figure 4.2. Comparison of the same painting created with IMPaSTo under different lighting conditions. Left, painting digitally illuminated by a 5600K bulb. Right, painting digitally illuminated by CIE Fluorescent Illuminant F8. The spectra below represent the light spectra (blue), 8 sample wavelength used by IMPaSTo (red) and CIE XYZ integrating functions (black).[5]

Not only paint and paintings are digitally recreated, photorealistic rendering of virtual objects in order to insert them into images of the real world is increasingly used. For example, in the (digital) catalogue of IKEA where digital models of furniture are rendered and inserted into images of a real-life photo set. Physically based methods are studied by Kronander to simulate how light propagates in a mathematical model of the augmented scene. He discusses four areas related to photorealistic rendering, HDR (High Dynamic Range) imaging, IBL (Image Based Lighting), reflectance modelling and efficient rendering. Next to that, two BRDF models are proposed for surfaces which exhibit wide angle gloss. The algorithm proposed by Kronander enables efficient rendering of scenes which contain glossy transfer and heterogeneous participating media.[36]

Matusik set up a method to use the BRDF data of a set of materials as input for renders using Mitsuba. The set of materials contains for example multiple metals and fabrics. An example of the render is shown in Figure 4.3 where the specular reflection is varied resulting in more matte or more glossy surfaces.



Figure 4.3. Variation in specular reflection applied to the BRDF of a black plastic with increasing specularity from left to right.[43]

#### 4.2- Ray Tracing

Ray tracing is a rendering technique where light rays are traced back from the observer via a digital scene to the digital light source. Tracing the light rays in reverse is preferred over tracing light rays from the light source because it is more efficient than tracing the rays emitted in every direction by the light source. The technique uses physically accurate reflections, refractions, shadows and indirect lighting to create a computer graphics image of a digital scene for example for architecture purposes. The principle of ray tracing is schematically shown in Figure 4.4 where the light rays are traced from the camera after which the rays might reflect from an object, pass through it or be blocked. The different interactions of the light rays with the objects in the scene result in reflections, refractions and shadows. These interactions are combined to produce an illumination and colour pixel which is displayed on the screen. A more intensive form of ray tracing is path tracing in which hundreds or thousands of rays are traced through each pixel. The light rays are followed through multiple bounces off or through objects before reaching the light source. Path tracing is done to collect information on colour and lighting of a scene.[52] The Mitsuba render engine is based on ray tracing and path tracing to create the computer graphics images.

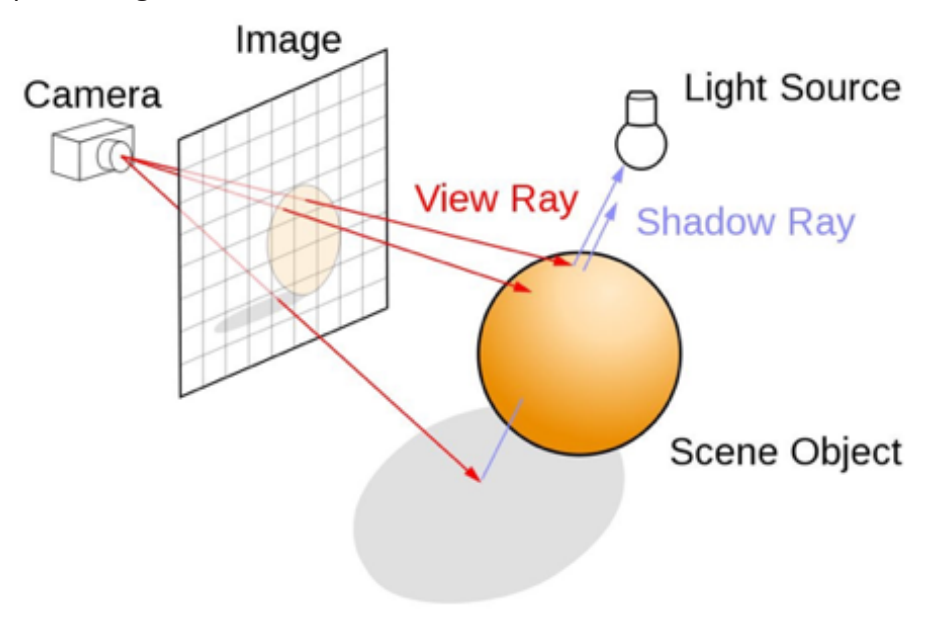


Figure 4.4. Schematic representation of ray tracing where light rays are traced back from the camera or observer via the objects in the digital scene to the light source.[52]

# 5 - Experiment - 3D model and Simulation

A 3D model is created using the layer thickness data from OCT scans to digitally recreate the topography and layered structure of the painting. Autodesk Maya is used to build the 3D model and create the environment scene around the painting containing the light sources and camera. The measured optical properties of the paints discussed in Chapter 3 should provide enough information to simulate the appearance of the painting using the render software Mitsuba. A first effort is made in corporation with Jerry Guo, PhD candidate at Computer Graphics and Visualisation, TU Delft to test the capabilities of the render engine to simulate the appearance of paint layers and to simulate the painting with and without the glaze layer.

#### 5.1- Assumptions made within Experiment

During the creation of the 3D model and render simulation of the painting, several assumptions needed to be made since a layered paint system might be difficult to model exactly. The first, 0<sup>th</sup> order, model will be based on homogeneous paint layers where the scattering of pigment particles is not present due to the dissolved pigment particles in the glaze. The refractive index (RI) was not retrieved from the ellipsometry measurements, therefore refractive indices from literature are used. When the refractive indices of a pigment and a binding medium are close to each other, the resulting paint is more translucent. Since the glaze layer is translucent, if the pigment particles have not dissolved into the oil, it can be assumed that the RI of the indigo and weld pigment is close to the RI of the linseed oil binding medium of the glaze. The RI of fresh linseed oil is, using the immersion method, determined to be 1.480 by Laurie. Of a 10 year old film of linseed oil, the RI is 1.512.[38] The refractive index of indigo is between 1.49 and 1.52 according to literature, which confirms the assumption that the RI of indigo is similar to that of linseed oil.[49] Refractive indices of 1.480 and 1.512 are taken for the glaze to simulate once the fresh paint and once aged paint. The black underpainting is as a first approximation considered to reflect no light. In a later stage, the reflection of the underpainting in sample OP\_19 measured using the micro spectrophotometer and the BRDF reflectance of sample RM\_1 are used as input for that specific layer.



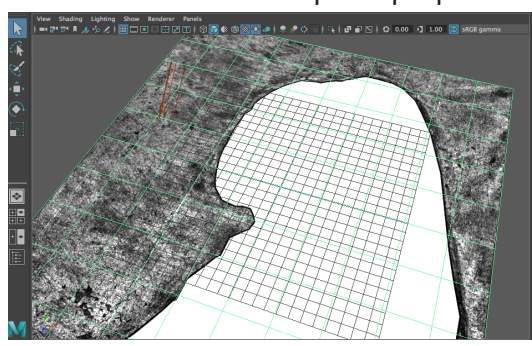
Figure 5.1. The assumption of isotropy means that the painting will appear the same under influence of reflection when viewed from for example the left or the right.

The painting is assumed to be an isotropic object, this means the painting will have the same reflection and therefore will appear the same when observing it from different angles. (see Figure 5.1) It should not make a difference when the painting is viewed before or after rotating it in its own plane. The OCT measurements do not provide the thickness of the varnish layer; therefore, the assumption is made that the thickness of the varnish layer is homogeneous over the entire background. The thickness is based on the thicknesses observed in the cross sections of the original painting.

#### 5.2- Creation of 3D Model

The OCT measurements performed by Callewaert have determined the layer thicknesses of the varnish and glaze layer.[8] The height maps resulting from the measurements are used as input

parameters to create a 3D computer model of the layered structure of the painting. The 3D model was created using Autodesk Maya, in Figure 5.2 an exaggerated glaze topography can be seen. The grey scale height map is converted to a 3D model by assigning displacement values to the specific grey tones where the white areas are the highest and the black areas are lowest. The 3D model is built up from two different meshes. The height map of the painting represents the thickness of the entire painting, which ranges in the height map from 0 to  $250 \,\mu\text{m}$ .[9] The varnish layer present in the cross section of sample OP\_19 is 5  $\mu$ m thick, the varnish layer is assumed to be homogeneous throughout the background of the painting. This varnish layer is subtracted from the thickness of the painting and created into a mesh. The thickness of the glaze layer is provided by the OCT data and used to create a second mesh. The thickness of the glaze layer is roughly 20 to 30  $\mu$ m thick. Large thicknesses in the height map are likely caused by noise. The meshes created from the height maps form the layers of the 3D model to which the optical properties are assigned using render software Mitsuba.



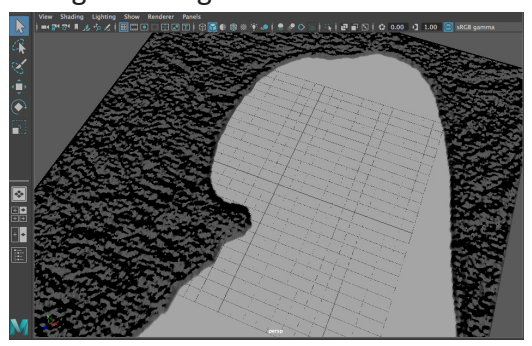


Figure 5.2. Impression of 3D model based on OCT map of the glaze layer thickness in the background. In the mesh on the right a displacement is applied to the height map with the height differences exagerrated.

### 5.3- Rendering using Mitsuba

The 3D model is used as a framework for the Mitsuba render engine. The measured absorption spectra and BRDF data have been used as input for the optical properties of the layers in the 3D model. Since the ellipsometry measurements did not result in refractive indices of the samples, refractive indices from literature are used. These are based on the real part of the RI of fresh linseed oil (1.480) and aged linseed oil (1.512).

The measured absorption spectra are in a comparably high resolution with 1197 segments of 0.35 nm bandwidth. Mitsuba is configured to use 15 bins for storing the absorption data. To improve the accuracy, the number of bins was increased to 50 bins of 9.4 nm band width.[26] This, however, resulted in a large rendering time. The colour data is therefore converted to RGB values with only three input values.

The implementation of BRDF in Mitsuba is an adaption of the method created by Matusik. The measured resolution is lower compared to the number of geometries used by Matusik. Instead of 2,916,000 (90x90x360) bins used by Matusik to divide the data, only 96 variables were used during the BRDF measurements. [43] Interpolation of the measured data is therefore done to provide Mitsuba with the necessary number of data points. Together with the BRDF measurements, the CIELab colour measurements.

This research focusses on the background of the painting. During rendering, the face of the girl is assumed to be diffuse so it appears the same from each illumination and viewing angle.

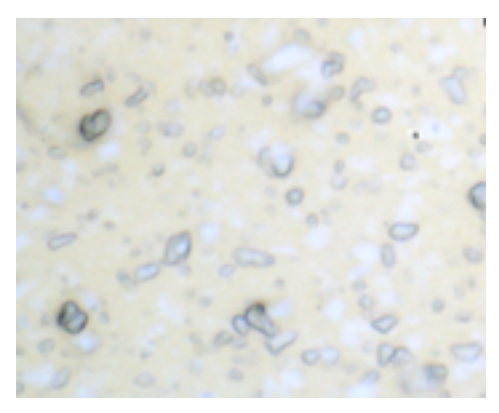
#### 5.4- Results

The measured optical parameters discussed in Chapter 3 are used as input for render software Mitsuba. The render model is built up in steps where during the first test only the measured absorption spectra are used. Following steps should be implementing the measured BRDF and CIELab colour data are used as input for the model. In the last step, refractive indices from literature are implemented in the render model.

#### 5.4.1 - Absorption spectra as input

The absorption spectra measured during the first part of the experiment is used as input for the Mitsuba render engine. Mitsuba uses the input spectra as reflection spectra which results in negative colours when

implementing the absorption spectra. As visible in Figure 5.3, the colour of the render does not match with the paint sample of which the absorption spectrum is measured. This problem is resolved by using the inverse absorption spectrum or reflectance spectrum as is shown in Figure 5.4 and 5.5.



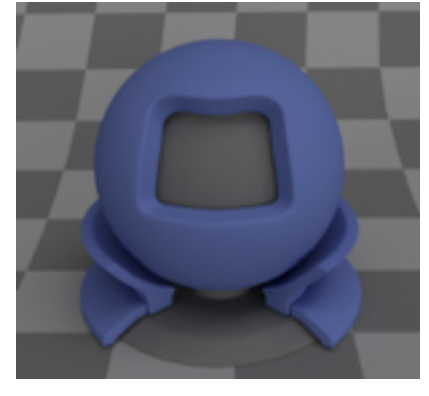
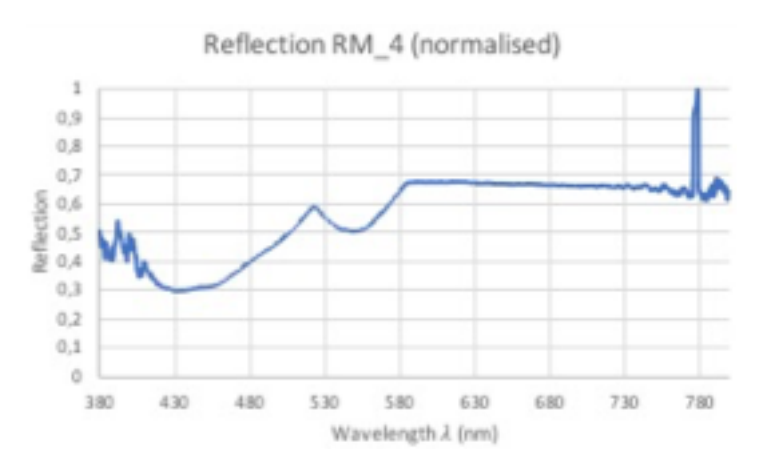


Figure 5.3. Left: microscope image of sample RM\_4, thinly applied on a microscope slide. Right: render created with the measured absorption spectrum. Colours do not match since the blue does not correspond to the yellow colour of the paint sample.



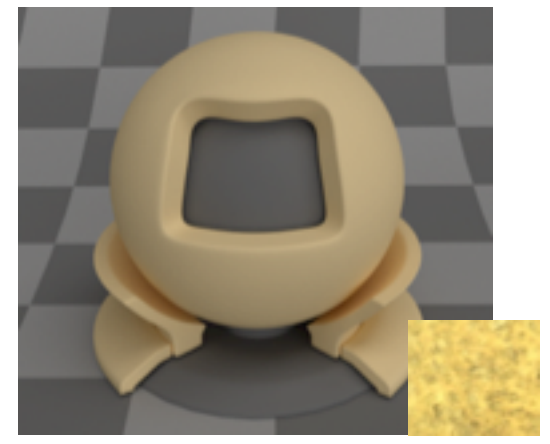
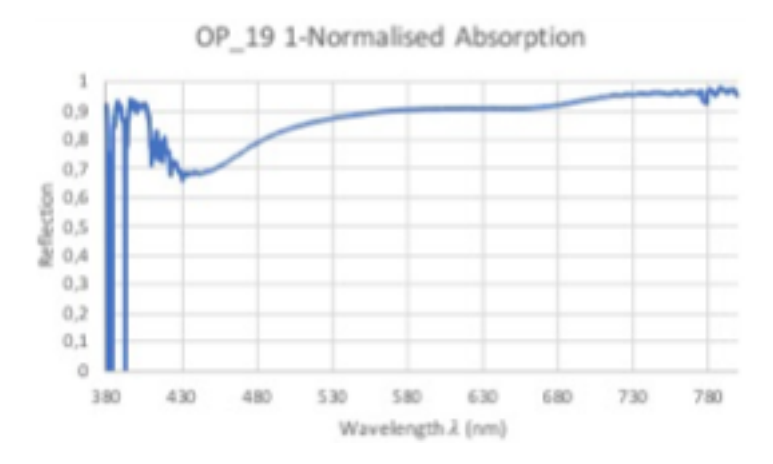


Figure 5.4. Left: the reflectance spectrum measured with micro spectrophotometer of reconstruction RM\_4 (Stil de grain) with added linseed oil used as input for Mitsuba. Right: render image with microscope image of RM\_4 in the insert.



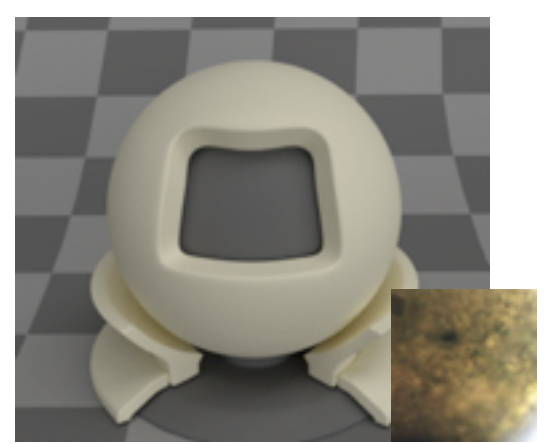


Figure 5.5. Left: the normalised absorption spectrum subtracted from 1 of sample OP\_19 used as input for Mitsuba. Right: render image with microscope image of OP\_19 in the insert.

The first tests done with the measured absorption data show promising results, implementing the measured BRDF data and refractive indices from literature is the next step in this research. In order to implement the BRDF data, the method designed by Matusik will be used as a base.

### 6 - Discussion and Conclusion

The research focussed on the determination of optical properties of paint and glaze layers in *Girl with a Pearl Earring* and of reconstructions created to approximate the paint present in the original painting. Both absorption and BRDF measurements were done on a set of samples. The measured properties in combination with OCT data provided by Callewaert should provide the imput needed to digitally recreate the painting which could lead to more insight regarding the optical effect of the glaze layer present in the background.

#### 6.1- Discussion

Measurements on samples of the original painting and reconstructions have been done to determine optical properties of the glaze and paint. On the samples of the original painting only absorption measurements using the micro spectrophotometer could be done due to the configuration of the samples. Determination of the refractive indices and BRDFs (Bidirectional Reflectance Distribution Function) is therefore done only on the reconstructions.

The reconstructions have been made to approximate the original glaze and paint as well as possible. Creating an exact replica of the original glaze and paint is almost impossible. Analytical techniques used to determine the composition of the original paint and glaze are only qualitative, meaning that the presence of certain components can be confirmed. [25] However, the exact ratio in which the components are present can be difficult to determine. This is also complicated by the fact that in this case only local samples of the background are available. Next to that, the original painting has aged for roughly 350 years, the reconstructions made during this research have aged only several weeks.

The absorption spectra normalised to the yellow pigment peak (Figure 3.12) show that the spectra of both samples of the original painting (OP\_19 and OP\_26) are very similar. This suggests that the glaze layer is similar throughout the painting. In order to confirm this, more samples need to be analysed since a set of two samples is not large enough to provide a reliable result. A limiting factor here is the configuration of the samples of the painting since paint samples are usually processed to cross sections embedded in resin making absorption measurements more difficult.

The absorption spectra of the reconstructions show that the peak of the yellow pigment only shifts about 5 nm compared to the original samples. Indicating that the yellow pigment in the reconstructions is a reasonable approximation of the weld in the original painting. The yellow pigment peaks are 75 to 100 nm wide, much narrower than the peaks for the indigo pigment. A peak width of 50 to 150 nm is expected for oil paint samples at room temperature, this is mainly caused by a combination of electronic and vibrational transitions within the molecules. Because these transitions usually display inhomogeneous broadening due to the oil environment of the pigment, the peaks of these paints are often broad bumps rather than sharp peaks. Subtracting the indigo spectrum of OP\_19 from the green glaze spectrum of that sample results in a spectrum showing mainly the peak for the yellow pigment. The absorption spectra also show absorption between 450 nm and 600 nm suggesting that the green glaze is a mixture of not only the yellow and blue pigment. The composition of the glaze of only weld and indigo is therefore a simplification of the situation but these are the main components of the glaze and therefore a good first approximation.

The noise at the edges of the measured spectrum are likely to be caused by the paint, since the measured reference spectra of the microscope slides show no noise. Having measured first in transmission and then the absorption, could cause the high sharp peaks since a very low intensity is measured and the logarithm of a value close to zero is calculated which results in a sharp high peak.[2] Reproducing the measurements and averaging the spectra should reduce the level of noise, improve the signal to noise ratio which should result in cleaner spectra. Measurements were done at different areas in the samples, however averaging these spectra did not yet result in spectra with a better signal to noise ratio.

Determination of the refractive index of paint layers has proven to be difficult. Usually, in the field of restoration and conservation of paintings, the RI is only determined by the immersion method. This could be because in restoration the relative RI (the RI compared to a binding medium) is mostly relevant. This determines the translucency of a paint. The visual appearance of for example a retouch applied by a restorer should be as close as possible to the original paint as possible. The appearance is often tested by the naked eye. The measurement done on sample RM\_2 gave a promising first result. Unfortunately, the thickness of the paint layer and its opacity resulted in reflected light intensity too low to be properly detected by the ellipsometer. The method has proven to be suitable for the determination of the refractive index (RI) and thickness of a varnish layer. [50] A varnish layer is a homogeneous layer whereas a paint layer contains pigment particles that might induce scattering of the light. The scattering of light caused by pigment particles could be the reason why the RI of paint layers is difficult to determine. It could be possible that ellipsometry measurements on a glaze layer will produce better results compared to the paint because the pigment particles have dissolved into the binding medium. Next to that, the application of the paint using a spatula resulted in a relatively thick and uneven layer to ellipsometry standards. This should be improved if further measurements are carried out.

BRDF measurements have been carried out only on paint and glaze reconstructions since the samples of the original painting were not suitable for the measurements. It is therefore not possible to determine how accurate the reconstructions are compared to the original painting based on the BRDF measurements alone. The visual appearance of the renders can be an indication of how well the reconstructions approximate the original painting. The measurement results show a dependence of the BRDF values on the substrate on which the paint is applied. This could be caused by the translucency of the paint and glaze causing subsurface scattering. The BRDF measurements on the reconstructions can therefore only be compared with each other when done on paint applied on the same substrate. The question rises whether the BRDF results are reliable enough or whether BSSRDF (Bidirectional Scattering-Surface Reflectance Distribution Function) would yield better results since it takes into account the translucency of the glaze layer.

The effect of the glaze layer applied on top of the black underpainting could be observed in the reconstruction and during BRDF measurements. From specific angles, the black underpainting with green glaze applied on top of it appears darker compared to a layer of black underpainting. (see Figure 3.15) Different appearances of the black underpainting with or without glaze layer is caused by several factors: texture, gloss, scattering due to pigment particles and the angles of illumination and observation. These effects can be observed when looking at the painted reconstruction. The black paint layer shows an irregular surface, i.e. more texture compared to the glaze layer. This difference is partially caused by the fact that an additional layer is applied and partially by the fluidity of the glaze resulting in a smoother surface. The glossy surface of the glaze layer is influenced by the surface texture and could be also caused by the relatively larger amount of binding medium present in the glaze layer. The reflected light of the black underpainting surface is more diffuse because the pigment particles have not dissolved into the binding medium and scattering takes place within the black paint layer.

It is clear from the BRDF results that the black underpainting does not absorb all light but reflects a small portion of the light. Therefore, the first assumption for the render simulation that the black layer absorbs all light is not valid. The light is reflected more specular from the glaze layer which could be because of the amount of texture as well as the fact that the pigment particles have dissolved into the binding medium and therefore scattering within the glaze layer does not occur as in the black paint. From specific angles the glaze layer appears darker or lighter because of the difference in the reflection of light. (see Figure 3.14)

Tests with rendering of the painting were done using the render engine Mitsuba which is created to digitally visualise layered structures as realistically as possible. This is still work in progress. The input parameters for Mitsuba are the absorption spectra, refractive indices and BRDFs of the paint samples. The number of bins (containers to store the data in) used by Mitsuba to divide the absorption data is limited making the resolution of the used absorption data very low compared to the measured data, especially when the RGB values -only 3 bins- are used as input. The lower resolution results in less accurate colours, however, increasing the number of bins used leads to a longer render time. Using the measured CIELab and CIEXYZ values as input instead might be a solution for this problem.

The resolution of the BRDF measurements is very low compared to the required resolution for the system set up by Matusik.[43] Interpolation of the data is therefore needed and to simplify the system, the assumption is made that the painting is isotropic. For a more accurate result, BRDF measurements should be done at a higher resolution which will result in a higher running time for the measurements.

As a first approximation for rendering, it was assumed that the glaze layer is a homogeneous layer in which no scattering takes place due to pigment particles. In order to determine if this assumption was valid, more time needs to be invested in the rendering of the glaze layer. The simplified version of the paint layer system used during this research might need to be finetuned to approach the glaze and paint in the painting as well as possible. When the system provides realistic results it might be possible to apply it in more cases. For paintings with similar pigments and glazes, it could be applied to recreate the other paintings. Optical properties such as the absorption, refractive index and BRDF are different for each paint and therefore painting. Application of this system would mean that the required optical and physical properties of the other paintings need to be determined as well. If a larger selection of paints and pigments is studied in multiple pigment and binding medium ratios, a database of optical properties could be created. When the optical properties of pigments present in a painting are available in such a database, a digital reconstruction could be made of more paintings, provided the layer thicknesses and topography of the painting and pigment distribution is available. Creating a set of more digitally recreated paintings might make it easier to compare the paints and paintings without the need for transportation. Before this is possible, multiple years of research are probably required.

#### 6.2.- Conclusions

As defined earlier, the aim of this research is to create an approach to determine optical properties suitable as input for digital simulation of the glaze layer present in *Girl with a Pearl Earring*. It has been proven that absorption measurements using micro spectrophotometry and BRDF measurements were successful. Determination of the refractive index using ellipsometry has not yet delivered conclusive results. More time should be invested since it is a promising technique for determining the refractive index of a glaze layer.

Micro spectrophotometry was used for measurements on original paint samples and reconstructions in order to determine the absorption of the paints and glazes. Micro spectrophotometer is proven to be an effective method to determine the absorption spectra of individual paint layers and paint samples applied on a microscope slide. There is much noise at the edges of the spectra which could be caused by absorption by the paint at these wavelengths. A larger set of measurements could improve the signal to noise ratio and result in spectra with less noise.

The BRDF measurements have been done on reconstructions to provide reflection data as input for the render engine. The spectral distribution of the BRDF indicated the darker appearance of the glaze layer applied on top of a black paint when viewed from specific angles. This is a clear indication of the influence of the glaze layer on the appearance of the painting since the light is reflected less in certain directions. Both the reflectance and CIELab colour results during the BRDF measurements indicate a difference in appearance depending on the surface on which the paint is applied. The colour changes and the amount of reflected light changes with the substrate.

First tests with rendering were done using the measured absorption data to get an indication of the performances of the render engine and the significance of the measured data. The high resolution absorption measurements were converted to a lower resolution to match with the input bins in Mitsuba. The resolution of the BRDF measurements was very low compared to the method proposed by Matusik. The measured data needed to be interpolated to provide reflection data from more angles than measured. This will lead to a less accurate render result. The layer thicknesses determined by OCT scans [9] were used to create a 3D model of the painting to which the optical properties can be assigned.

In the future, the current simplified version of the paint layer system used during this research could be further refined to approach the glaze and paint in the painting as well as possible.

#### 6.3-Limitations

One of the main limitations during this research was the uncertainty of the composition of the paint and glaze. The exact paint recipe cannot be determined for the entire glaze layer because quantitative analysis on paint is difficult. Next to that paint and glaze are inhomogeneous substances meaning that the composition varies throughout the surface of the painting. The assumptions made were done to simplify the paint layer system and create a first approximation. This leads to another limitation, the system set up for rendering the image of the painting is a rough approximation in which multiple assumptions needed to be made due to the fact that a lot of information is unknown. An example here is the refractive index of oil paint. Due to the lack of research done on the exact determination of the RI of paint so far, assumptions needed to be made based on the few values available in literature.

The assumption of a glaze layer being homogeneous could implicate that the simulation will not properly run for a regular paint. The measurement of the absorption and BRDF should cause no problems but the render model might need to be adjusted. The resolution of the render engine compared to the analysis techniques could be improved to achieve more accurate results.

When there is interest to apply this system to other paintings as well, much more data needs to be collected on the paints present in other paintings. At the moment it is not yet an easy implementation for other situations.

#### 6.4.- Recommendations

The first test to determine the refractive index of paint using ellipsometry indicated that there are possibilities for using this technique. In future research, the paint samples need to be applied thinner and it should be taken into account that ellipsometry might only work for glazes where the pigment has dissolved into the binding medium.

An interesting test would be to examine the difference in appearance for glazes of different colours. If the render system works for a green glaze, the absorption spectrum of a cochineal glaze could be used to get a quick indication of the appearance of the painting with a different colour glaze.

During the 17th century, the Golden Age for the Netherlands, only a limited amount of pigments was available to painters. This small group of pigments could be analysed in a similar way to the analysis during this research to form a database. When more data is available of the composition and layered structure of paintings from that era, this could be combined with the measured optical properties and BRDFs of the database. In that way, digital reconstructions can be created of 17th century paintings to preserve them for the future.

The measured optical properties of the paint can be used to compare the optical properties of paint with ink used in 3D printing. When the Mitsuba render engine provides a realistic digital representation of the paint based on the optical properties, this render engine can be used to get an indication of a 3D printed reproduction before it is printed, possibly leading to an improvement of the quality of 3D printed reproductions. A next step is to test the render engine in combination with 3D printed samples.

# Acknowledgements

First of all a thank you to my parents and Christian who supported me during my studies and especially during my graduation project.

Prof. dr. Joris Dik (3mE, TU Delft) and prof. dr. ir. Jo Geraedts (IO, TU Delft), you presented me this subject and made this research possible. I had the priviledge to work in many different fields and without the help of the following people it wouldn't have been possible to get to this result.

The measurements on the samples of the original painting would not have been possible without dr. Abbie Vandivere (Mauritshuis) and Annelies van Loon (Mauritshuis). Thank you Abbie for answering my many questions even when you were so busy yourself. Your enthusiasm for the research on *Girl with a Pearl Earring* is infectious.

Willemijn Elkhuizen (TU Delft), you always had interesting input, shared your data with me and made time to discuss my research even when you did not really have time. Thank you, Tom Callewaert (TU Delft) for sharing your OCT data with me.

For one of the sets of reconstructions I got offered the help of Fahed Ibrahim (UvA), he dedicated a couple days to help me create paint on which I could do my measurements. The micro spectrophotometry measurements would not have been possible without Muriel Geldof (RCE), thank you for letting me use the instrument for my measurements. The ellipsometry measurements were a small gamble but ing. Marc Zuiddam (TNW, TU Deflt) was open to try the measurements on the paint. Thank you for letting me experience a clean room for the first time. The BRDF measurements would not have been possible without the help of two people, Eric Kirchner (AkzoNobel) thank you for answering my questions and for getting me in touch with Alejandro Ferrero (CSIC, Madrid). Many thanks to Alejandro for making it possible for me to do BRDF measurements on the paint reconstructions on such a short notice. I learned a lot and you contributed a lot by helping me with the measurements.

A big thanks for Jerry Guo (EWI, TU Delft) for the hours you spent on this project to get a working code to implement my measured data in Mitsuba. I have asked a lot from you and I really appreciate your help. Prof. dr. Elmar Eisemann (EWI, TU Delft), your interest in the subject from lead to the possibility to introduce computer visualisation in the project, thank you for making that possible.

# Bibliography

- [1] Acharya, R. (2017). Interaction of waves with medium. In *Satellite Signal Propagation, Impairments and Mitigation*, 57-86. doi:10.1016/b978-0-12-809732-8.00003-x
- [2] Ariese, F. (2019). [Personal Communication on Absorption Spectra]
- [3] ASTM E179-17. (2017). Standard Guide for Selection of Geometric Conditions for Measurement of Reflection and Transmission Properties of Materials. In *Summary of Guide:* ASTM International
- [4] Batsanov, S. S., Ruchkin, E. D., & Poroshina, I. A. (2016). Methods of Measuring Refractive Indices. *Refractive Indices of Solids* Springer Briefs in Applied Sciences and Technology, 9-15. doi:10.1007/978-981-10-0797-2\_2
- [5] Baxter, W., Wendt, J., & Lin, M. C. (2004). *IMPaSTo: A Realistic, Interactive Model for Paint*. Paper presented at the Proceedings of the 3rd International Symposium on Non-Photorealistic Animation and Rendering, Annecy, France
- [6] Berns, R. S., & René de la Rie, E. (2003). The Effect of the Refractive Index of a Varnish on the Appearance of Oil Paintings. *Studies in Conservation*, 48(4), 251-262. doi:10.1179/sic.2003.48.4.251
- [7] Callewaert, T., Dik, J., & Kalkman, J. (2017). Segmentation of thin corrugated layers in high-resolution OCT images. Optics Express, 25(26), 32816. doi:10.1364/oe.25.032816
- [8] Callewaert, T. (2018). [Personal Communication on OCT Scans].
- [9] Callewaert, T. (2019). [Personal Communication on OCT Scans and Data].
- [10] Chen, T.-E., Huang, T.-S., Lin, W.-C., & Chuang, J.-H. (2017). Simulating Painted Appearance of BTF Materials. *Multi-med Tools Appl*, 77, 7153-7169
- [11] Cheung, C. S., Spring, M., & Liang, H. (2015). Ultra-high resolution Fourier domain optical coherence tomography for old master paintings. *Optics Express*, 23(8), 10145-10157
- [12] Craic. (2012). Microspectrophotometer Design. Retrieved at April 13 2019 from http://www.craictechnologies.com/support/service-contracts/microspectrophotometer-design
- [13] Dong, Y., Wang, J., Pellacini, F., Tong, X., & Guo, B. (2010). Fabricating Spatially-Varying Subsurface Scattering. *ACM Transactions on Graphics*, 29(4)
- [14] Dorsey, J., Rushmeier, H., & Sillion, F. (2010). Digital Modeling of Material Appearance. Burlington: Elsevier Science.
- [15] Eastaugh, N., Walsh, V., Chaplin, T., & Siddall, R. (2008). *Pigment Compendium, A Dictionary and Optical Microscopy of Historical Pigments*. Oxford: Elsevier
- [16] Elkhuizen, W. S., Essers, T. T. W., Lenseigne, B., Weijkamp, C., Song, Y., Post, S. C., Dik, J., et al. (2017). *Reproduction of Gloss, Color and Relief of Paintings using 3D Scanning and 3D Printing*. Paper presented at the Eurographics
- [17] Elkhuizen, W. S., Zaman, T., Verhofstad, W., Jonker, P., Dik, J., & Geraedts, J. M. P. (2014). Topographical scanning and reproduction of near-planar surfaces of paintings. *Proceedings of SPIE, 9018* (Measuring, Modeling, and Reproducing Material Appearance)
- [18] Ellipsometry Data Analysis. (2019). Retrieved at April 27 2019 from https://www.jawoollam.com/resources/ellipsometry-tutorial/ellipsometry-data-analysis
- [19] Ellipsometry Measurements. (2019). Retrieved at April 20 2019 from https://www.jawoollam.com/resources/ellipsometry-tutorial/ellipsometry-measurements

- [20] Emmel, P., & Hersch, R. D. (2000). A Unified Model for Color Prediction of Halftoned Prints. *Journal of Imaging Science and Technology*, 44(4), 351-360
- [21] Ferrero, A., Bernad, B., Velázquez, J. L., Pons, A., Hernanz, M. L., Jaanson, P., Campos, J., et al. (2015). *Measurement of Goniofluorescence in Photoluminiscent Materials*. Paper presented at the 28th CIE Session
- [22] Ferrero, A., Campos, J., Rabal, A. M., Pons, A., Hernanz, M. L., & Corróns, A. (2011). Principal Components Analysis on the Spectral Bidirectional Reflectance Distribution Function of Ceramic Colour Standards. *Optics Express*, 19(20)
- [23] Ferrero, A., Rabal, A. M., Campos, J., Martínez-Verdú, F. M., Chorro, E., Perales, E., Hernanz, M. L., et al. (2013). Spectral BRDF-based Determination of Proper Measurement Geometries to Characterize Color Shift of Special Effect Coating. *Optical Society of America*, 30(2), 206-214
- [24] Geldof, M., Gaibor, A. N. P., Ligterink, F., Hendriks, E., & Kirchner, E. (2018). Reconstructing Van Gogh's Palette to Determine the Optical Characteristics of his Paints. *Heritage Science*, 6(17)
- [25] Groen, K. M., Werf, I. D. v. d., Berg, K. J. v. d., & Boon, J. J. (1998). Scientific Examination of Vermeer's Girl with a Pearl Earring. *Studies in the History of Art*, 55, 168-183
- [26] Guo, J. (2019, March 26 2019). [Personal Communication on Rendering Using Mitsuba]
- [27] Hammond, H. K., & Dean, T. J. (1972). Color and Light. In Paint Testing Manual (13 ed.). Philadelphia
- [28] Hébert, M., Mazauric, S., & Simonot, L. (2016). Assessing the capacity of two-flux models to predict the spectral properties of layered materials. Paper presented at the IS&T International Symposium on Electronic Imaging, San Fransisco, United States
- [29] Isaac and Rebecca, Known as 'The Jewish Bride', Rembrandt van Rijn, c. 1665 c. 1669. Retrieved at May 12 2019 from https://www.rijksmuseum.nl/en/collection/SK-C-216
- [30] Jakob, W., d'Eon, E., Jakob, O., & Marschner, S. (2014). A Comprehensive Framework for Rendering Layered Materials. *ACM Transactions on Graphics*, 33(4)
- [31] Janson, J. (2018a). Glazing. Retrieved at April 18 2019 from http://www.essentialvermeer.com/technique/technique glazing.html#.XLn2IS-iHOQ
- [32] Janson, J. (2018b). Weld. Retrieved at November 14 2018 from http://www.essentialvermeer.com/palette/palette weld.html#.W-xe-C9x OQ
- [33] Jenkins, F. A., & White, H. E. (2001). Fundamentals of Optics (S. Grall Ed. Fourth ed.)
- [34] Jones, J. (2002, 2 November). Girl With a Pearl Earring, Jan Vermeer (c1665). *The Guardian*. Retrieved at November 13 2018 from https://www.theguardian.com/culture/2002/nov/02/art
- [35] Joshi, J. J., Vaidya, D. B., & Shah, H. S. (2000). Application of Multi-Flux Theory Based on Mie Scattering to the Problem of Modeling the Optical Characteristics of Colored Pigmented Paint Films. Color Research an Application, 26(3), 234-245
- [36] Kronander, J. (2015). *Physically Based Rendering of Synthetic Objects in Real Environments*. Linköping University, Norrköping
- [37] Kubelka, P., & Munk, F. (1931). An Article on Optics of Paint Layers. In Fuer Tekn. Physik, 12 593-609
- [38] Laurie, A. P. (1937). The Refractive Index of a Solid Film of Linseed Oil Rise in Refractive Index with Age. *Proceedings of the Royal Society of London. Series A, Mathematical and Physical Sciences*, 159(896), 123-133
- [39] Lee, K. J., Kim, D. H., Yun, I. D., & Lee, S. U. (2007). Three-dimensional Oil Painting Reconstruction with Stroke Based Rendering. *The Visual Computer*, 23(9-11), 873-880

- [40] Levin, A., Glasner, D., Xiong, Y., Durand, F., Freeman, W., Matusik, W., & Zickler, T. (2013). Fabricating BRDFs at High Spatial Resolution Using Wave Optics. *ACM Transactions on Graphics*, 32(4)
- [41] Light and Materials. (2019). Retrieved at April 20 2019 from https://www.jawoollam.com/resources/ellipsome-try-tutorial/light-and-materials
- [42] Loon, A. v. (2019, February 27 2019). [Personal Communication on Samples Girl with a Pearl Earring]
- [43] Matusik, W., Pfister, H., Brand, M., & McMillan, L. (2003). A Data-Driven Reflectance Model. *ACM Transactions on Graphics*, 22(3), 759-769
- [44] Mauritshuis. Meisje met de parel. Mauritshuis Museum, Den Haag.
- [45] McCrackin, F. L., Passaglia, E., Stromberg, R. R., & Steinberg, H. L. (1963). Measurement of the Thickness and Refractive Index of Very Thin Films and the Optical Properties of Surfaces by Ellipsometry. *Journal of Research*, 67A(4), 363-377.
- [46] Mouw, T. (2018). LAB Color Values. Retrieved at April 27 2019 from https://www.xrite.com/blog/lab-color-space
- [47] Nave, C. R. (2017). Refraction of Light. Retrieved at March 3 2019 from http://hyperphysics.phy-astr.gsu.edu/hbase/geoopt/refr.html#c3
- [48] New Light for Old Master Paintings. (2015). Retrieved at November 13 2018 from https://www.osa.org/en-us/about\_osa/newsroom/news\_releases/2015/new\_light\_for\_old\_master\_paintings/
- [49] O'Hanlon, G. (2013, June 12 2013). Why Some Paints are Transparent and Others Opaque. Retrieved at May 6 2019 from https://www.naturalpigments.com/artist-materials/transparent-opaque-paints/
- [50] Polikreti, K., Othonos, A., & Christofides, C. (2005). Optical Characterization of Varnish Films by Spectroscopic Ellipsometry for Application in Artwork Conservation. *Applied Spectroscopy*, 59(1), 94-99
- [51] Rabal, A. M., Ferrero, A., Campos, J., Fontecha, J. L., Pons, A., Rubiño, A. M., & Corróns, A. (2012). Automatic Gonio-Spectrophotometer for the Absolute Measurement of the Spectral BRDF at in- out-of-plane and Retroreflection Geometries. *Metrologia*, 49, 213-223
- [52] Ray Tracing. (2019). Retrieved at April 20 2019 from https://developer.nvidia.com/discover/ray-tracing
- [53] Steadman, P. (2011, 17-02-2011). Vermeer and the Camera Obscura. Retrieved at November 13 2018 from http://www.bbc.co.uk/history/british/empire\_seapower/vermeer\_camera\_01.shtml
- [54] Stich, M. (2018). Introduction to NVIDIA RTX and DirectX Ray Tracing. Retrieved at May 12 2019 from https://developer.nvidia.com/discover/ray-tracing
- [55] Taft, W. S., & Mayer, J. W. (2000). The Science of Paintings. New York: Springer-Verlag New York, Inc.
- [56] Tan, J., DiVerdi, S., Lu, J., & Gingold, Y. (2018). Pigmento: Pigment-Based Image Analysis and Editing. *IEEE Transactions on Visualization and Computer Graphics*
- [57] Vandivere, A. (2018, 9 November 2018). [Personal Communication on MMdP for TU Delft\_samples 19 and 26]
- [58] Viguerie, L. d., Walter, P., Laval, E., Mottin, B., & Solé, V. A. (2010). Revealing the sfumato Technique of Leonardo da Vinci by X-Ray Fluorescence Spectroscopy. *Angewandte Chemie International Edition*, 49(35), 6125-6128
- [59] Weidlich, A., & Wilkie, A. (2007). *Arbitrarily Layered Micro-Facet Surfaces*. Paper presented at the GRAPHITE, Perth, Australia.
- [60] Weld dye. (2016). Retrieved at March 8 2019 from http://cameo.mfa.org/wiki/Weld\_dye
- [61] Wetering, E. v. d. (2000). Rembrandt: The Painter at Work. Amsterdam University Press

- [62] Yan, N., Baar, T., Segovia, M. O., & Allebach, J. (2016). Fitting analytical BRDF models to low-resolution measurements of light scattered from relief printing samples. Paper presented at the IS&T International Symposium of Electronic Imaging 2016
- [63] Yushanov, S., Crompton, J. S., & Koppenhoefer, K. C. (2013). *Mie Scattering of Electromagnetic Waves*. Paper presented at the COMSOL, Boston
- [64] Zaman, T., Dik, J., & Jonker, P. (2013, November 2013). Modern Digitization for Cultural Heritage: Simultaneous Capture of 3D Topography and Colour in Paintings of Van Gogh and Rembrandt. *AR[t] Augmented Reality, Art and Technology*, 56-59
- [65] Zaman, T., Jonker, P., Lenseigne, B., & Dik, J. (2014). Simultaneous capture of the color and topography of paintings using fringe encoded stereo vision. *Heritage Science*, 2(23)
- [66] Zegeling, M. (2017). Het Geheim van de Meester. Amsterdam: MarkMedia & Art

# Appendix A - Sample Preparation

#### A1- Overview of samples

The preparation of the paint and glaze samples is described in this appendix. It includes an overview of all the samples that were created and which analysis is done on each sample.

The collection of samples is listed in Table A.1 with in the first column the sample names. In the second column the substrates on which the paint was applied are listed:

- opacity chart (OC)
- microscope slide (MS)
- microscope cover slide (CS)
- single crystal silicon wafer (W)
- canvas board (CB)

Next to the samples from the original painting, two sets of reconstructions are made. One set is created in corporation with Technical Art History student Fahed Ibrahim at the University of Amsterdam (UvA). These samples are made with pigments similar to the pigments present in the painting. The pigments were ground with heatbodied linseed oil which has been at the window sill of Abbie Vandiver causing the oil to thicken.

Sample name	Applied on	Sample description	Optical microscopy	Absorption (micro spectrophoto-meter)	Ellipsometry	BRDF
OP_19		Original Painting				
		dispersion, bottom right				
		corner, property of				
		Mauritshuis (sample				
		1687-19, 4048 A)				
OP_26		Original Painting thin				
		section, left from				
		forehead, property of				
		Mauritshuis (sample				
RU_1	OC, MS, CS,	1687-26, 4054 B) Reconstruction UvA,				ОС
NO_1	W	charcoal black				OC
RU_1a	MS	Charcoal black				
RU_2	OC, MS, CS,	Weld				ОС
	W	110.0				
RU 2a	MS	Weld				
RU_3	OC, MS, CS,	Indigo				ОС
_	W					
RU_3a	MS	Indigo				
RU_3b	MS	Indigo				
RU_4	OC, MS, CS	Weld and Indigo mixed				OC, MS
		(ratio 30:1)				
RU_4a	MS	Weld and Indigo mixed				
		(ratio 30:1)				
RU_5	OC, MS, CS,	Weld and Indigo mixed				OC, MS
DII E	W	(ratio 20:1)				
RU_5a	MS	Weld and Indigo mixed				
RU_6	OC, MS, CS	(ratio 20:1) Charcoal black				
RU_6a	MS	Charcoal black				
RM_1	MS, CS, CB	Reconstruction of				СВ
I/I/VI_±	1013, C3, CB	Modern Paint, Ivory				CD
		black				
RM_2	MS, CS, CB	Stil de grain				
RM_3	MS, CS, CB	Indigo				
RM_4	MS, CS, CB	Stil de grain with added				
		linseed oil				
RM_5	MS, CS, CB	Indigo with added				
		linseed oil				
RM_6	MS, CS, CB	Stil de grain and Indigo				MS, CB
		mixed (ratio 3:1)				
RM_7	MS, CS, CB	Stil de grain with added				
		linseed oil and Indigo				
		with added linseed oil mixed (ratio 3:1)				
RM_8	MS, CS	Linseed oil				
RM_9	MS, CS	Linseed oil				
RM_10	MS, CS, CB	Ivory black				
RM_11	MS, CS, CB	Stil de grain			1	
RM_12	MS, CS, CB	Indigo				
RM_13	MS, CS, CB	Stil de grain with added				
±3	, 05, 05	linseed oil				
RM_14	MS, CS, CB	Indigo with added				
	1, 22, 32	linseed oil				

RM_15	MS, CS, CB	Stil de grain mixed with Indigo (ratio 3:1)		
RM_16	MS, CS, CB	Stil de grain with added linseed oil and Indigo with added linseed oil mixed (ratio 3:1)		
RM_17	MS, CS	Linseed oil		

### A.2- Reconstructions made with pigments which can be found in the original painting

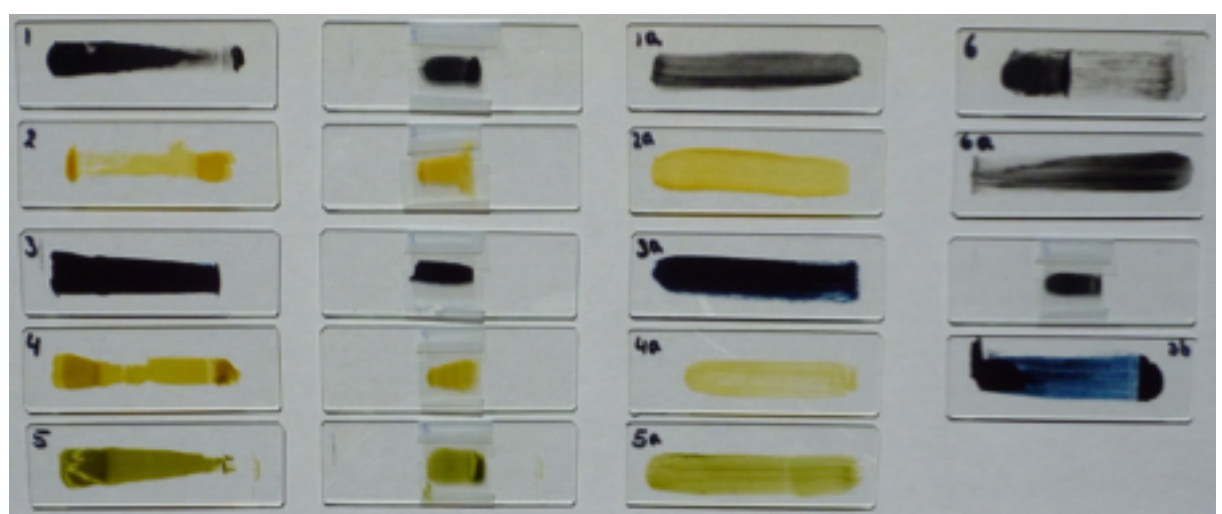


Figure A1.1 Reconstructions created using pigments found in the original painting. First two columns applied using a drawdown bar  $(50\mu\text{m})$ . 1) Charcoal black  $(RU_1)$ , 2) Weld  $(RU_2)$ , 3) Indigo  $(RU_3)$ , 4) Weld and Indigo mixed in 30:1 ratio  $(RU_4)$ , 5) Weld and Indigo mixed in 20:1 ratio  $(RU_5)$ . Third column applied by brush, 1a) Charcoal black  $(RU_1)$ , 2a) Weld  $(RU_2)$ , 3a) Indigo  $(RU_3)$ , 4a) Weld and Indigo mixed in 30:1 ratio  $(RU_4)$ , 5a) Weld and Indigo mixed in 20:1 ratio  $(RU_5)$ . Fourth column, 6) Charcoal black applied by drawdown bar  $(50\mu\text{m})$  on microscope slide and microscope cover slide  $(RU_6)$ , 6a) Charcoal black applied by brush  $(RU_6)$ , 3b) Indigo applied by drawdown bar  $(50\mu\text{m})$  on microscope slide  $(RU_3)$ .

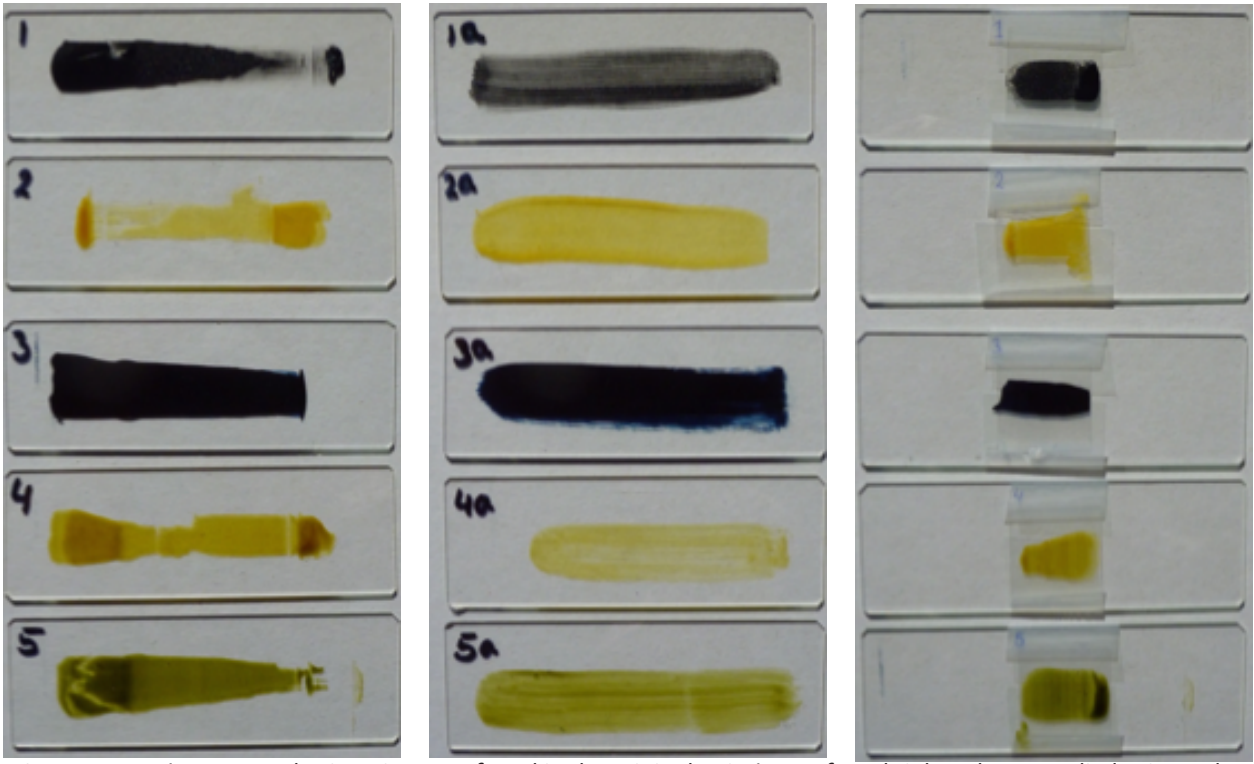


Figure A1.2 Reconstructions created using pigments found in the original painting. Left and right column applied using a drawdown bar (50µm) onto microscope slides (left) and microscope cover slides (right). 1) Charcoal black, 2) Weld, 3) Indigo, 4) Weld and Indigo mixed in 30:1 ratio, 5) Weld and Indigo mixed in 20:1 ratio. Right column applied by brush, 1a) Charcoal black, 2a) Weld, 3a) Indigo, 4a) Weld and Indigo mixed in 30:1 ratio, 5a) Weld and Indigo mixed in 20:1 ratio.

application method and the substrate on which the paint is applied are listed. Table A.2 Overview of the preparation of the reconstructions with pigments similar to the pigments found in the original painting. The paint recipes, the

			B (1a) B (6a)			
	S (4b)	D (6)	D (6)			5 min. (RU_1, RU_6)
	B (4a)	D (1)	D (1)	D (4)	D (4)	Charcoal black from beech 47800, Kremer (0.502 g) mixed with linseed oil (0.570 g) ground for
-52	S (3b)		B (5a)			(RU_5)
2	B (3a)	D (5)	D (5)	D (3)		Mixture of Weld and Indigo (ratio roughly 20:1)
			B (4a)			(RU_4)
		D (4)	D (4)		D (3)	Mixture of Weld and Indigo (ratio roughly 30:1)
			B (3a)			(RU_3)
	S (2b)		D (3b)			mixed with linseed oil (0.515 g) ground for 4 min.
	B (2a)	D (3)	D (3)	D (2)	D (2)	Indigo 'tinctoria' from Couleur Garance (0.500 g)
						Pigment made April 12th 2018 by TAH (RU_2)
	S (1b)		B (2a)			mixed with linseed oil (0.100 g) ground for 3 min.
	B (1a)	D (2)	D (2)	D (1)	D (1)	Weld+potash and CaCO3 (0.230 g)
າກ wafer	Single crystal silicon wafer	Microscope cover slide	Microscope slide	Opacity chart 5C	Opacity chart 2A-2	

D = Application with drawdown bar, 50  $\mu$ m

B = Application with a brush

S = Application with a spatula

(1,2,3...) = Slide/sample number

Linseed oil used: heat bodied linseed oil from

sill Abbie Vandivere mill 'Het Pink', aged for 22 months from window

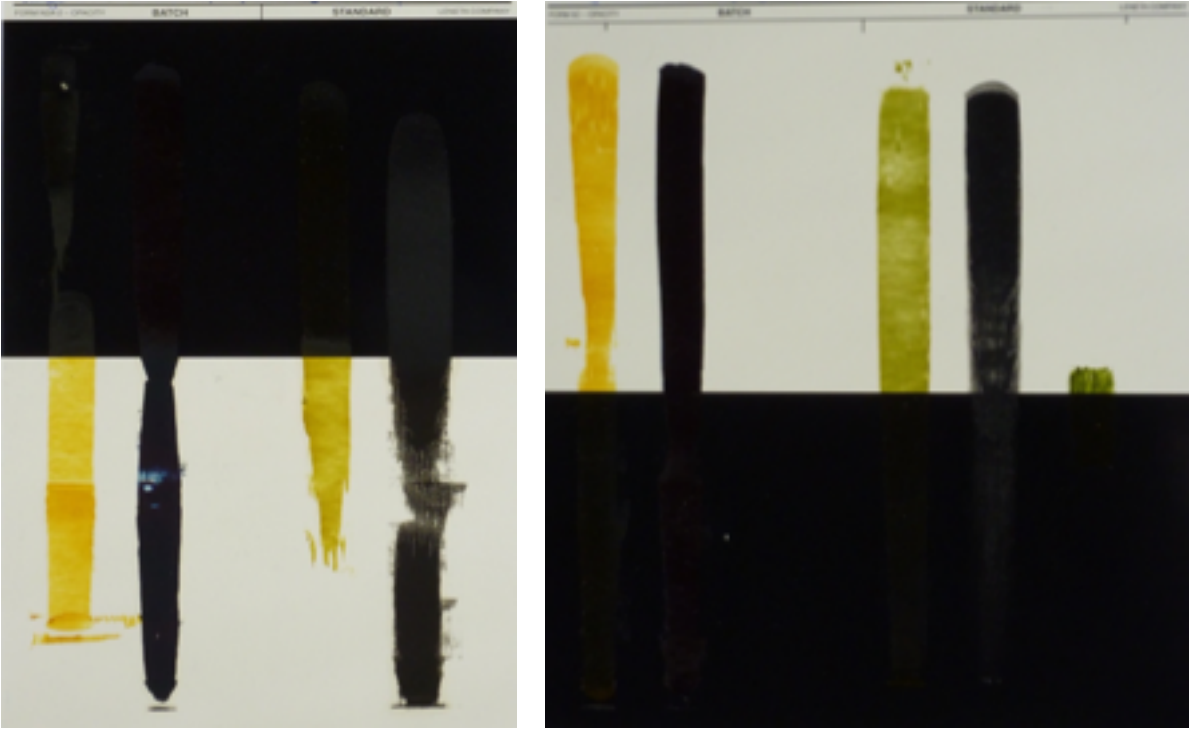
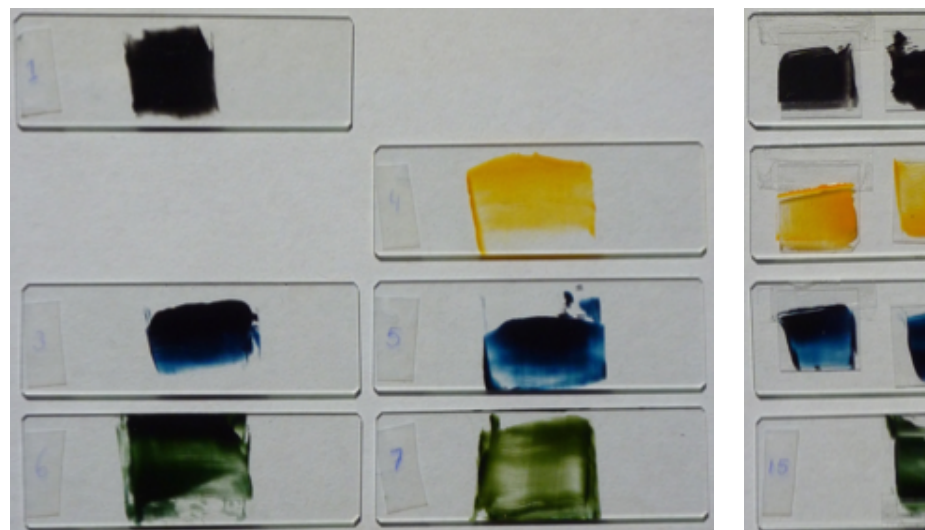


Figure A1.3 Reconstructions created using pigments found in the original painting. Left image Leneta Opacity Chart N2A-2 unsealed. Paint is applied with a drawdown bar ( $50\mu m$ ). From left to right: Weld ( $RU_2$ ), Indigo ( $RU_3$ ), Weld and Indigo mixed (30:1 ratio) ( $RU_4$ ), Charcoal black ( $RU_1$ ).

Right image Leneta Opacity Chart 5C, first 4 paints are applied with a drawdown bar (50μm), right paint applied with a brush. From left to right: Weld (RU\_2), Indigo (RU\_3), Weld and Indigo mixed (20:1 ratio) (RU\_5), Charcoal black (RU\_1), Weld and Indigo mixed (20:1 ratio) (RU\_5).

### A.3- Reconstructions made from modern paint



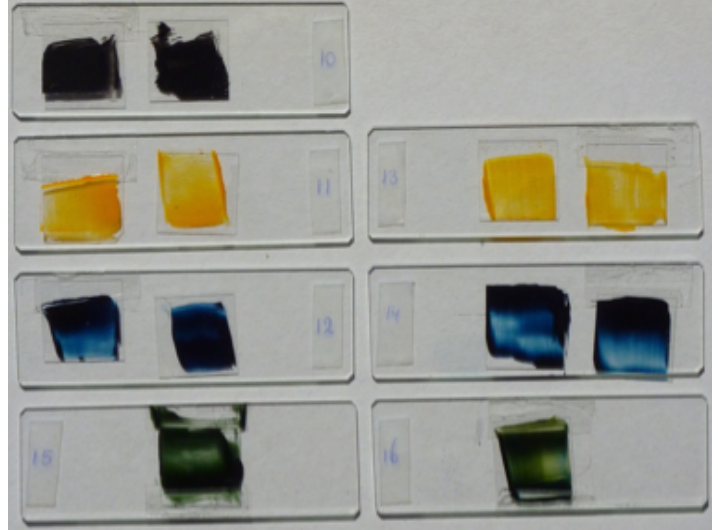


Figure A1.4 Left: Reconstructions created of modern oil paint (Rembrandt series by Talens) applied onto microscope slides using a spatula. 1) Ivory black, 2) Stil de grain, 3) Indigo, 4) Stil de grain with added linseed oil, 5) Indigo with added linseed oil, 6) Stil de grain and Indigo mixed in 3:1 ratio.

Right: Reconstructions created of modern oil paint (Rembrandt series by Talens) applied onto microscope cover slides using a spatula. 10) Ivory black, 11) Stil de grain, 12) Indigo, 13) Stil de grain with added linseed oil, 14) Indigo with added linseed oil, 15) Stil de grain and Indigo mixed in 3:1 ratio, 16) Stil de grain and Indigo with added linseed oil mixed in 3:1 ratio.

Table A.3 Overview the reconstructions made with modern paint. Ratios and substrate on which the paint is applied are listed.

	Microscope slide	Microscope cover slide	Single crystal silicon wafer
Stil de grain (Rembrandt series, Talens)	S (RM_2)	S (RM_11)	S (RM_W2a) S (RM_W2b)
Stil de grain (1.5 cm of paint from the tube) mixed with 2 drops of linseed oil			S (RM_W4a) S (RM_W4b)
Stil de grain (0.5 cm of paint from the tube) mixed with 1 drop of linseed oil	S (RM_4)	S (RM_13)	
Indigo (Rembrandt series, Talens)	S (RM_3)	S (RM_12)	S (RM_W3a) S (RM_W3b)
Indigo (1.5 cm of paint from the tube) mixed with 2 drops of linseed oil			S (RM_W5a) S (RM_W5b)
Indigo (0.5 cm of paint from the tube) mixed with 1 drop of linseed oil	S (RM_5)	S (RM_14)	
Mixture Stil de grain and Indigo (ratio 3:1)	S (RM_6)	S (RM_15)	S (RM_W6a) S (RM_W6b)
Mixture of Stil de grain and Indigo with linseed oil (ratio 3:1)	S (RM_7)	S (RM_16)	S (RM_W7a) S (RM_W7b)
Ivory black (Rembrandt series, Talens)	S (RM_1) S (RM_18)	S (RM_10)	S (RM_W1a) S (RM_W1b)
Bleached linseed oil (Talens)	S (RM_8)	S (RM_17)	S (RM_W8)
Blank	(RM_9)		(RM_W9)
S = Application with a spatula (1,2,3) = Slide/sample number			

# Graduation project MS53000



Literature study Guusje Harteveld (4007522)

Supervisors Joris Dik and Jo Geraedts

# Table of contents

1 Introduction - A painting	-3-
2 Previous research	-4-
3 Data acquisition of a painting	-6-
3.1 Optical scan - colour	-6-
3.2 Optical scan - topography	-7-
3.3 Optical scan - OCT	-7-
3.4 Optical scan - gloss	-8-
3.5 Refractive index	-8-
3.6 Ellipsometry	-8-
3.7 Absorption	-9-
4 Models	-10-
4.1 Theoretical model - Kubelka-Munk	-10-
4.2 Theoretical model - Fresnel	-11-
4.3 Computer models - digitally simulating paint	-12-
4.4 Computer models - digitally simulating paintings	-13-
5 3D printing	-17-
6 Conclusion	-20-
7 Bibliography	-21-

## 1 Introduction - A painting

The painting Girl with a Pearl Earring (c. 1665-1666) (Figure 1) by Johannes Vermeer is one of the most iconic and well-known paintings in the world. Next to Rembrandt van Rijn and Jan Steen, Vermeer is one of the famous painters from the Dutch Golden Age. Girl with a Pearl Earring shows the portrait of a girl with a blue headdress and an earring in front of a dark background. The portrait appeals to many viewers because of its appearance and mystery. There is a soft-focus effect in the painting that, up until this date, raises questions amongst art historians. Some suggest that Vermeer might have used a camera obscura to create the almost photograph-like effect of the portrait. (Jones, 2002) In the television programme Het Geheim van de Meester a test is done with a camera obscura to study the effect and compare it to the painting. The soft-focus effect in the painting



Figure 1. Girl with a Pearl Earring (c.1665-1666)
(Mauritshuis, 2018)

was visible using the camera obscura, which could be a suggestion that Vermeer might have looked through a camera obscura and used the effect as inspiration for the Girl with a Pearl Earring. (Zegeling, 2017) When comparing looking at an object through a lens and with the naked eye, the dynamic range can be significantly reduced when looking through the lens. This could result in the dark areas appearing darker and the light areas appearing lighter.

A painting is a layered structure as schematically shown in Figure 2. The canvas is the base of the painting on top of which a layer of ground paint is applied. On top of the ground, one or more layers of paint are applied which form the image of the painting. Often a varnish layer is applied on top of the paint to preserve the paint and bring out the colours and depth of the painting. (Taft et al., 2000) The optical properties of the varnish and paint determine how a painting is seen by the viewer. Light rays from a light source interact with the painting and penetrate into the layers of the painting and are reflected in different manners. In general, the surface and composition of a material influence the type of reflection. There is a distinction between specular (mirror-like) and diffuse reflection. The spectral distribution of the light source combined with the wavelengths absorbed by a material determine the colour the material appears to be to the observer. A red object appears red because the material absorbs all wavelengths of the visible spectrum except for the red.

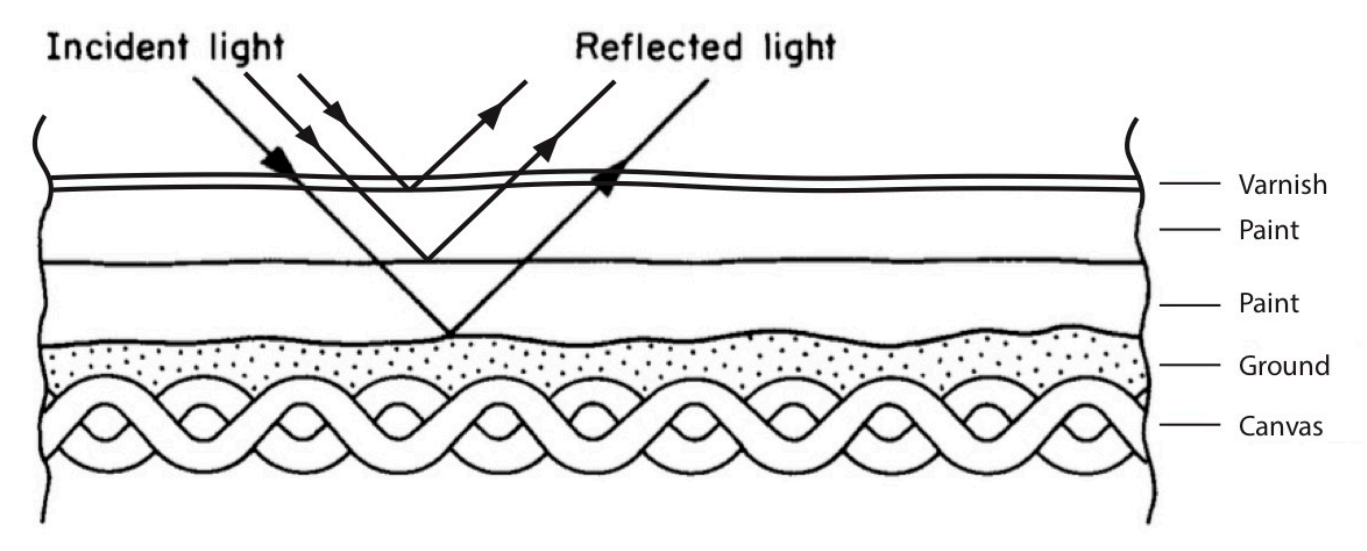


Figure 2. Schematic cross section of a painting, after Taft. (Taft et al., 2000)

#### 2 Previous research

Coming back to the Girl with a Pearl Earring, in 1994-1995 the painting was examined and restored extensively at the Mauritshuis museum. (Groen et al., 1998) During the examination it was confirmed that earlier restorations had been rough. Several pieces of paint had become dislodged and some were stuck upside down on top of the paint surface. These pieces of paint provided samples from the painting without having to cut into the painting. The old retouches appeared to have shielded the original paint from moisture and light. That is probably the reason why areas underneath the retouches were darker compared to the other areas. (Groen et al., 1998) Figure 3 shows a cross section of the background and the green colour of the paint is visible in the left image. The cross section originates from the background between the left side of the painting and the forehead of the girl (Figure 4, sample 26).

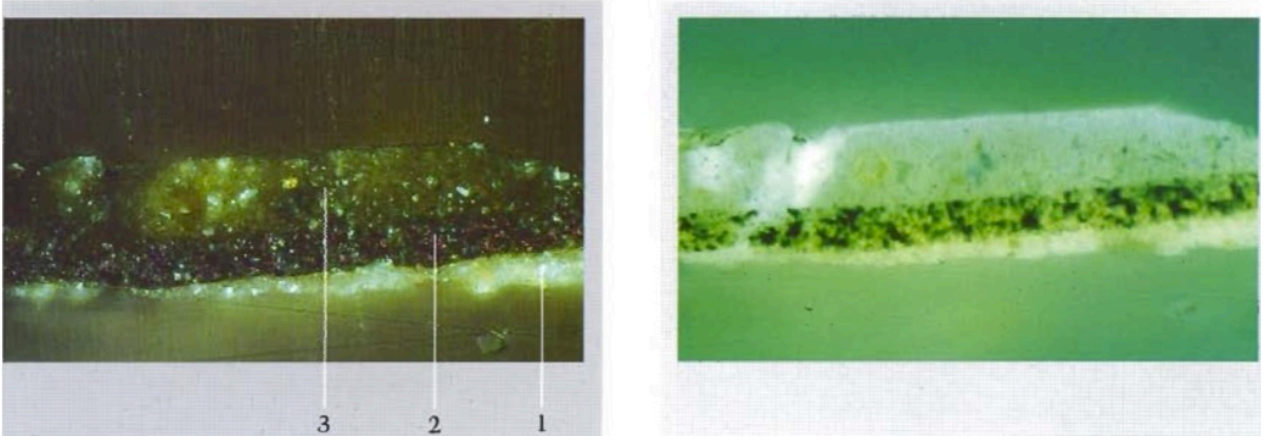


Figure 3. Cross section of a background sample (sample 26) left of the forehead of Girl with a Pearl Earring. The left image was taken under regular light, the right image under fluorescent light both with 305x magnification. 1 Indicates the ground, 2 the black underpaint of 12  $\mu$ m thickness and 3 is the translucent green glaze layer of 28  $\mu$ m containing weld, chalk, indigo and a little red ochre. (Groen et al., 1998)

In the cross section in Figure 3 three distinct layers are visible. The bottom layer (1) is the ground, consisting of chalk, lead white, a little fine ochre and black. The 12  $\mu$ m middle layer (2) is a black underpaint, according to the latest research probably consisting of a combination of charcoal black and bone black, pigments created by burning wood and bones. The top layer visible in the cross section (3) is a 28  $\mu$ m thick translucent green layer

consisting of ultramarine, indigo, chalk and a little red ochre. The High-Performance Liquid Chromatography (HPLC) results show the presence of a proteinaceous material, probably weld which might originate from woollen textiles dyed with weld used as a pigment in the paint. (Vandivere, 2018) Weld is a natural yellow dye obtained from the Reseda luteola and was used for dying woollen and silk materials. It is very transparent and therefore an ideal pigment for glazes. (Janson)

The background of the painting, around the image of the girl (Figure 4), appears black at first sight. However, the glaze layer on top of the dark underpaint is a green translucent glaze



layer present as seen in the cross section. The glaze is applied on top of a black layer of paint. The question rises why the glaze layer is applied on top of a black layer and whether the presence of the glaze layer influences the visual appearance of the background compared to only a black layer of paint. A hypothesis is that the combination of the glaze layer and the textured black paint beneath it cause the soft-focus or camera obscura effect. To test this, research should be done on the role of the glaze layer and whether the effect can be simulated to relate it to the characteristic appearance of the portrait painted by Vermeer.

Figure 4. Overview of samples available of the painting (Vandivere, 2018)

To test the effect of the glaze layer, a computer model based on the properties of the painting could be used to simulate the appearance of the paint layers. This computer model could perhaps also be used as a base for a 3D printed reproduction of a painting. Recent research in the reproduction of fine art has focused on reproduction by 3D printing however the reproduction of gloss and texture could still be improved. (Elkhuizen et al., 2014) The digital reproduction of paint has mainly focussed on car paint for car commercials and animating the application of paint on a canvas. The current state of the research can be categorised into three sections. Firstly, novel techniques are used to take measurements of physical parameters of paint and paintings in order to collect data and gather knowledge on the properties of paintings. Secondly, models which use the gathered data and transform this into reproducible data, for example an as realistic as possible digital render of paint. Lastly the 3D printing where the aforementioned models can be applied to create a physical reproduction of the art work.

## 3 Data acquisition of a painting

To make cultural heritage more accessible to the general public, museums tend to digitize their collections. The database created in this way is useful for accessibility, education, art historical research and conservation and restoration purposes. Paintings are seen as a 2D representation of the 3D world; however, a painting does have a certain topography and is not completely flat. The images in the database are a 2D representation of the paintings, the topography information of the painting is lost in the images. Next to photographs and examinations using a microscope, more advanced techniques are being developed to register physical parameters of paintings. Physical parameters such as colour, gloss, texture and translucency influence each other and the visual appearance of a painting (Figure 5). This data represents the 3D character of the paintings in a more precise manner and can be used for 3D printed reproductions in a later state.

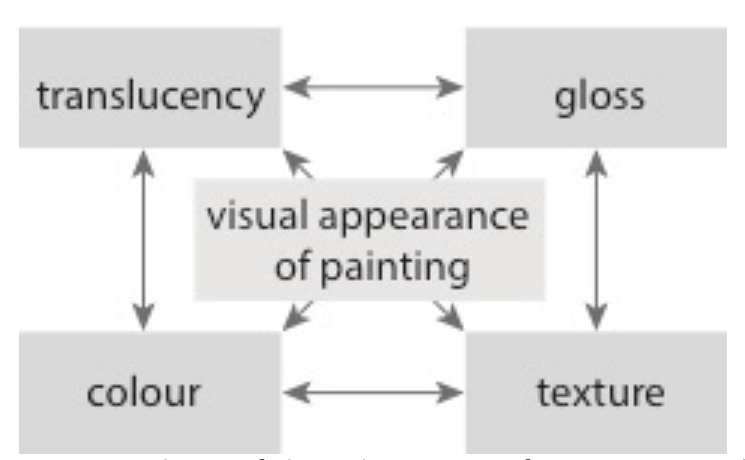


Figure 5. Relation of physical properties of a painting to each other and the visual appearance of a painting.

### 3.1 Optical scan - colour

Former graduate student Zaman developed a hybrid system of a stereo vision camera rig and a fringe projection to collect high resolution topography and colour data of a painting. The scanner provided the researchers with enough data to recreate paintings of Van Gogh and Rembrandt using a 3D printer of Océ. (Zaman et al., 2013; Zaman et al., 2014) The reconstructions are created by a 3D relief print with the addition of one or several ink layers on top of the relief. This leads to a print with minimal translucency and gloss variations. Therefore, the 3D print is similar to 2D posters except for the topography. Research by Elkhuizen on the capturing (Figure 6) and reproduction of gloss variation of the paint layers has led to more life-like reproductions of fine art. Variations in gloss give the 3D print a different appearance compared to a 2D poster and therefore makes it look more like the original painting. The colour matching could however be improved as could the edge sharpness. By changing the illumination at the moment of capture and viewing or the amount of print colours used could improve the colour matching of the print to the original. The sharpness of the edges needs further research, the cause of the lack of sharpness is not clear yet but could have something to do with the size of the ink drops and the drying time. Further research is also needed on the viewing distance and therefore resolution of the prints and whether this is attainable by the 3D scanner and printer. (Elkhuizen et al., 2017; Elkhuizen et al., 2014)

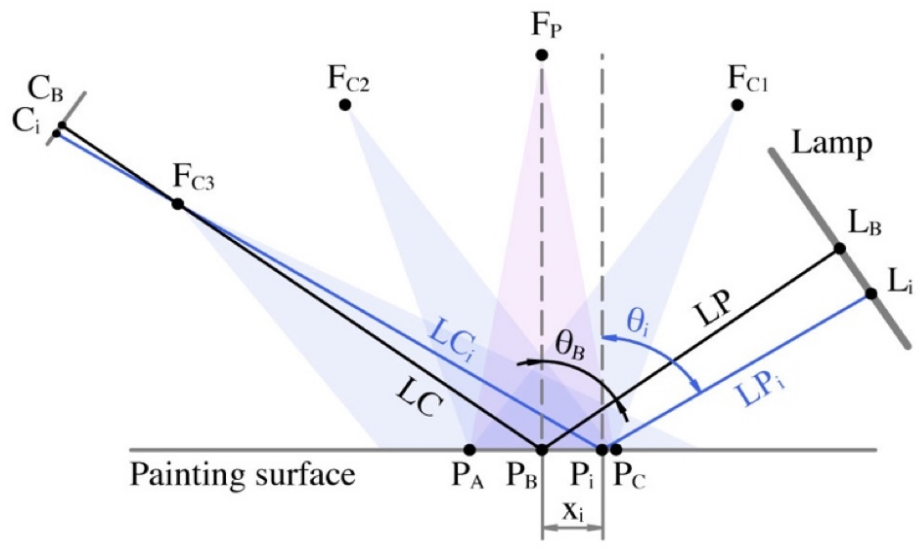


Figure 6. Setup of scanner by Elkhuizen measuring gloss of the surface of a painting. The camera is positioned at C on the left and a lamp positioned on the right. The Brewster angle is based on the averaged refractive index of oil paint and is used as the angle between line  $F_pP_B$  and  $L_BP_B$ . (Elkhuizen et al., 2017)

## 3.2 Optical scan - topography

The surface topography of a painting is an important indicator of the fact that a painting is not a 2D object. Van Hengstum used a stereo camera setup related to the one used by Elkhuizen to visualise the craquelures present in Girl with a Pearl Earring. The craquelures could be visualised in 3D and it is clearly visible that they consist of a small ridge next to the valley. The setup Van Hengstum is practically used to create a height map of the surface of the painting. (Van Hengstum et al., 2018)

#### 3.3 Optical scan - OCT

A technique recently applied for the first time in the field of fine art is Optical Coherence Tomography (OCT). The technique is based on the differences in the penetration of light in the different layers of a structure. A beam of light is split where half of the beam is directed to a reference mirror and the other half of the beam is directed to the sample. The light scattering of the surfaces is compared to the reference beam reflected of the mirror. By doing so, the penetration depth of the light into the sample can be determined. Repeating this over the area of the sample, will result in a cross-sectional map of the sample which represents the 3D build-up of the layers of the sample. ("New Light for Old Master Paintings," 2015) OCT is usually applied in medical situations where it is used for example for the examination of eyes. The depth resolution of the regular system does not meet the accuracy required for the examination of the thin layers present in a painting. To accommodate for this, Cheung used ultra-high resolution Fourier domain OCT to examine the stratigraphy of the paint and varnish layers. Because of its high dynamic range and depth selection capabilities it is a very sensitive technique for revealing preparatory drawings and the topography of the paint layers. The technique can be applied to research on the changes that occur in the ageing of a painting or the cleaning process in a case of restoration. (Cheung et al., 2015) During recent research on the Girl with a Pearl Earring, OCT scans were made of the painting by Callewaert. (Callewaert, 2018) Due to the absorbance of the black layer in the background of the Girl with a Pearl Earring, no data is retrieved from underneath that layer. A dark layer of paint is therefore a limiting factor in the use of OCT scans in the examination of paintings.

#### 3.4 Optical scan - gloss

Next to the measurements of the topography of the painting surface and paint layers, the optical properties of the paint itself are also necessary in order to simulate the visual appearance of the painting. The absorption and reflection of light by the paint influences the colour of the paint and next to the topography is the reflection also an indication of the glossiness of the paint. (Elkhuizen et al., 2018) The refractive index (RI) of the materials provides the relation between the transmitted and reflected light at an interface between two materials. These factors all influence the appearance of the paint and therefore need to be taken into account when simulating the visual appearance of the paint.

#### 3.5 Refractive index

The addition of a varnish layer on top of a painting can alter the appearance of the painting drastically. The change depends on the properties of the paint layer, the varnish, the method of application and the optical contact between the varnish and the paint layer. The varnish layer usually reduces the surface roughness which can result in an increase in contrast, spatial image quality and colour gamut. (Taft et al., 2000) The refractive index of the varnish compared to that of the underlying paint is an indication of how transparent the varnish layer appears to be to the human eye. To visualise the effect of the RI of the varnish layer on the appearance of a painting, Berns created a computer simulation to model varnish layers with different RI on paintings. (Berns et al., 2003) The effect of the refractive index on the appearance of a painting is made clear by Berns. In the field of conservation and restoration of paintings, determination of the RI is usually done using the immersion method. In order to determine if a pigment for restoration will appear similar to the pigment present in the painting its refractive index (RI) compared to the binding medium can be useful. The closer the RI of the pigment is to the RI of the binding medium, the more transparent it will appear. By immersing pigment in binding medium of a known RI, an estimation can be made of the RI of the pigment. In order to get a close approximation of the RI of the pigment, a set of oils with different, known RI need to be used. (Batsanov et al., 2016) For conservation and restoration purposes, the exact refractive index is often not necessary so usually the pigment is only tested in commonly used binding media.

#### 3.6 Ellipsometry

Ellipsometry is a technique which can be used for the exact determination of the refractive index and thickness of a very thin film (in the order of nanometers) on a solid surface. The technique is based on the measurement of changes in the polarisation state of light after reflection from a surface. Due to the thickness and RI of the film, there is an additional change in the light reflected from the film compared to the light reflected from the surface on which the film is applied. These changes can be used to determine the thickness and refractive index (per wavelength) of the film. (McCrackin et al., 1963) The technique discussed here can be applied for the optical characterisation of varnish films on paintings which can be useful in the field of conservation and restoration. Polikreti examined two different fresh varnishes using spectroscopic ellipsometry in order to determine whether they could determine the optical properties of the varnishes, the thicknesses and whether a distinction could be made between the two varnishes. This technique shows promising results as it might be a non-destructive method to determine the varnish present on a painting which is useful for conservation and restoration purposes. (Polikreti et al., 2005) The absence of pigment particles in the varnish, compared to paint, probably contributed to the

promising results of this research. Up until now, the RI and thickness of paint layers have not been examined using ellipsometry.

### 3.7 Absorption

As mentioned earlier, the absorption and reflection of the paint influence the colour which is perceived by the viewer. The reflected wavelengths are registered by our eyes and brain which results in the observed colour of the object. The reflection of an object is wavelength dependent, which means that an object appears different under different wavelengths. This can be caused by the difference in the wavelength distribution emitted by light sources. The reflection and absorption can be measured using a spectrophotometer. For extremely small samples, for example paint samples, a micro spectrophotometer can be used to measure the absorption of an area with a resolution up to 1 by 1  $\mu$ m. A possible setup for a micro spectrophotometer is shown in Figure 7 where a spectroscopic segment is added to a regular microscope. The microscope with transmission illumination contains a condenser which focusses the light onto the sample from below. The microscope objective is used to collect the light transmitted through the sample and focus it on the spectrophotometer aperture. This spectrophotometer measures the intensity of the light transmitted through the sample per wavelength. This can be processed into an absorption spectrum of the sample.(Craic, 2012)

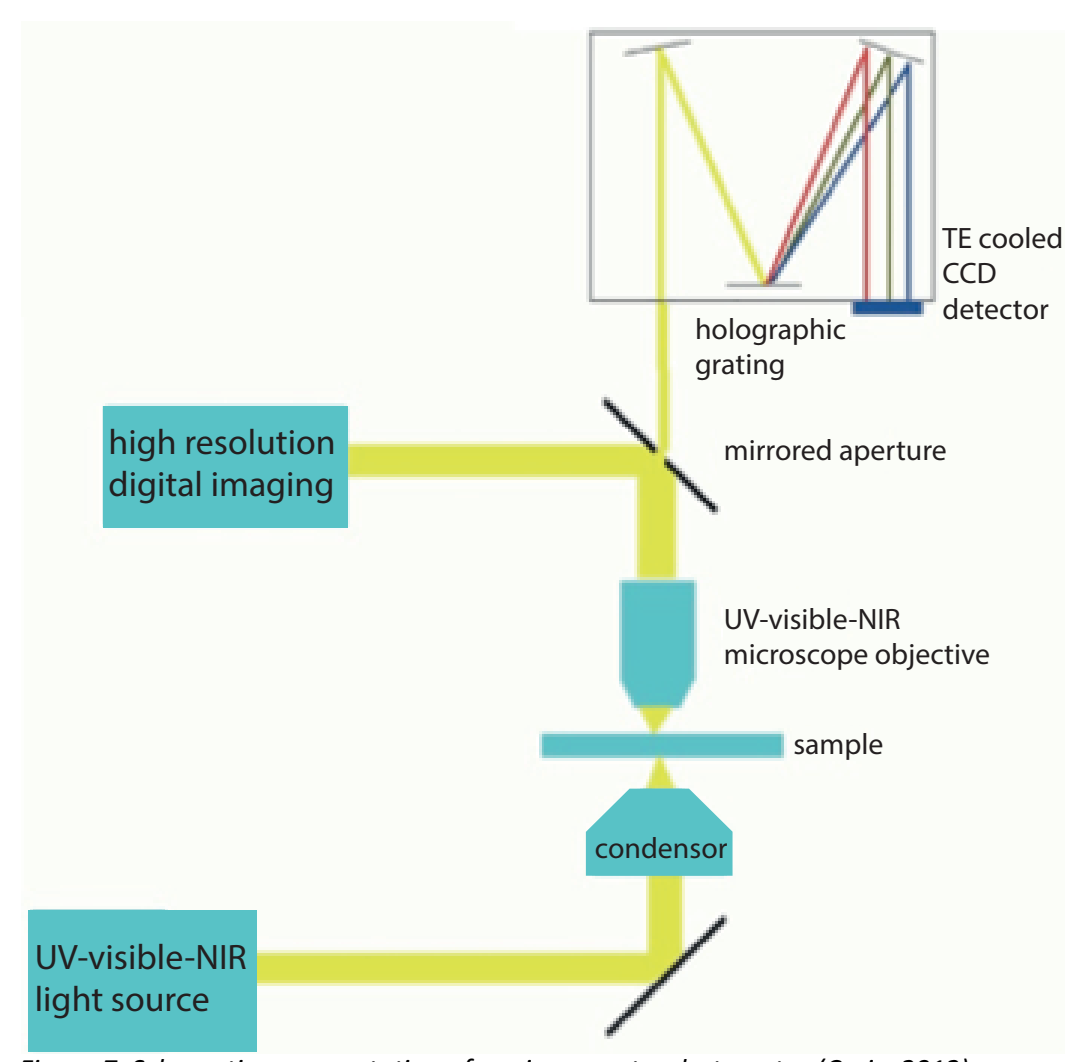


Figure 7. Schematic representation of a micro spectrophotometer. (Craic, 2012)

Reflection measurements are for example done by Geldof to retrieve input for the Kubelka-Munk theory mentioned below to simulate the original appearance of the Field with irises near Arles painting by Van Gogh. The painting degraded significantly over the past ninety years and the aim of the research was to digitally reconstruct the original appearance of the painting. Geldof calculated the absorption and reflection parameters of different mixtures of paint in order to extrapolate these and to determine what would have been the ratio of the original paint and therefore the appearance of the painting when it was just painted. (Geldof et al., 2018)

### 4 Models

Simulating the optical behaviour of paint can be done by developing a model which could be used to process the measured physical data of a painting to perception parameters in order to create a digital visualisation or 3D print. Several models are available and further developed to fit the properties of a painting, digital model and 3D print. The models can be divided into the theoretical models and the applications of the theoretical models.

#### 4.1 Theoretical model - Kubelka-Munk

The Kubelka-Munk (K-M) theory is used to model the behaviour of light in multi-layer structures. The most simplified version of the K-M theory is based on the optical behaviour of a single layer on top of a substrate. The albedo of the surface of a material and the intensity of a light ray incident on the surface influence the amount of light that is reflected from the surface. The intensity of the light ray incident on the layer surface (I) multiplied with the albedo (H) of the surface results in the reflected (J) light, which is a portion of the incident light. In the paint layer, at a point at distance x from the surface, the light fluxes going into and out of the paint layer are given by equation 2.1. The intensity of light going downwards into the layer is given by i in equation 2.1. The intensity of the light going upwards due to reflection, refraction and diffraction is given by j. The absorption constant (s) and scattering constant (r) influence the portion of incident light being reflected and absorbed. The scattering constant is determined by the scattering properties of the pigment particles and the absorption constant is determined by the absorption of the bulk material which is mainly the binding medium of the paint. (Kubelka et al., 1931)

$$\begin{array}{rcl} -di &=& -(r+s)i\;dx+r\;j\;dx\\ dj &=& -(r+s)j\;dx+r\;i\;dx \end{array}$$
 eq. 2.1

For a thin layer, some of the light is also transmitted through the layer, this can then get to the surface of a second layer. This flux of light within the layer is used for the prediction of the behaviour of a stack of materials. (Kubelka et al., 1931) The classical version of the theory is applicable in the case of strongly scattering layers which are in optical contact with each other. The Kubelka-Munk model has been used by Geldof in the investigation of the original colour used by Van Gogh when painting his Field of irises in Arles. To predict the measured reflection of the paint, an adapted version of the K-M theory (eq. 2.2), the Saunderson correction (eq. 2.3) was used.

$$R_{t} = \frac{(a+b)(a-b-R_{g})exp(-2bSD) - (a+b-R_{g})(a-b)}{(a-b-R_{g})exp(-2bSD) - (a+b-R_{g})}$$
eq. 2.2

$$a=1+rac{K}{S}$$
 
$$b=\sqrt{a^2-1}$$
 eq. 2.2a

R<sub>t</sub> is the theoretical reflectance of the paint including the influence from the substrate. The thickness of the paint layer is given by D, S is the scattering parameter and K the absorption parameter.

$$R_{m} = \alpha k_{1} + \frac{(1 - k_{1})(1 - k_{2})R_{t}}{1 - k_{2}R_{t}}$$
 eq. 2.3 
$$\left(\frac{K}{S}\right)_{mixture} = \frac{c_{1}K_{1} + c_{2}K_{2} + \dots + c_{N}K_{N}}{c_{1}S_{1} + c_{2}S_{2} + \dots + c_{N}S_{N}}$$
 eq. 2.4

The measured reflection data was used as input for the relationship proposed by Duncan (eq. 2.4) to determine the reflectance factors of a mixture of N pigments with weight concentration c. This was used as a basis to determine the appearance of the original paint and create a digital reproduction of the original painting. (Geldof et al., 2018)

#### 4.2 Theoretical model - Fresnel

When a light ray travels from one medium to another, the wave is bent when it crosses the interface between the two different media. The strength of this refraction depends on the refractive indices of the materials which are characteristic for the materials. The refractive index of a material is the ratio between the speed of light through vacuum compared to the speed with which light travels through that particular material. The Fresnel equations (eq. 2.5) relate the refractive indices and incident angle with the reflection and transmission of the light into a medium.  $R_s$  and  $R_p$  are the reflection coefficients that correspond to the perpendicular and parallel directions to the surface.(Elkhuizen et al., 2017)

$$R_{s}(\theta) = \left(\frac{n_{1}\cos\theta_{i} - n_{2}\cos\theta_{t}}{n_{1}\cos\theta_{i} + n_{2}\cos\theta_{t}}\right)^{2}$$

$$R_{p}(\theta) = \left(\frac{n_{1}\cos\theta_{t} - n_{2}\cos\theta_{t}}{n_{1}\cos\theta_{t} + n_{2}\cos\theta_{t}}\right)^{2}$$
eq. 2.5

When the refractive index of medium 2 (Figure 8) is larger than medium 1, the angle of the transmitted light ray with the normal is decreased compared to the angle of incidence. Snell's Law relates the refractive indices of the two media and the propagation angles of the light rays. Snell's Law is derived from the Fresnel equations and can be seen as a simplified version of these equations, suitable for dielectric materials. (Jenkins et al., 2001; Nave, 2017)

Elkhuizen used the Fresnel equations and the simplified Snell's law (eq. 2.6) to determine the Brewster angle during the gloss measurements of painting surfaces.

$$\frac{n_2}{n_1} = \frac{\sin(\theta_i)}{\sin(\theta_t)} \quad \Rightarrow \quad \cos(\theta_t) = \sqrt{1 - \left(\frac{n_1}{n_2}\sin(\theta_i)\right)^2}$$
 eq. 2.6

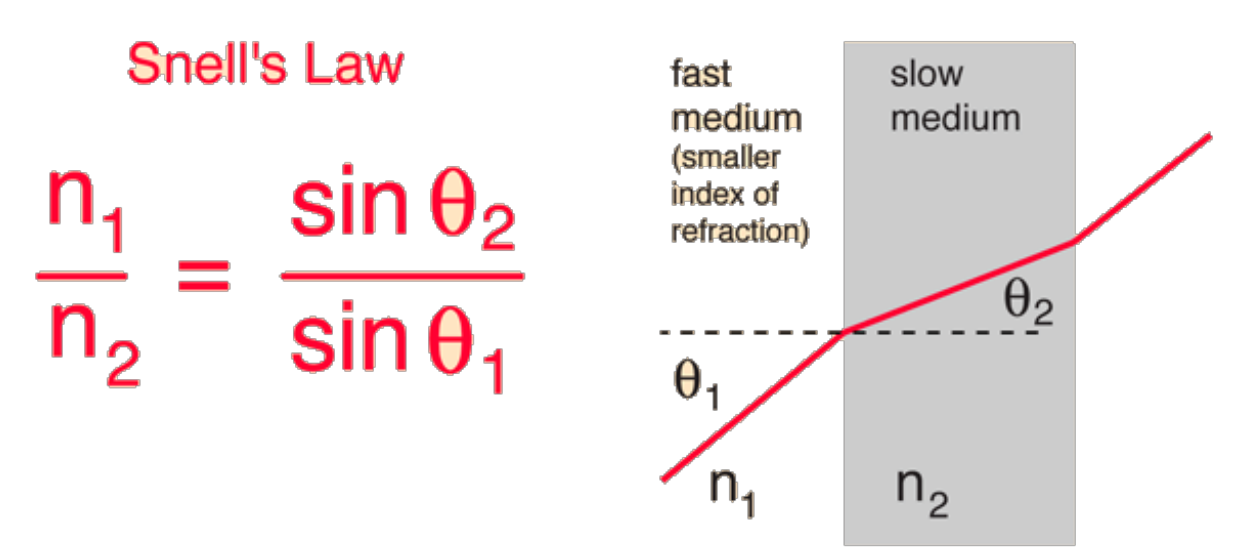


Figure 8. Snell's Law relating the refractive indices to the angles to the normal of the refracted beam. The fast medium 1 has a smaller refractive index compared to medium 2, resulting in a smaller  $\theta_2$  compared to  $\theta_1$ . (Nave, 2017)

The aforementioned Fresnel equations describe the reflection and transmission of electromagnetic waves at an interface. Different from Kubelka-Munk, Fresnel uses the refractive indices of materials and the angles of the light beams to determine the reflection and transmission. Scattering of pigment particles in a paint layer are not considered in the Fresnel model.

## 4.3 Computer models - digitally simulating paint

Based on Kubelka-Munk two-flux and four-flux computer models are designed to simulate the spectral behaviour of layered materials. (Hébert et al., 2016) A discrete version can be used in the case of a stack of non-scattering materials. This poses a limitation of the K-M theory, the layers within the stack need to be in optical contact in order for the model to work. The classical and discrete versions are the most general of the theory. Four other versions meant for different stacks are discussed by Hébert. The continuous-symmetrical version for cases of uniform scattering use the classical K-M formulas. The discrete-symmetrical version is created for stacks of identical layers which have the same reflectance on either face. A discrete non-symmetrical version for stacks of identical layers with different reflectance on either face. Lastly a continuous non-symmetrical version for stacks of layers that have different absorption and scattering coefficients according to the forward and backward flux directions. The accuracy of these generalised models still need to be tested with stacks of halftone ink layers. (Hébert et al., 2016)

Four-flux models have been developed to increase the accuracy of the prediction of the appearance of a layered structure. Song combined optical models and measurements in a multiscale solution in order to predict the reflectance and transmittance of ink layers. A radiative transfer four-flux model is used which is based on microscopic characteristics of the inks used. The characteristics of the print support were measured separately. Tests of the model were done by printing ink stacks of different thicknesses on a transparent support to measure the reflectance and transmittance of the inks. The initial results show that the radiative transfer four-flux model is suitable for the prediction of image rendering with different combinations of ink and print support. (Song et al., 2018; Song et al., 2016) The question is whether this model is suitable for the inks currently used in 3D printing.

The Bidirectional Reflection Distribution Function (BRDF) is a mathematical model to characterise the relation between the incident and reflected energy when light hits a surface. BRDF is used by Yan as a base to create four different analytical models. Two empirical models (Blinn-Phong model and Ward model) and two microfacet-based models (Cook-Torrance model and Ashikhim-Shirley model) are tested on their performance. The Ward model showed the best results in terms of accuracy and speed. This is used as a starting point for further research to develop the BRDF model. (Yan et al., 2016) A BRDF model for subsurface scattering is set up by Dong. The Bidirectional subsurface scattering reflection distribution function (BSSRDF) is a general model to describe the surface appearance of translucent materials. The description is in terms of the light transport between every pair of surface points. This is used to compute the optimal layer layout of the output volume, thickness of the layers and the distribution of basis materials. (Dong et al., 2010)

Monte-Carlo simulation with a numerical optimizer is used by Elek as a base for the simulation of heterogeneous scattering. The researchers aim at creating a pipeline to print a sharp surface texture. It is, however, subject to physical limitations. The simulation is posed as a method to acquire the optical properties of the printing materials currently available. (Elek et al., 2017) Whether this is also suitable for ink requires further research. Another pipeline for the reproduction process is investigated by Hasan. They propose a pipeline for the entire process including measuring, modelling and fabricating objects with certain subsurface scattering behaviours. (Hasan et al., 2010) This research seems to have focused more on stone-like reproductions rather than paintings. Whether the pipeline is different from the reproduction of paintings could be investigated.

A last interesting option is the use of a traversal algorithm for voxel (volume of a pixel) surfaces as researched by Brunton. This makes it possible to transfer the existing error diffusion algorithms from 2D printing to 3D printing. In other words, it is possible to map 2D error diffusion filters onto a surface in a consistently oriented way. Since a lot of research has already been done on 2D printing, it can be very useful if that knowledge can be transferred to 3D printing. Especially since colour imaging and colour management are different for 3D printing compared to 2D printing. Brunton proposed algorithms for precise and efficient control of material placement in multi-jet 3D printers for the purposes of halftoning. (Brunton et al., 2015)

#### 4.4 Computer models - digitally simulating paintings

Theoretical calculations and calculations made using the theoretical models like described above can be used to calculate and simulate the behaviour of a layered paint structure. Rendering software could visualise the paint layers digitally and provide more insight in the visual appearance of paintings. Several analytical reflectance models have been developed for the field of computer graphics which can be divided into empirical and physically based models. The physically based computations focus on the interaction of light with matter to create realistic depictions of surfaces.

Jakob developed a method for rendering and in that way simulating layered materials. By using transport-theoretical models of isotropic or anisotropic scattering layers and smooth

or rough boundaries of dielectrics and conductors as input, BSDFs (Bidirectional Scattering Distribution Function) of layered materials can be computed. Therefore, more realistic rendering results can be achieved because the multiple scattering within and between layers can be simulated using their systems reflectance models. The system can be considered a computational language for describing surface structure which can be combined to describe a layered structure. This forms the basis for the Mitsuba render engine. To solve the scattering matrices of medium layers, this system uses the adding-doubling technique which assumes that multiple scattering is a higher-order effect that can be neglected for sufficiently thin layers. These very thin layers are used to find the scattering matrices of a layer double the thickness by joining two identical layers. This process of joining two identical layers is repeated until the desired thickness is achieved. (Jakob et al., 2014)

Weidlich proposed a physically plausible BRDF model capable of simulating smooth and rough multi-layered surfaces. The model includes absorption within the layers and the total internal reflection. They have tested several layered structures with different material properties in order to replicate the visual appearances of multiple types of paint. (see Figure 9) The glossy paint (Figure 9a) consists of a clear varnish on top of a coloured solid. This is the application of a Lambertian surface, with diffuse reflection, covered with a smooth layer. It can be a simulation of a paint layer covered with a varnish. The tinted glazing (Figure 9b) is a Lambertian colourless surface covered with a tinted varnish or glaze layer. (Weidlich et al., 2007) A combination of these two models could be an approximation of the paint layers present in the background of the Girl with a Pearl Earring. The model proposed by Weidlich does however still fail to reproduce wave effects like iridescence.

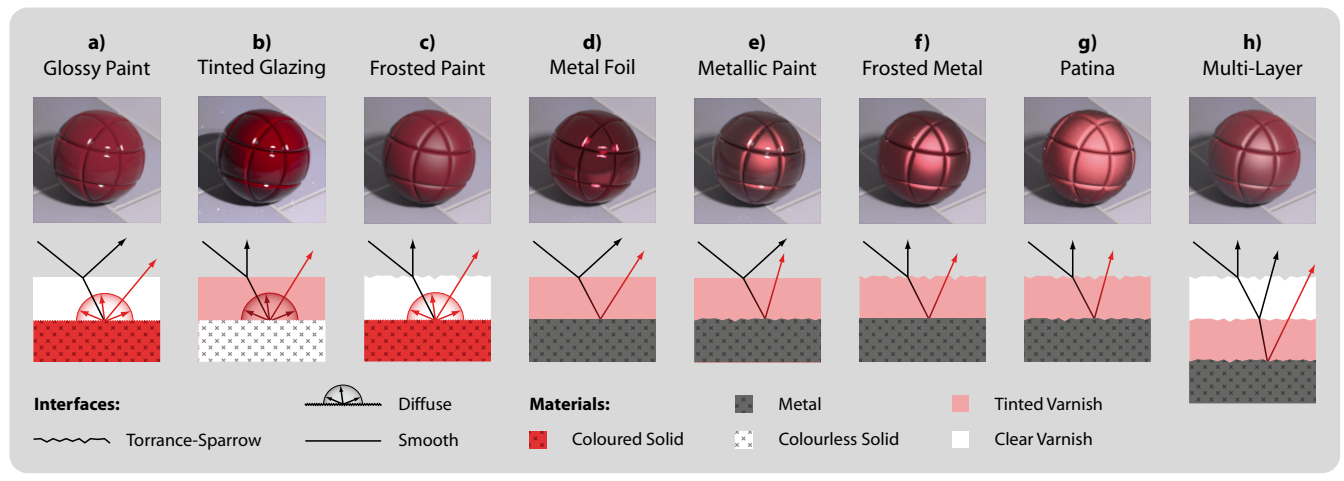


Figure 9. Examples of various surface types generated using the layered model created by Weidlich, Spheres are rendered under same illumination conditions. To distinguish the various cases, the micro-facets of the surface are much smaller than the layer thickness in the drawings. (Weidlich et al., 2007)

Levin set up a method to construct the spatially varying reflectance at resolutions up to 220 dpi. A consequence of the higher resolution is a lower angular resolution. Levin presents an analysis of incoherent reflectance based on wave optics which provides guidelines for the relation between the shape and size of particles and their reflectance functions. Wave optics are taken into account when, beyond a certain scale, geometric optics models do not apply. Other than the model from Weidlich, this model does take into account wave interference in order to fabricate a range of reflection effects.(Levin et al., 2013)

Moving more towards the realistic depiction of real objects in the digital environment, there

are several researches done on digitally imaging paint and other objects. In several cases of the paint simulation, Kubelka-Munk is used as a basis to calculate the absorption and reflection parameters in order to digitally replicate the paint.

An example of digitally recreating a painting is Pigmento. It consists of an algorithm created by Tan to model a per-pixel mixture of a limited number of pigments with an RGB image as input. The multispectral scattering and absorption coefficients of the pigments are determined by using the K-M model. The system makes is possible to build up an original RGB image of pigments in order to make tonal adjustments by editing the properties of the pigments. Several applications are possible, for example recolouring, selection masking, edge enhancement and more. In the future it might be possible to use this technique for the identification of pigments in paintings from RGB images. There are at the moment still some limitations regarding the pigment database and the number of primary pigments used in the reconstruction of the image. Next to that, the approach does only provide plausible results enabling paint-like editing.(Tan et al., 2018)

Chen simulated the appearance of paint applied on a BTF (Bidirectional Texture Function) material. The BTF is a function representing the appearance of the surface of a material as a function of location, viewing direction and lighting direction. It is captured from a real material and can therefore produce a realistic digital representation of that material. This BTF data is used to set up the physical information of the surface including the geometry and reflectance. The properties of the paint are added to this model. The reflectance of the paint is computed using the K-M model. The use of the K-M model has its limitations and causes this system to not yet support complex lighting effects due to the directions of the fluxes in the K-M model. A more physically accurate model could lead to a more realistic result. (Chen et al., 2017)

To create a realistic depiction of a painting while it is being made, Baxter created a model which can be used in interactive painting systems. This model simulates both the numerical aspect as the physical flow of paint during the application on a surface. It can be used on paint styles similar to oil and acrylic paint and several different painting styles are possible, for example thick impasto and semi-transparent glazes. The user of the model can draw on a tablet the brush strokes of the painting and the system will calculate the behaviour of the applied paint and its interaction with the surface and the brush. One active wet layer is taken into account together with an unlimited number of dry paint layers and each layer is represented by a height field. A set of pigments was selected by the developers in advance to build up the images. The spectral properties of the pigments were included in the set. By representing the colours in terms of the set of pigments rather than RGB allows the system to show the painting under different lighting conditions because the appearance of the pigments can be adjusted with the emitted spectrum of the light source. (Figure 10) The physical flow of paint is used to simulate the application of paint live, however, the simulation is based on approximations with added heuristics which model the behaviours not covered by the physical terms. The full-spectrum reflectance of several oil paints commonly used were measured and imported into the system for users to work with. To model as accurate as possible the chromatic behaviour of paint blending, a colour blending and compositing engine based on the Kubelka-Munk model is added to the system as well. Limitations of the model are the limited resolution due to computational costs and the fact

that K-M is an idealisation of the situation which does not exactly simulate the light transport through the paint layer. (Baxter et al., 2004) Creating the appearance of a painted surface from a 2D image is done by Lee. An algorithm was generated to introduce 3D brush strokes to a 2D photograph to create the suggestion of an oil painting. Using a photometric stereo technique, brush strokes have been converted into 3D models. These could be integrated into the image by decreasing brush stroke radius to approach the effect of the painted image. (Lee et al., 2007)

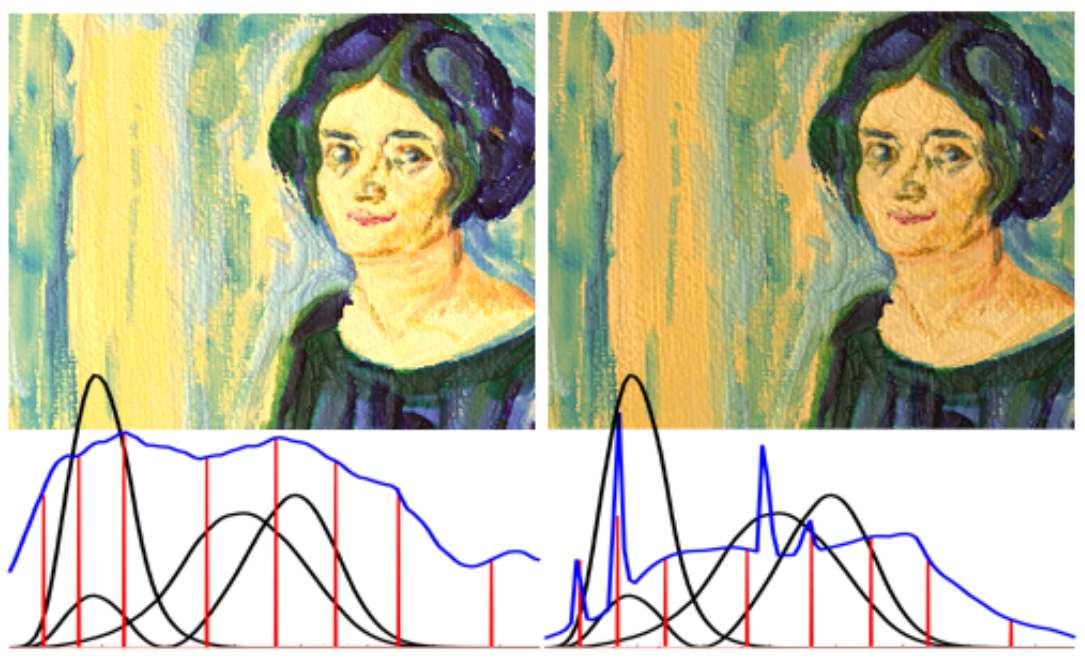


Figure 10. Comparison of the same painting created with IMPaSTo under different lighting conditions. Left, painting digitally illuminated by a 5600K bulb. Right, painting digitally illuminated by CIE Fluorescent Illuminant F8. The spectra below represent the light spectra (blue), 8 sample wavelength used by IMPaSTo (red) and CIE XYZ integrating functions (black).(Baxter et al., 2004)

Not only paint and paintings are digitally recreated, photorealistic rendering of virtual objects in order to insert them into images of the real world is increasingly used. For example, in the (web) catalogue of IKEA where digital models of furniture are rendered and inserted into images of a real-life photo set. Physically based methods are studied by Kronander to simulate how light propagates in a mathematical model of the augmented scene. He discusses four areas related to photorealistic rendering, HDR (High Dynamic Range) imaging, IBL (Image Based Lighting), reflectance modelling and efficient rendering. Next to that, two BRDF models are proposed for surfaces which exhibit wide angle gloss. The algorithm proposed by Kronander enables efficient rendering of scenes which contain glossy transfer and heterogeneous participating media. (Kronander, 2015)

To conclude, several different models are tried for layered and partially translucent structures like the materials used in paintings and 3D printing. The optical properties of the paint present in original paintings, paint reconstructions and ink currently used for the 3D printed reproductions of paintings could be used to test (one of) these models. Testing the models can provide more insight in the use of computer models to predict the results of the 3D printing with the data retrieved from the original objects.

# 5 3D printing

3D printers have become more available in the last decade and the amount of research done on the applications of 3D printing has increased drastically. Next to extrusion printing and laser sintering printing, printing with UV-curable ink has been developed. This last one is based on droplets of ink which are deposited on a surface and cured using UV light. It is developed by Océ and used already in several reproductions of paintings. (Elkhuizen et al., 2017; Océ, 2018; Zaman et al., 2013) The aim of the fine art reproductions is to get the same visual effect as the original painting while built up out of a different material as visualised in Figure 10. A study on the perception of gloss on a print surface is done by Baar, where the psychophysical relationship between measurable gloss levels and gloss perception and its dependence on the print surface colour and texture is determined. This relation can be described by a single roughness parameter which make it possible to estimate the optical properties of surface characteristics. (Baar, 2015)

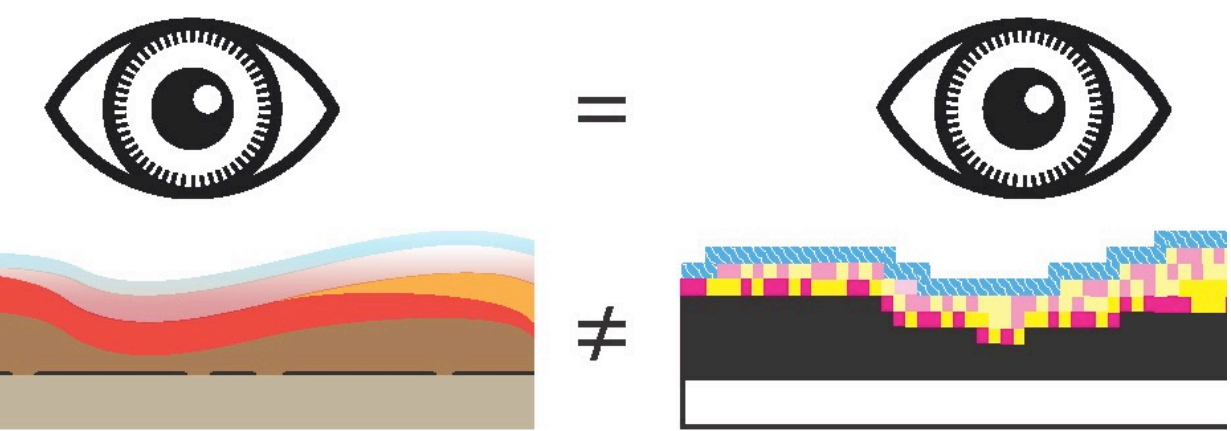


Figure 10. Aim for the same visual observation while the materials used to make the reconstruction are different. (Elkhuizen et al., 2014)

In printing, images can be created by placing ink droplets next to each other. Halftoning is a printing technique where dots are either coloured or not. In Figure 11 an example is given for the gradient from white to black. Within a certain area, more and more dots are black when moving to the right side of the image. Colour can be created by printing cyan, magenta, yellow and black (CMYK) ink droplets next to each other in specific compositions. To create, for example, orange small dots of red and yellow are placed next to each other to create the appearance of orange.(Fraser, 2006) Shi combined contoning with halftoning, where the size of the ink dot is varied to create colour and shading, in order to simultaneously solve the layout discretisation and colour quantisation problems with only contoning or halftoning. Their work has focused on the accurate reproduction of colour using a 3D printer equipped with ten inks. The ink library and physical prediction model need further development.(Shi et al., 2018) This research, other than Elkhuizen, has not focussed on gloss, combining both could lead to more realistic reproductions.

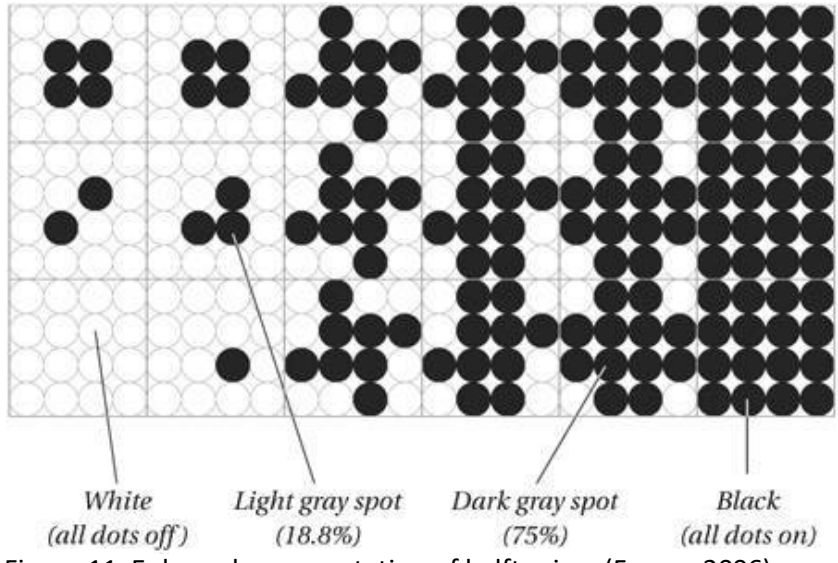
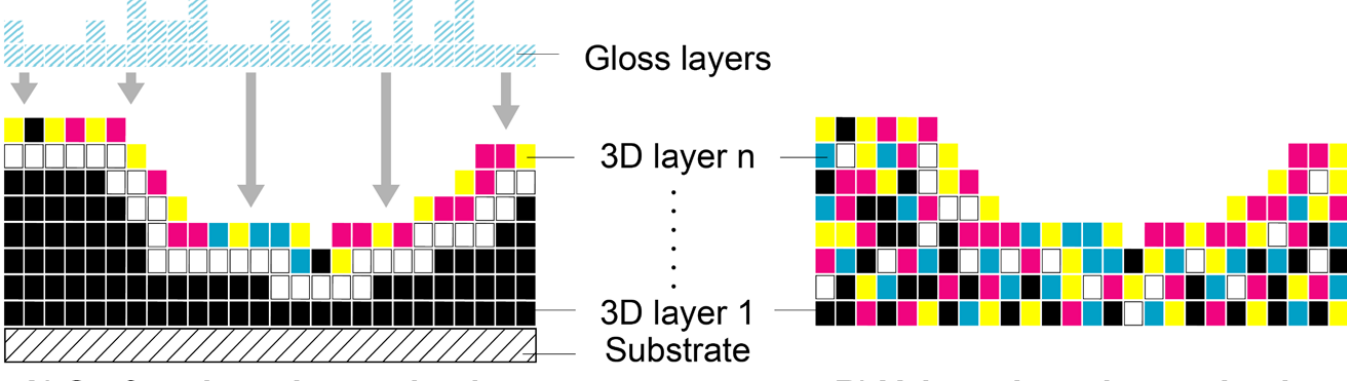


Figure 11. Enlarged representation of halftoning. (Fraser, 2006)

The resolution of the 3D printed reproductions has so far mostly been based on the resolution the human eye can observe at a distance of 75 cm.(Zaman et al., 2013) Observing the reproduction up close makes it possible to distinguish pixels. Subsurface scattering effects also hinder the perception of finer details in a print, especially in the case of (semi-) transparent ink. The adoption of shape enhancement approaches could increase the readability of tiny details, for example by pre-computing an ad hoc surface shading to colour the surface of the print. This could enhance the perception of the geometric shape of the print which improves the appearance of the fine details.(Scopigno et al., 2015) The method proposed by Elek should result in a sharper surface texture, however this method is aimed at the processing of the data rather than adjusting the printing technique.(Elek et al., 2017)

Current research focusses more on the printing technique and processing of data to convert the measurements of paintings to be able to use these for 3D printing. There is less focus on development of the material used to print. Baar proposed to influence aspects such as ink deposition and drying time by utilizing different parameters of a printing system. This impacts the roughness of the print surface on a micro level. (Baar et al., 2015) A 3D print of a painting can be constructed in two different manners, surface-based and volume-based (Figure 12). Elkhuizen evaluated these two material jetting systems. The inner volume of a surface-based reproduction is built up with ink and creates the relief of the painting. CMYK, white and transparent ink form the outer layer. The advantage here is that only the top layers need to be printed in colour, a disadvantage is the lack of perception of depth. A volume-based 3D printer uses 5 translucent, CMYK and white inks. The colour here is created through consecutive layers of pixels or 3D half-toning. The surface-based system is more accurate in colour reproduction. When gloss layers are added, the reproduction is even more life-like. With the volume-based technique colours appear to blend a little causing the overall image to look less sharp. Next to that more colours are needed to obtain more accurate colours. (Babaei et al., 2017; Elkhuizen et al., 2018) The described effect can be observed in Figure 13, the original painting and surface-based and volume-based reproductions are shown under different lighting and viewing conditions. The image of volume-based reproduction is clearly less sharp compared to the original and surface-based reproduction. Perhaps the adjustment of print parameters as in the research of Baar (2016) could create a more realistic surface edge sharpness.



A) Surface-based reproduction

# B) Volume-based reproduction

Figure 12. Two different methods to build up a 3D printed reproduction. Left surface-based where a base structure is made to create the relief and the colour and gloss are printed on top of the base. Right is volume-based where the entire print is built up out of coloured ink. (Elkhuizen, Doubrovski, et al., 2018)



Figure 13. Comparison of the original artefact with 2 3D printed reproductions. Gloss variation is clearly visible in the surface-based colour reproduction. The volume-based reconstruction is highly translucent but also more blurred. (Elkhuizen, Doubrovski, et al., 2018)

The focus mainly lies on the 3D printing techniques rather than the development of new materials. The resolution used so far is around 300 dpi which is similar to the resolution of the human eye from a distance of 75 cm.(Zaman et al., 2014) Some researchers have focussed on creating a variation in gloss on the printed surface to create more life-like reproductions. More research could be done on the materials used for the 3D prints.

With the development of new 3D printing inks, the measured optical properties of original paints could be taken into account. If rendering of paints will provide a realistic representation of the paint in real life, the render software can be used for further development of realistic 3D printed reproductions. Rendering images of paint and paintings with measured optical properties of paints and inks can give an indication of the visual appearance of the 3D print without physically printing. When the rendered image can reproduce the visual appearance of a glaze layer, this data can be useful for better reproducing a glaze layer using a 3D printer.

### 6 Conclusion

Research on the Girl with a Pearl Earring was done in '94-'95 by Groen and the focus was on chemical research to determine the composition of the paint in the painting. The background of the painting consists of a black underpaint with a green glaze layer applied on top. The exact function of this glaze layer and its influence on the appearance of the painting is still unknown. (Groen et al., 1998)

A painting consists of layers of paint on top of a canvas. The individual paint layers have distinct physical properties (colour, gloss, translucency, texture) which determine the visual appearance of the painting. The physical parameters of paint and paintings can be determined by several means of analysis. Spectrophotometry and ellipsometry are techniques which could be suitable to determine optical properties of paint, for example the colour and translucency. Novel techniques have been developed by Elkhuizen to measure the level of gloss and to create a map of the surface topography of the painting surface.(Van Hengstum et al., 2018)

The measured physical properties of paint and paintings can be used as input for theoretical and computer models to predict and simulate the visual appearance of the paint and painting. To verify for example the computer models, renders need to be made and these should be compared to the original painting. If the computer model can provide a realistic representation of the painting using the measured physical parameters as input, the model could be useful for further development of 3D printed reproductions of paintings.

3D printed reproductions of paintings can be used for conservation and restoration purposes and make art more accessible to a large public. Using the physical parameters of 3D printing ink as input, a proper computer model can give a prediction of the appearance of a 3D print before having to physically print it. When a 3D print is created after a 3D model and computer model, test prints would need to be made and their characteristics would have to be compared to a painted and rendered version.

Future research can focus on the optical properties of the paint and glaze layer present in the background of Girl with a Pearl Earring. These optical properties, possibly combined with other physical properties of the painting (surface texture, layer thickness, gloss) can be used as input for a computer model to digitally recreate the painting and test the influence of the glaze layer on the visual appearance of the painting. Research on the printing technique and materials will be extensive and too much for the current graduation project.

Baar, T. (2015). Optimisation of print quality with multi-channel printing. (PHD), ParisTech, Paris.

Baar, T., Brettel, H., & Segovia, M. O. (2015). Relating Optical and Geometric Surface Characteristics for Gloss Management in Printing Applications. *Journal of Imaging Science and Technology*, *59*(6), 60404-60401-60404-60414.

Babaei, V., Vidimce, K., Foshey, M., Kaspar, A., Didyk, P., & Matusik, W. (2017). Color Contoning for 3D Printing. *ACM Transactions on Graphics*, *36*(4), 1-15.

Batsanov, S. S., Ruchkin, E. D., & Poroshina, I. A. (2016). Methods of Measuring Refractive Indices. In *Refractive Indices of Solids* (pp. 9-15): Springer.

Baxter, W., Wendt, J., & Lin, M. C. (2004). *IMPaSTo: A Realistic, Interactive Model for Paint*. Paper presented at the Proceedings of the 3rd International Symposium on Non-Photorealistic Animation and Rendering, Annecy, France.

Berns, R. S., & Rie, E. R. d. l. (2003). The Effect of the Refractive Index of a Varnish on the Appearance of Oil Paintings. *Studies in Conservation*, 48(4), 251-262.

Brunton, A., Arikan, C. A., & Urban, P. (2015). Pushing the limits of 3D color printing - Error diffusion with translucent materials *ACM Transactions on Graphics*, *35*(1). Callewaert, T. (2018).

Chen, T.-E., Huang, T.-S., Lin, W.-C., & Chuang, J.-H. (2017). Simulating Painted Appearance of BTF Materials. *Multimed Tools Appl, 77*, 7153-7169.

Cheung, C. S., Spring, M., & Liang, H. (2015). Ultra-high resolution Fourier domain optical coherence tomography for old master paintings. *Optics Express, 23*(8), 10145-10157. Craic. (2012). Microspectrophotometer Design. Retrieved April 14 2019 from <a href="http://www.craictechnologies.com/support/service-contracts/microspectrophotometer-design">http://www.craictechnologies.com/support/service-contracts/microspectrophotometer-design</a>

Dong, Y., Wang, J., Pellacini, F., Tong, X., & Guo, B. (2010). Fabricating Spatially-Varying Subsurface Scattering. *ACM Transactions on Graphics*, *29*(4).

Elek, O., Sumin, D., Zhang, R., Weyrich, T., Myszkowski, K., Bickel, B., . . . Krivánek, J. (2017). Scattering-aware Texture Reproduction for 3D Printing. *ACM Transactions on Graphics*, *36*(6), 241:241-241:215.

Elkhuizen, W. S., Doubrovski, E. L., Apeldoorn, N. v., Essers, T. T. W., & Geraedts, J. M. P. (2018). *Digital Manufacturing of Fine Art Reproductions for Appearance*. Paper presented at the 3rd International Conference on Innovation in Art Research and Technology (inArt 2018). Elkhuizen, W. S., Essers, T. T. W., Lenseigne, B., Weijkamp, C., Song, Y., Post, S. C., . . . Dik, J. (2017). *Reproduction of Gloss, Color and Relief of Paintings using 3D Scanning and 3D Printing*. Paper presented at the Eurographics.

Elkhuizen, W. S., Essers, T. T. W., Song, Y., Pont, S. C., Geraedts, J. M. P., & Dik, J. (2018). Gloss Calibration and Gloss Gamut Mapping for Material Appearance Reproduction of Paintings. Paper presented at the Eurographics Workshop on Graphics and Cultural Heritage, Viena.

Elkhuizen, W. S., Zaman, T., Verhofstad, W., Jonker, P., Dik, J., & Geraedts, J. M. P. (2014). Topographical scanning and reproduction of near-planar surfaces of paintings. *Proceedings of SPIE, 9018* (Measuring, Modeling, and Reproducing Material Appearance). Fraser, B. (2006). *Real World Adobe Photoshop CS2: Industrial-strength Production Techniques*.

Geldof, M., Gaibor, A. N. P., Ligterink, F., Hendriks, E., & Kirchner, E. (2018). Reconstructing Van Gogh's Palette to Determine the Optical Characteristics of his Paints. *Heritage Science*, *6*(17).

Groen, K. M., Werf, I. D. v. d., Berg, K. J. v. d., & Boon, J. J. (1998). Scientific Examination of Vermeer's Girl with a Pearl Earring. *Studies in the History of Art*, 55, 168-183.

Hasan, M., Fuchs, M., Matusik, W., Pfister, H., & Rusinkiewicz, S. (2010). Physical Reproduction of Materials with Specified Subsurface Scattering. *ACM Transactions on Graphics*, *29*(4).

Hébert, M., Mazauric, S., & Simonot, L. (2016). Assessing the capacity of two-flux models to predict the spectral properties of layered materials. Paper presented at the IS&T International Symposium on Electronic Imaging, San Fransisco, United States.

Hengstum, M. J. W. v., Essers, T. T. W., Elkhuizen, W. S., Dodou, D., Song, Y., Geraedts, J. M., & Dik, J. (2018). *Development of a High Resolution Topography and Color Scanner to Capture Crack Patterns of Paintings*. Paper presented at the Eurographics Workshop on Graphics and Cultural Heritage, Viena.

Jakob, W., d'Eon, E., Jakob, O., & Marschner, S. (2014). A Comprehensive Framework for Rendering Layered Materials. *ACM Transactions on Graphics*, *33*(4).

Janson, J. Weld. Retrieved November 14 2018 from

http://www.essentialvermeer.com/palette/palette\_weld.html#.W-xe-C9x\_OQ

Jenkins, F. A., & White, H. E. (2001). *Fundamentals of Optics* (S. Grall Ed. Fourth ed.). Jones, J. (2002, 2 November). Girl With a Pearl Earring, Jan Vermeer (c1665). *The Guardian*. Retrieved November 13 2018 from <a href="https://www.theguardian.com/culture/2002/nov/02/art">https://www.theguardian.com/culture/2002/nov/02/art</a>

Kronander, J. (2015). *Physically Based Rendering of Synthetic Objects in Real Environments*. Linköping University, Norrköping.

Kubelka, P., & Munk, F. (1931). An Article on Optics of Paint Layers. Retrieved from Lee, K. J., Kim, D. H., Yun, I. D., & Lee, S. U. (2007). Three-dimensional Oil Painting Reconstruction with Stroke Based Rendering. *The Visual Computer, 23*(9-11), 873-880. Levin, A., Glasner, D., Xiong, Y., Durand, F., Freeman, W., Matusik, W., & Zickler, T. (2013). Fabricating BRDFs at High Spatial Resolution Using Wave Optics. *ACM Transactions on Graphics, 32*(4).

Mauritshuis. Meisje met de parel. In. Den Haag: Mauritshuis.

McCrackin, F. L., Passaglia, E., Stromberg, R. R., & Steinberg, H. L. (1963). Measurement of the Thickness and Refractive Index of Very Thin Films and the Optical Properties of Surfaces by Ellipsometry. *Journal of Research*, 67A(4), 363-377.

Nave, C. R. (2017). Refraction of Light. Retrieved March 11 2019 from http://hyperphysics.phy-astr.gsu.edu/hbase/geoopt/refr.html#c3

New Light for Old Master Paintings. (2015). Retrieved November 13 2018 from https://www.osa.org/en-

<u>us/about\_osa/newsroom/news\_releases/2015/new\_light\_for\_old\_master\_paintings/</u>
Océ. (2018). UVgel. Retrieved November 15 2018 from <a href="https://www.oce.com/products/oce-uvgel/">https://www.oce.com/products/oce-uvgel/</a></u>

Polikreti, K., Othonos, A., & Christofides, C. (2005). Optical Characterization of Varnish Films by Spectroscopic Ellipsometry for Application in Artwork Conservation. *Applied Spectroscopy*, *59*(1), 94-99.

Scopigno, R., Cignoni, P., Pietroni, N., Callieri, M., & Dellepiane, M. (2015). Digital Fabrication Techniques for Cultural Heritage: A Survey. *Computer Graphics Forum, 36*(1), 6-21.

- Shi, L., Babaei, V., Kim, C., Foshey, M., Hu, Y., Sitthi-Amorn, P., . . . Matusik, W. (2018). *Deep Multispectral Painting Reproduction via Multi-Layer, Custom-Ink Printing*. Paper presented at the ACM SIGGRAPH ASIA 2018, Tokyo.
- Song, T. P. V., Andraud, C., Sapaico, L. R., & Segovia, M. O. (2018). *Color prediction based on individual characterizations of ink layers and print support*. Paper presented at the IS&T International Symposium on Electronic Imaging 2018, Burlingame, California.
- Song, T. P. V., Andraud, C., & Segovia, M. O. (2016). *Implementation of the four-flux model for spectral and color prediction of 2.5D prints*. Paper presented at the Printing for Fabrication 2016, Manchester.
- Taft, W. S., & Mayer, J. W. (2000). *The Science of Paintings*. New York: Springer-Verlag New York, Inc.
- Tan, J., DiVerdi, S., Lu, J., & Gingold, Y. (2018). Pigmento: Pigment-Based Image Analysis and Editing. *IEEE Transactions on Visualization and Computer Graphics*.
- Vandivere, A. (2018, 9 November 2018). [MMdP for TU Delft\_samples 19 and 26].
- Weidlich, A., & Wilkie, A. (2007). *Arbitrarily Layered Micro-Facet Surfaces*. Paper presented at the GRAPHITE, Perth, Australia.
- Yan, N., Baar, T., Segovia, M. O., & Allebach, J. (2016). Fitting analytical BRDF models to low-resolution measurements of light scattered from relief printing samples. Paper presented at the IS&T International Symposium of Electronic Imaging 2016.
- Zaman, T., Dik, J., & Jonker, P. (2013, November 2013). Modern Digitization for Cultural Heritage: Simultaneous Capture of 3D Topography and Colour in Paintings of Van Gogh and Rembrandt. *AR[t] Augmented Reality, Art and Technology,* 56-59.
- Zaman, T., Jonker, P., Lenseigne, B., & Dik, J. (2014). Simultaneous capture of the color and topography of paintings using fringe encoded stereo vision. *Heritage Science*, 2(23).
- Zegeling, M. (2017). Het Geheim van de Meester. Amsterdam: MarkMedia & Art.



